

CONTACT RELATIONS BETWEEN
THE NEW ROSS LEUCOMONZOGRAHITE AND THE
FALLS LAKE MAFIC PORPHYRY:
EVIDENCE FOR MAGMA-MAGMA INTERACTIONS
IN THE SOUTH MOUNTAIN BATHOLITH

Vincent Charles DeWolfe

Submitted in Partial Fulfilment of the Requirements
for the Degree of Bachelor of Science, Honours
Department of Earth Sciences
Dalhousie University, Halifax, Nova Scotia
March 1994



Dalhousie University

Department of Earth Sciences

Halifax, Nova Scotia

Canada B3H 3J5

(902) 494-2358

FAX (902) 494-6889

DATE April 22, 1994

AUTHOR Vincent Charles DeWolfe

TITLE Contact Relations Between the New Ross Leucomonzogranite and the
Falls Lake Mafic Porphyry: Evidence for Magma-Magma Interactions
in the South Mountain Batholith.

Degree Honours BSc. Convocation Spring Year 1994

Permission is herewith granted to Dalhousie University to circulate and to have copied for non-commercial purposes, at its discretion, the above title upon the request of individuals or institutions.

THE AUTHOR RESERVES OTHER PUBLICATION RIGHTS, AND NEITHER THE THESIS NOR EXTENSIVE EXTRACTS FROM IT MAY BE PRINTED OR OTHERWISE REPRODUCED WITHOUT THE AUTHOR'S WRITTEN PERMISSION.

THE AUTHOR ATTESTS THAT PERMISSION HAS BEEN OBTAINED FOR THE USE OF ANY COPYRIGHTED MATERIAL APPEARING IN THIS THESIS (OTHER THAN BRIEF EXCERPTS REQUIRING ONLY PROPER ACKNOWLEDGEMENT IN SCHOLARLY WRITING) AND THAT ALL SUCH USE IS CLEARLY ACKNOWLEDGED.

Distribution License

DalSpace requires agreement to this non-exclusive distribution license before your item can appear on DalSpace.

NON-EXCLUSIVE DISTRIBUTION LICENSE

You (the author(s) or copyright owner) grant to Dalhousie University the non-exclusive right to reproduce and distribute your submission worldwide in any medium.

You agree that Dalhousie University may, without changing the content, reformat the submission for the purpose of preservation.

You also agree that Dalhousie University may keep more than one copy of this submission for purposes of security, back-up and preservation.

You agree that the submission is your original work, and that you have the right to grant the rights contained in this license. You also agree that your submission does not, to the best of your knowledge, infringe upon anyone's copyright.

If the submission contains material for which you do not hold copyright, you agree that you have obtained the unrestricted permission of the copyright owner to grant Dalhousie University the rights required by this license, and that such third-party owned material is clearly identified and acknowledged within the text or content of the submission.

If the submission is based upon work that has been sponsored or supported by an agency or organization other than Dalhousie University, you assert that you have fulfilled any right of review or other obligations required by such contract or agreement.

Dalhousie University will clearly identify your name(s) as the author(s) or owner(s) of the submission, and will not make any alteration to the content of the files that you have submitted.

If you have questions regarding this license please contact the repository manager at dalspace@dal.ca.

Grant the distribution license by signing and dating below.

Name of signatory

Date

ABSTRACT

The South Mountain Batholith is a peraluminous composite batholith that intruded over a short interval of time. The batholith consists of 260 intrusive bodies, thus the possibility of magma-magma interactions is high. The types of contacts that form when one granite intrudes another granite depends on the temperatures, viscosities, densities, and the degree of crystallization of the two granites at the time of intrusion. In the New Ross Pluton, a wide range of unusual contact relations occur between the New Ross Leucomonzogranite and Falls Lake Mafic Porphyry. Contacts between these units are commonly lobate and crenulate, and have a fractal nature. Contacts between the leucomonzogranite and mafic porphyry are diffuse and irregular, and large grains from the leucomonzogranite cut across contacts, and locally occur as xenocrysts in the mafic porphyry. Contact relations between the New Ross Leucomonzogranite and Falls Lake Mafic Porphyry suggest that the leucomonzogranite postdates the mafic porphyry, and that the degree of crystallization of the mafic porphyry was variable when the leucomonzogranite intruded. Field relations and petrography provide evidence that mingling of the leucomonzogranite and mafic porphyry occurred. Mineral compositions provide evidence that a limited degree of mixing accompanied mingling processes. Variances in the degree of crystallization (C) of the mafic porphyry result in sharp contacts where C is high, and irregular, crenulate contacts where C is lower.

Key Words: composite intrusion, leucomonzogranite, mafic porphyry, crenulate, fractal, contact relations, mingling, mixing.

This thesis is dedicated to my parents and grandparents, who have inspired and encouraged me during my years at Dalhousie.

TABLE OF CONTENTS

CHAPTER 1. Introduction

1.1	Introduction	1.
1.2	Types and Features of Igneous-Igneous Contacts	1.
1.3	General Geology	8.
1.4	Purpose and Scope	9.
1.5	Organization	10.

CHAPTER 2. Field Work

2.1	Introduction	11.
2.2	Geology of the New Ross Pluton	11.
2.3	Unit Descriptions	12.
	2.3.1 Unit 1. New Ross Leucomonzogranite	12.
	2.3.2 Unit 2. Falls Lake Mafic Porphyry	12.
2.4	Mapping and Methodology	15.
2.5	Observed Contact Relations	16.
	2.5.1 Xenoliths of Mafic Porphyry in Leucomonzogranite	16.
	2.5.2 Dykes of Leucomonzogranite in Mafic Porphyry	20.
	2.5.3 Nature of Contacts between Leucomonzogranite and Mafic Porphyry	20.
2.6	Discussion	24.
2.7	Conclusions	29.

CHAPTER 3. Petrography

3.1	Introduction	30.
3.2	Petrographic Descriptions	30.
	3.2.1 Unit 1. New Ross Leucomonzogranite	30.
	3.2.2 Unit 2. Falls Lake Mafic Porphyry	32.
	3.2.3 Contact Descriptions	36.
3.3	Discussion	42.
3.4	Conclusions	48.

CHAPTER 4. Mineral Chemistry

4.1	Introduction	49.
4.2	Mineral Chemistry	49.
4.2.1	Background	49.
4.2.2	Mineral Chemistry	53.
4.2.2.1	Biotite compositions	53.
4.2.2.2	Plagioclase chemistry	54.
4.2.2.3	Alkali feldspar chemistry	54.
4.3	Discussion	56.
4.4	Conclusions	57.

CHAPTER 5. Discussion

5.1	Introduction	58.
5.2	Review of Data	58.
5.2.1	Review	58.
5.2.2	Evidence of Mingling	58.
5.2.3	Evidence of Mixing	66.
5.3	Discussion	67.
5.4	Possible Models and Explanations	68.
5.5	Conclusions	69.

CHAPTER 6. Conclusions

6.1	Conclusions	70.
-----	-------------	-----

References	72.
------------	-----

Appendix A: Petrographic Observations	A1.
---------------------------------------	-----

Appendix B: Mineral Chemistry	B1.
-------------------------------	-----

TABLE OF FIGURES

- Figure 1.1. Geologic map of the South Mountain Batholith showing the distribution of the various lithologic units and the location of the major fault and shear zones. 2.
- Figure 1.2. a) Post magmatic fracturing with negligible intergranular fluid present. b) Late-magmatic fracturing with about 10% intergranular hydrous melt present. c) Late-main magmatic fracturing with as much as 30% intergranular melt present. 5.
- Figure 1.3. The different types of exchange occurring between two coexisting and contrasting magmas in a dynamic magma system, and their combination into mixing or mingling processes. 6.
- Figure 2.1. Photograph showing the nature of the New Ross Leucomonzogranite and Falls Lake Mafic Porphyry. 13.
- Figure 2.2. Quartz-alkali-plagioclase plot for the New Ross Leucomonzogranite and Falls Lake Mafic Porphyry. 14.
- Figure 2.3. Detailed map of the study area, showing patchy outcrop of mafic porphyry and locations of various sampling localities. 17.
- Figure 2.4. Photograph showing mafic porphyry xenoliths present in a leucomonzogranite dyke. 18.
- Figure 2.5. Enlarged section of Figure 2.4 showing the elongate, oval shape of mafic porphyry xenoliths. 18.
- Figure 2.6. Photograph showing a mafic porphyry xenolith with chilled and altered margins. 19.
- Figure 2.7. Photograph showing the megascopically sharp linear nature of leucomonzogranite contacts which occur where leucomonzogranite intrudes the mafic porphyry. 19.
- Figure 2.8. Photograph showing the megascopically sharp linear nature of leucomonzogranite dyke contacts, which show curvilinear contacts at smaller scale. 20.
- Figure 2.9. Photograph showing the irregular diffuse contact between leucomonzogranite and the mafic porphyry. 20.
- Figure 2.10. Photograph showing alkali feldspar megacrysts which align at the edge of the leucomonzogranite dyke, and cut across the contact. 22.

- Figure 2.11. Photograph showing dyking of leucomonzogranite, which is marked by fine-grained leucomonzogranite which contains a mafic porphyry xenolith, and a concentration of alkali feldspar megacrysts in mafic porphyry. 22.
- Figure 2.12. Photograph showing a megascopically sharp, linear contact between the leucomonzogranite and mafic porphyry units. 23.
- Figure 2.13. Photograph showing an irregular leucomonzogranite/mafic porphyry contact, where alkali feldspar megacrysts cut across the contact and protrude into the mafic porphyry. 23.
- Figure 2.14. Photograph showing an irregular crenulate contact between the leucomonzogranite and mafic porphyry units. 25.
- Figure 2.15. Photograph showing phenocrysts of alkali feldspar which cut across the leucomonzogranite/ mafic porphyry contact. 25.
- Figure 2.16. Photograph showing irregular contact where feldspar phenocrysts from the leucomonzogranite penetrate the mafic porphyry. 26.
- Figure 2.17. Photograph showing the arcuate shape and nature of leucomonzogranite/mafic porphyry contacts. 27.
- Figure 2.18. Photograph showing crenulate and cusped contacts between leucomonzogranite and mafic porphyry. 27.
- Figure 2.19. Sketch of Figure 2.19 showing contacts between leucomonzogranite and mafic porphyry at various scales. 28.
- Figure 3.1. Photograph showing an instance where small biotite plates occur as inclusions in other grains. 31.
- Figure 3.2. Photograph showing muscovite phases in the leucomonzogranite that occur as euhedral plates that replace alkali feldspar. 31.
- Figure 3.3. a) Photograph of plagioclase in the leucomonzogranite showing Carlsbad twinning and albite twinning. b) Photograph of plagioclase with a sausseritized core. 33.
- Figure 3.4. Photograph showing alkali feldspar megacrysts from the leucomonzogranite. 34.
- Figure 3.5. Photograph showing an inequigranular texture present in the mafic porphyry groundmass, and also the local occurrence of a micrographic texture between quartz and alkali feldspar. 34.

- Figure 3.6. Photograph of a cluster of biotite and muscovite in the mafic porphyry. 35.
- Figure 3.7. Photograph showing plagioclase grains that occur in the mafic porphyry groundmass. Plagioclase grains commonly display a) Carlsbad and b) albite twinning. 37.
- Figure 3.8. Photograph of alkali feldspar phases from the mafic porphyry. 38.
- Figure 3.9. Photograph of alkali feldspar megacrysts present in the mafic porphyry. 38.
- Figure 3.10. a) Photograph showing the irregular nature of leucomonzogranite/mafic porphyry contacts. 39.
- Figure 3.11. Photograph showing mingling between Falls Lake Mafic Porphyry and New Ross Leucomonzogranite. 40.
- Figure 3.12. Photograph showing concentric quartz grains in a alkali feldspar xenocryst in the Falls Lake Mafic Porphyry. 41.
- Figure 3.13. Photograph showing zoned plagioclase grains in the Falls Lake Mafic Porphyry near contacts. 41.
- Figure 3.14. a) Plagioclase grain with inclusion-rich plagioclase rim of different extinction. b) Photograph showing plagioclase with a rim of alkali feldspar. 43.
- Figure 3.15. Photograph showing corroded plagioclase grain in Falls Lake Mafic Porphyry. 44.
- Figure 3.16. Photograph of mafic porphyry near the dike-like contact shown in Figure 2.11. 44.
- Figure 4.1. Drawing showing how plagioclase compositions (Pl_x) change in response to: a) temperature changes, b) changes in water pressure, and c) magma mixing. 52.
- Figure 4.2. Drawing showing how plagioclase phases vary in the leucomonzogranite and mafic porphyry, near and away from contacts. 55.
- Figure 5.1. Sketch showing the various stages that may occur during the incorporation of mafic porphyry xenoliths by leucomonzogranite dykes. 61.
- Figure 5.2. Sketch showing how xenoliths of mafic porphyry may be incorporated at contacts between areas of leucomonzogranite and mafic porphyry. 62.

Figure 5.3. Drawing showing how the types of contacts between the leucomonzogranite and mafic porphyry vary according to differences in the degree of crystallization of the mafic porphyry. 63.

TABLE OF TABLES

Table 1.1. Comparisons between Case 1 and Case 2 igneous-igneous contacts for the various conditions listed.	4.
Table 3.1 Comparisons of New Ross Leucomonzogranite and Falls Lake Mafic Porphyry.	46.
Table 4.1 Comparison of compositions of phases from the New Ross Leucomonzogranite and Falls Lake Mafic Porphyry.	53.
Table 5.1. Evidence of mingling and mixing that occurs in field relations, petrography, mineral chemistry data.	59.
Table 5.2. Role of the various types of exchange at different structural levels, their causes, and results (from Barbarin and Didier 1992).	64.
Table 5.3. Criteria present where intrusive-intrusive contacts occur.	68.

Acknowledgements

The author wishes to thank Rick Horne for recognizing, and suggesting this thesis topic. The author also wishes to thank Rick Horne and Dr. D.B. Clarke for their suggestions and guidance during the production of this document. Thanks also go to J.P. Duggan for the use of his computer. Special thanks go to all other students in the department for their support, and for offering to help during the final stages of the production of this thesis.

CHAPTER 1:INTRODUCTION

1.1 Introduction

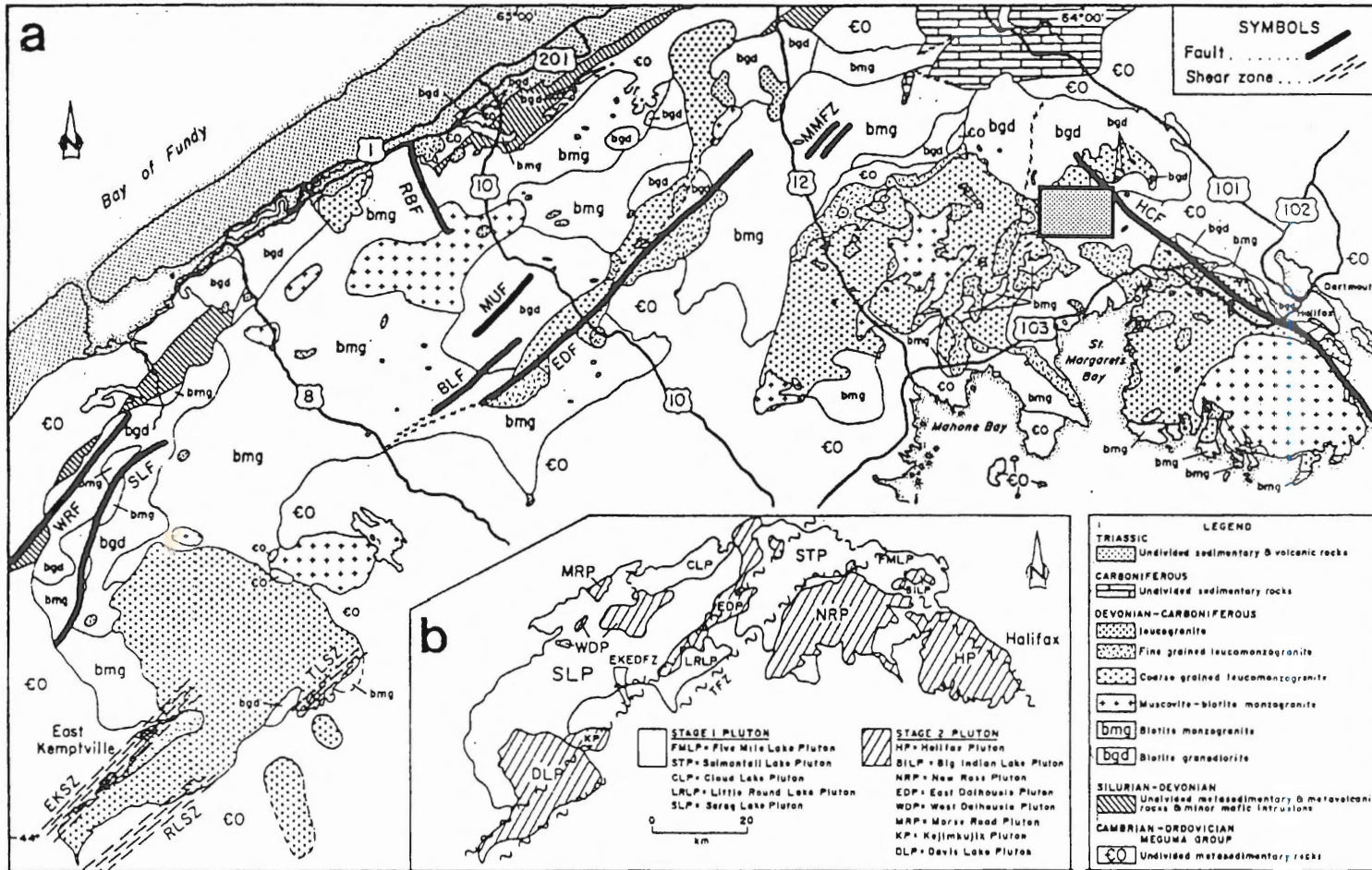
Large composite batholiths, such as the South Mountain Batholith (SMB), contain many smaller intrusive units (Fig. 1.1). MacDonald et al. (1992) identified 13 plutons consisting of 260 mappable intrusive bodies in the SMB. In the SMB, these smaller units intruded over a short interval, because the radiometric ages for all major intrusions in the SMB cluster around 370 Ma (Clarke et al. 1993 for discussion). The coeval nature of units in the SMB suggests a high probability of magma-magma interaction. Intrusive contacts exposed in one part of the New Ross Pluton show unusual contact relations, ranging from sharp to diffuse, and the relationship between the two units involved is unclear.

1.2 Types and Features of Igneous-Igneous Contacts

Igneous-igneous contacts form in two general settings (Table 1.1):

Type 1 (magma-solid). Type 1 contacts occur when an incompletely crystallized magma intrudes a completely crystallized igneous body. Type 1 contacts form when the period of time separating intrusive episodes allows earlier intrusions to solidify before later units intrude.

Type 1 contacts are sharp, and crystals in the solid body show truncation (Fig. 1.2a). Chilled margins may form where a crystallizing magma meets a much cooler, crystallized body. Assimilation of the host by the incompletely crystallized magma is likely, and wall-rock alteration may modify the host.



 Study Area

Figure 1.1. Geological map of the South Mountain Batholith showing the distribution of the various lithologic units and the location of the major fault and shear zones. The small inset map shows the Stage 1 and Stage 2 plutons. Study area shown in hatched box (after Horne et al. 1992).

Type 2 (magma-magma). Type 2 contacts form when two incompletely crystallized magmas meet. The range of contacts that occurs in this case is highly variable, and depends on the degree of crystallization of the materials involved. These contacts are likely to occur where the successive emplacement of plutons occurred over a short period.

Type 2 contacts involve two incompletely crystallized magmas. Two immiscible magmas can coexist if they are of contrasting compositions, densities, and viscosities (Barbarin and Didier 1992). At least temporary immiscibility can occur between melts of felsic and mafic composition; however, preserved contacts between two immiscible units rarely occur.

Type 2 contacts may show non-truncated and free-floating crystals (Fig. 1.2c) when one incompletely crystallized magma (magma A) intrudes another incompletely crystallized magma (magma B) (Hibbard and Watters 1985). If magma B has a higher degree of crystallization than magma A contacts may appear megascopically sharp, but show an interlocking texture at thin section scale (Fig. 1.2b). Whether only mingling (defined by mechanical mixing of the two magmas without homogenization (Fig. 1.3)), or mixing (defined by thermal, mechanical, and chemical exchanges between the two magmas leading to homogenization (Fig. 1.3)), occurs between two incompletely crystallized magmas depends on the differences in composition, temperature, density, and viscosity of the two magmas. As the differences in physical and chemical properties decrease, magma mixing will likely occur. The general

Table 1.1. Comparisons between Type 1 and Type 2 igneous-igneous contacts for the various conditions listed.

CONDITIONS	Type 1	Type 2
State of material A	completely crystallized $C \approx 1^*$	incompletely crystallized $0 < C < 0.74^{**}$
State of material B	incompletely crystallized $0 < C < 0.74$	incompletely crystallized $0 < C < 0.74$
Temperature difference	large	small
Time interval between intrusion of material A and material B	long	short
Degree of mingling/mixing	incorporation of enclaves little or no mixing	mingling and mixing depending on miscibility of materials A and B
Nature of contacts	sharp with truncation of grains	variable - sharp to diffuse no truncation

C = degree of crystallization (volume of crystal fraction)

* volume of crystal fraction ≈ 1 , 100% crystallization - behaves as a solid

** volume of crystal fraction between 0 and 0.74, 0% to 74% crystallization.

For $C > 0.74$ the intrusion is mechanically a solid (Abbott 1989).

shapes of contacts formed from mingling of two coeval magmas are locally straight, and are often lobate and cusped (Barbarin and Didier 1992; Seamen and Ramsey 1992; Barbarin 1988).

The nature of contacts formed during intrusion depends on the rheological properties of the intruding magma and intruded country material. The rheological properties of igneous melts depend on the initial temperature, composition, and effective viscosity (μ_{eff}) of the melt (Fernandez and Barbarin 1991; Barbarin 1988). The effective viscosity is the viscosity of the bulk magma, and it

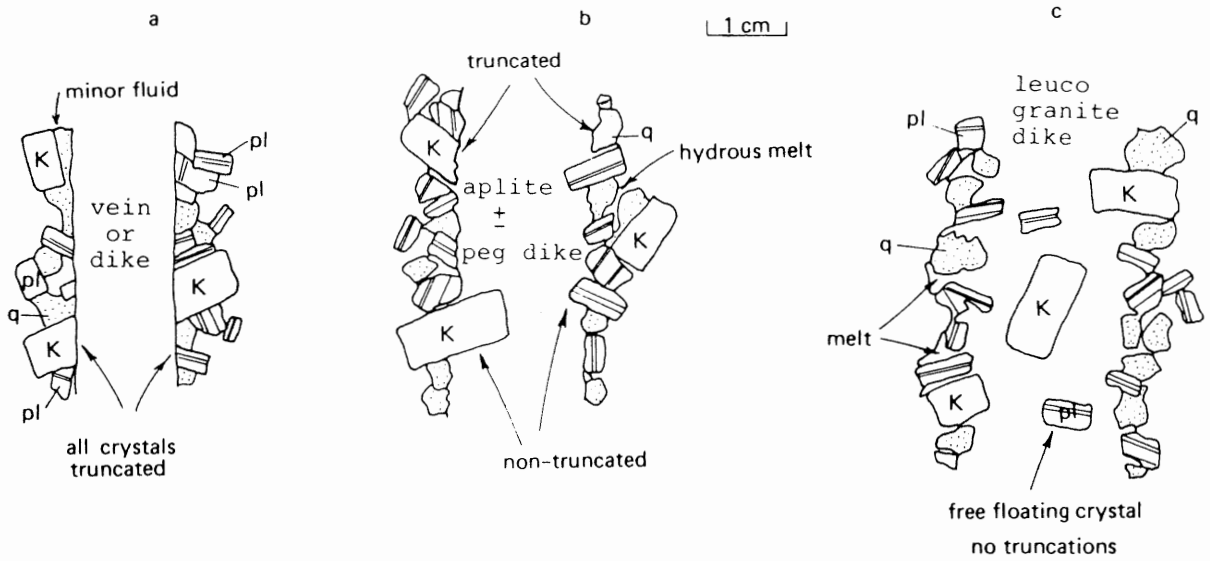


Figure 1.2. a) Post magmatic fracturing with negligible intergranular fluid present. b) Late-magmatic fracturing with about 10% intergranular hydrous melt present. c) Late-main magmatic fracturing with as much as 30% intergranular melt present (from Hibbard and Watters 1985).

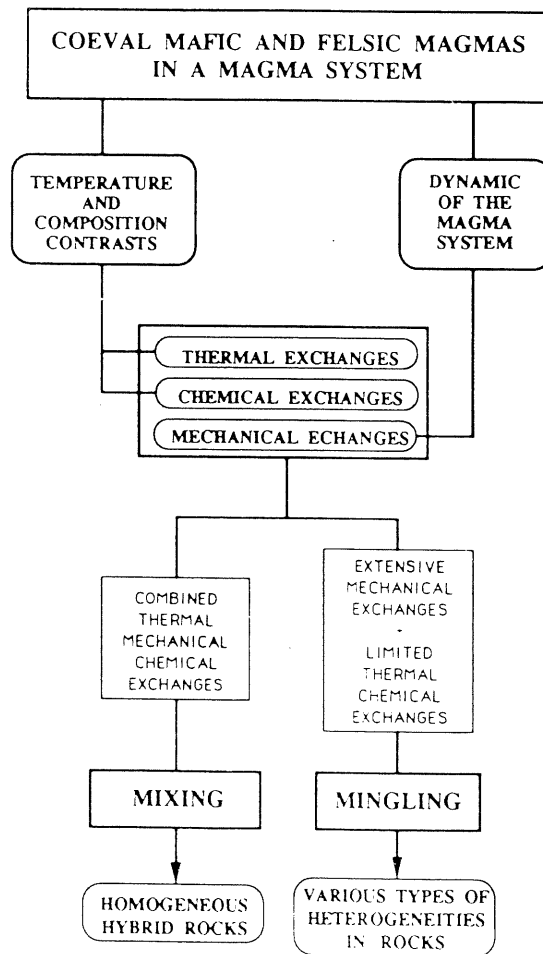


Figure 1.3. The different types of exchange occurring between two coexisting and contrasting magmas in a dynamic magma system, and their combination into mixing or mingling processes. Magma mingling occurs when the properties of the two units allow mechanical exchanges to occur between the two units, and when temperature and composition contrasts between the two units are small. Magma mixing occurs when temperature and composition contrasts are high, and mechanical, thermal, and chemical exchanges allow the two units to mix, forming hybrid rocks (after Barbarin and Didier 1992).

increases as the degree of crystallization of the magma increases; effective viscosity increases as the amount of suspended solids increases, and depends on the size, shape, and interaction of suspended solids (Arzi 1978, van der Molen and Paterson 1979).

As the effective viscosity of a melt increases, the melt gradually passes from a Newtonian substance to a Bingham substance, gaining a finite strength (Arzi 1978). A Newtonian substance behaves plastically under applied stress. A Bingham substance exhibits plastic deformation for stresses lower than its yield strength, and brittle deformation for stresses above the yield strength. The yield strength of a substance increases as the degree of crystallization of the substance increases.

Abbott (1989) stated that for monzogranites of the SMB, the Newtonian-Bingham boundary occurs at $C = 0.74$ ($C =$ the degree of crystallization of the melt). Equation 1.1 approximates the Newtonian-Bingham boundary using the effective viscosity (μ_{eff}) for a suspension of uniform spheres, here approximated by feldspar megacrysts, where C is the volume fraction of uniform rigid spheres in the melt, and μ_0 is the viscosity of the melt prior to crystallization.

$$\mu_{\text{eff}} = \mu_0 (1 - 1.35C)^{-2.5} \quad \text{Equation 1.1}$$

For C slightly less than 0.74, the melt behaves as a "crystal mush" (Abbott 1989). The resulting crystal mush will have variable viscosity and yield strength. Viscosity and yield strength of the crystal mush depend on the crystal size, crystal shape, and the degree of crystallization (Arzi 1978, van der Molen and Paterson 1979, Hibbard and Watters 1985, Abbott 1989). If the stress on the crystal mush exceeds the yield

strength, brittle deformation occurs. The degree of crystallization of the intruding material and intruded material determine the type of contact which forms (Fig. 1.2).

1.3 General Geology

The SMB is a peraluminous, composite batholith covering $\sim 7300 \text{ km}^2$ of southwestern Nova Scotia (Fig. 1.1). McKenzie and Clarke (1975) estimated the depth of intrusion of the SMB at between 4-10 km. The SMB intruded the Cambrian-Ordovician Meguma Group metasediments and conformably overlying Silurian and Lower Devonian metamorphic units (Fig. 1). Intrusion and uplift of the SMB are stratigraphically constrained by an Emsian age for the SMB host rocks, and Lower Carboniferous strata of Famennian age (Martel et al. 1993) that unconformably overlie the SMB. This short interval between intrusion of the SMB and deposition of strata suggests rapid uplift of the pluton.

Two major stages of intrusion occur in the SMB (Fig. 1.1b). Stage 1 intrusions consist primarily of biotite-bearing monzogranites and granodiorites, whereas Stage 2 plutons consist primarily of muscovite-bearing rocks. Horne et al. (1992) suggested that emplacement of Stage 2 plutons was partly controlled by NE- and NW-trending structures. The short interval between the emplacement of Stage 1 and 2 plutons suggests the possibility that the NE and NW structures formed in incompletely crystallized Stage 1 plutons.

1.4 Purpose and Scope

This thesis investigates the intrusive relationship between the New Ross Leucomonzogranite and Falls Lake Mafic Porphyry, which occur in the New Ross Pluton. Determination of the intrusion history and the relative ages of the two units requires an interpretation of field observations, thin section observations, and mineral compositions. The interpretation of field relations determines the relative ages of the two units, and the character of the contacts between the two units. Contact and age relations allow discussion of the methods of interaction of the New Ross Leucomonzogranite and Falls Lake Mafic Porphyry. Thin section observations provide a better understanding of the intrusive history when combined with field observations. The chemical compositions of feldspar megacrysts indicate the melt in which they formed. The origin of feldspar megacrysts in the Falls Lake Mafic Porphyry tests the results obtained from field observations and thin section observations. Determination of contact relations between the New Ross Leucomonzogranite and Falls Lake Mafic Porphyry establishes the intrusion history of these units and provides information on intrusive relations in the SMB. This thesis also provides criteria for identifying igneous/igneous contacts in general. The age and origin of the New Ross Leucomonzogranite and Falls Lake Mafic Porphyry are beyond the scope of this thesis.

1.5 Organization

Chapter 2 discusses field relations, which are used to determine the relative ages, and the character of contacts between the New Ross Leucomonzogranite and

Falls Lake Mafic Porphyry. Chapter 3 uses petrography to define the characteristics of the New Ross Leucomonzogranite and Falls Lake Mafic Porphyry at thin section scale. Determination of contact relations at thin section scale enhances field observations. Petrographic examinations of alkali feldspar megacrysts determine any similarities between megacrysts from the New Ross Leucomonzogranite and Falls Lake Mafic Porphyry. Chapter 4 examines results from mineral chemistry data from various phases. Mineral chemistry from alkali feldspar megacrysts from both units tests whether the feldspar megacrysts are of similar origin. The combination of mineral chemistry with observed contact relations further constrains the intrusive history of the two units. Chapter 5 reviews the data and discusses the possible models in terms of the interaction two igneous intrusions. Chapter 6 relates these results and addresses the model which best fits the observed contact relations.

CHAPTER 2: FIELD RELATIONS

2.1 Introduction

MacDonald et al. (1992) stated that 49 intrusive units, comprising 260 intrusive bodies, have been recognized in 13 plutons in the SMB. The definition of intrusive unit, intrusive body, and pluton is after MacDonald et al. (1992). Many intrusive units occur in a single pluton, giving most SMB plutons a composite nature. This chapter discusses the geology of the New Ross Pluton and describes the unusual contact relations that occur between the New Ross Leucomonzogranite and Falls Lake Mafic Porphyry.

2.2 Geology of the New Ross Pluton

The New Ross Pluton (Fig. 1.1) is a Stage 2 pluton that covers $\sim 870 \text{ km}^2$ (MacDonald et al. 1992). The pluton is roughly circular in shape, but is partially fault-bounded (MacDonald et al. 1992). The main lithologies of the New Ross Pluton are: coarse-grained leucomonzogranite, fine-grained leucomonzogranite, muscovite-biotite monzogranite, biotite granodiorite, and minor amounts of mafic porphyry (Fig. 1.1). Unusual contact relations that occur between the New Ross Leucomonzogranite (Fig. 1.1, stipple pattern) and Falls Lake Mafic Porphyry (not shown on map) outcrop near the eastern edge of the New Ross Pluton, and are the focus of this thesis. These units, especially the mafic porphyry, are poorly understood in terms of the intrusion history of the SMB.

2.3 Unit Descriptions

2.3.1 New Ross Leucomonzogranite

The term leucomonzogranite follows the definition of MacDonald et al. (1992), applying to monzogranitic rocks containing $\leq 6\%$ ferromagnesian minerals. The New Ross Leucomonzogranite is typically megacrystic with local equigranular areas, contains 4-6 % biotite, trace-2% muscovite, and local concentrations of alkali feldspar megacrysts (MacDonald et al. 1987) (Fig. 2.1). Megacrystic portions account for 30-40 % of the volume of this unit. Higher biotite percentages of 7-8 % occur near leucomonzogranite/granodiorite contacts (MacDonald et al. 1987).

2.3.2 Falls Lake Mafic Porphyry

The Falls Lake Mafic Porphyry has a high biotite content (10-18%; Ham and Horne 1986) and a porphyritic texture (Fig. 2.1). Porphyry is defined as a rock with a predominantly fine-grained groundmass and medium- to coarse grained-phenocrysts (MacDonald et al. 1992). The mafic porphyry contains phenocrysts of quartz, alkali feldspar, and plagioclase set in a fine-grained, biotite-rich matrix. Alkali feldspar megacrysts occur locally in the mafic porphyry, and are distinctly larger than alkali feldspar phenocrysts in the mafic porphyry. The mafic porphyry contains abundant biotite-rich xenoliths which vary in abundance at different outcrop (2-20% rock volume; Ham and Horne 1986).

Normative mineralogy for both the Falls Lake Mafic Porphyry and New Ross leucomonzogranite plot in the monzogranite field of a quartz-alkali feldspar-

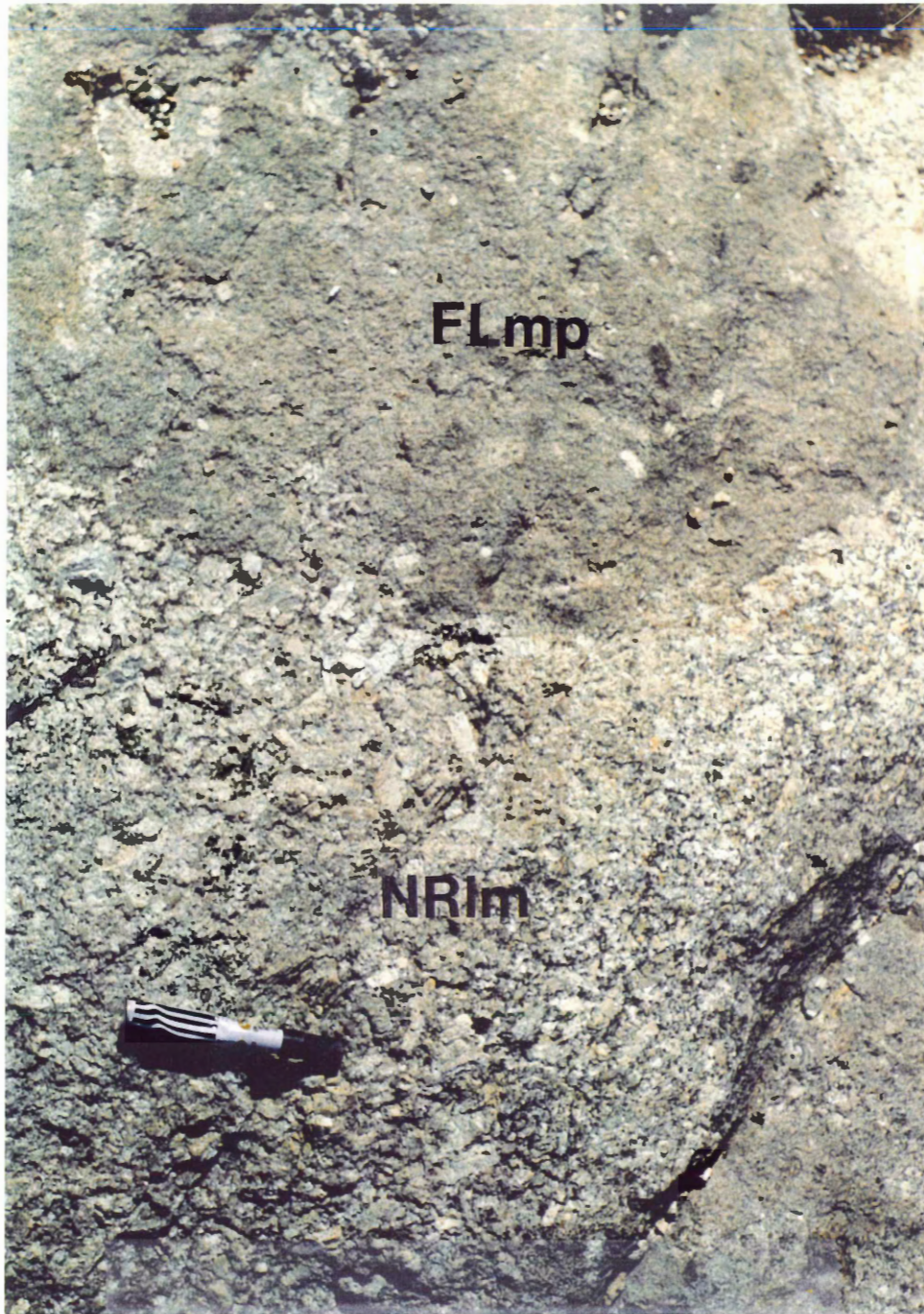


Figure 2.1. Photograph showing the nature of the New Ross Leucomonzogranite (NRIm) and Falls Lake Mafic Porphyry (FLmp) (marker (13 cm) for scale).

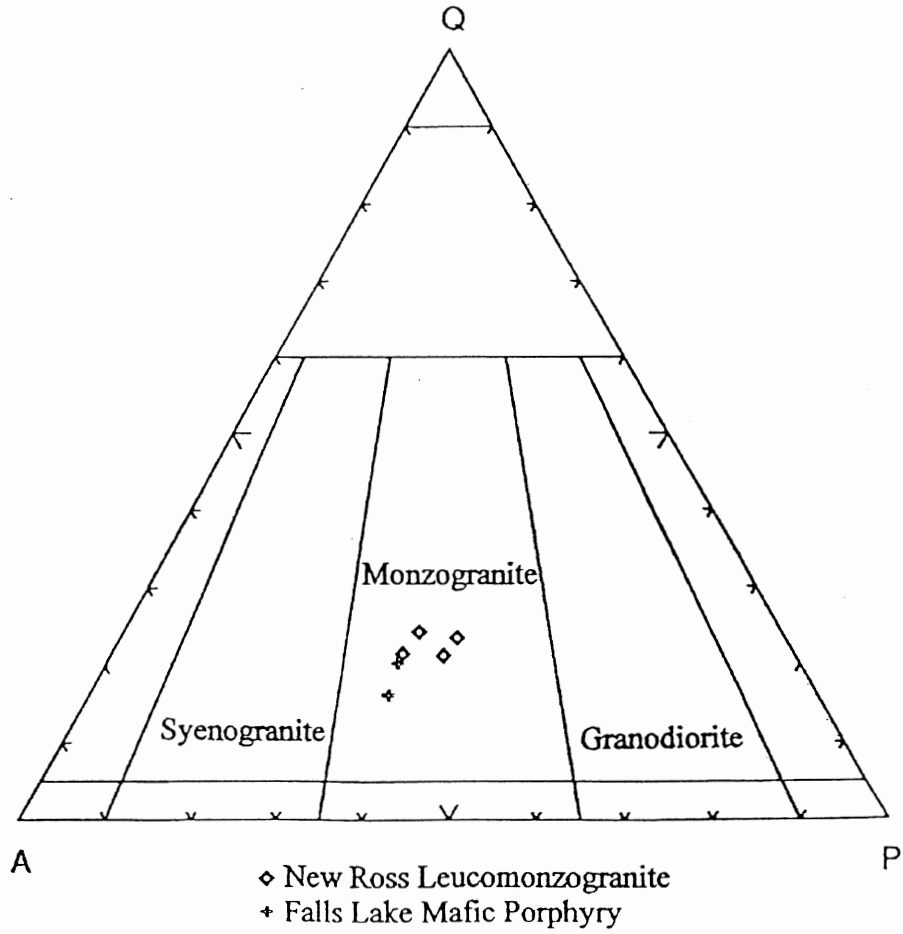


Figure 2.2. Quartz-alkali-plagioclase plot of normative mineralogy of the New Ross Leucomonzogranite and Falls Lake Mafic Porphyry. Normative mineralogy from Ham et al. (1989).

plagioclase plot (Fig. 2.2). Ham and Horne (1986) show the mafic porphyry associated with the Panuke Lake Leucomonzogranite. However, in the study area, the leucomonzogranite associated with the mafic porphyry more closely resembles the New Ross Leucomonzogranite (Horne 1993 pers comm). Unless otherwise stated, the term mafic porphyry refers to the Falls Lake Mafic Porphyry and the term leucomonzogranite refers to the New Ross Leucomonzogranite. The mafic porphyry is not well exposed, and where mafic porphyry is exposed it is associated with leucomonzogranite and occurs as several large areas (5-15 m²) within the leucomonzogranite rather than as one distinct intrusion (Fig. 2.3).

2.4 Mapping and Methodology

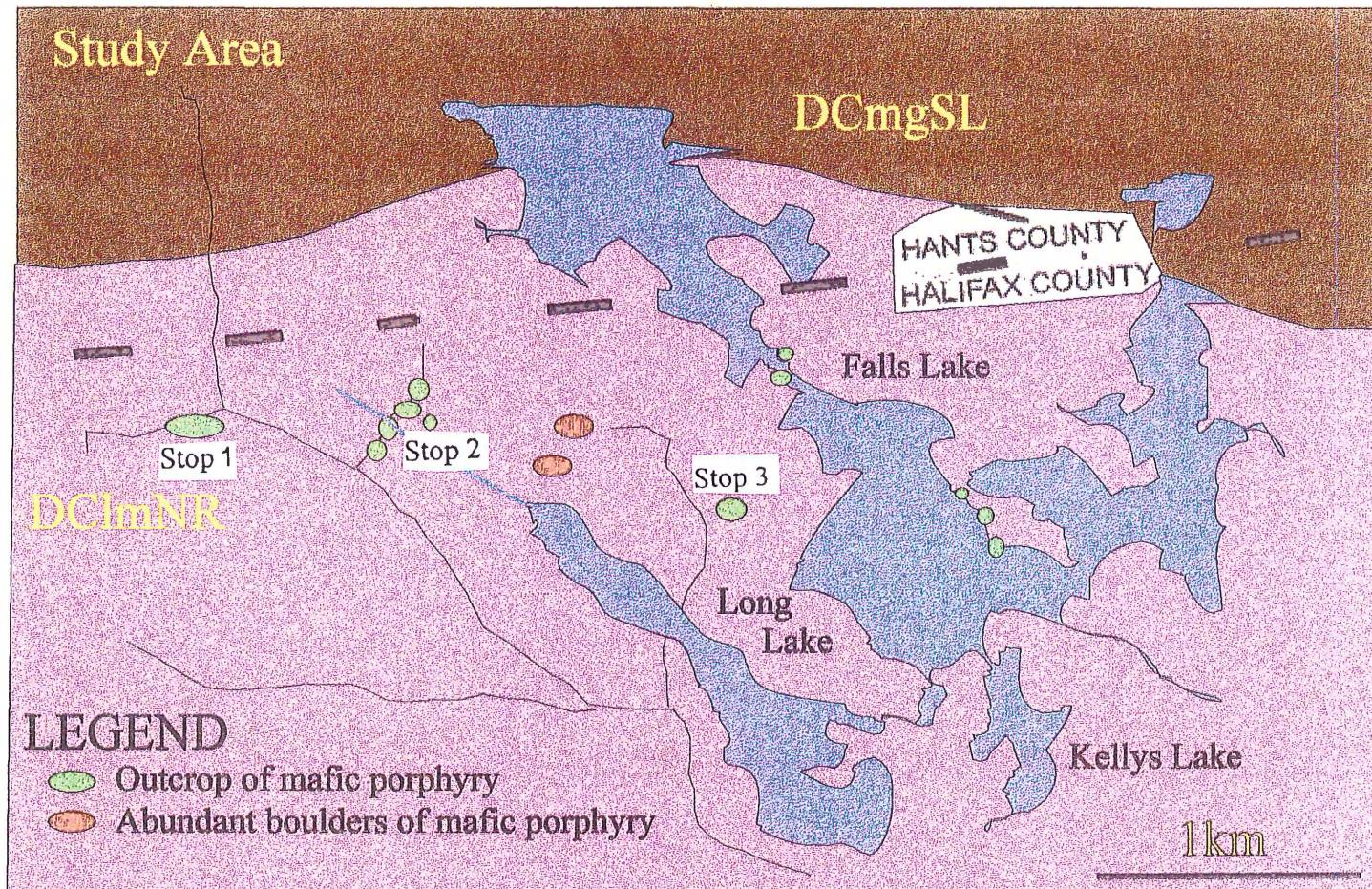
Ham and Horne (1987) most recently mapped the eastern portion of the New Ross Pluton, and defined the general distribution of the leucomonzogranite and mafic porphyry units. Mapping for this thesis was limited to outcrops displaying contacts between the leucomonzogranite and mafic porphyry units. Figure 2.3 shows a detailed map of the study area for this thesis. Samples of leucomonzogranite and mafic porphyry collected (Fig. 2.3) include: 1) New Ross Leucomonzogranite, 2) Falls Lake Mafic Porphyry, and 3) contact areas between these two units. Access to the study area for this thesis is provided by Bowater Mersey logging roads located on the north side of Highway 103, near the head of St. Margarets Bay (~ 10 km west of Exit 5).

2.5 Observed Contact Relations

A wide range of contact relations occurs between the leucomonzogranite and mafic porphyry where: 1) xenoliths of mafic porphyry occur in leucomonzogranite, 2) dykes of leucomonzogranite cut the mafic porphyry, and 3) the leucomonzogranite and mafic porphyry meet. Many exposures of the contact between these units occur in the study area and display unusual contact relations, as detailed below.

2.5.1 Xenoliths of mafic porphyry in leucomonzogranite

Xenoliths of mafic porphyry less than 30 cm in length (length:width ratio ~ 2:1) occur in leucomonzogranite dykes or near leucomonzogranite/mafic porphyry contacts. Xenoliths of mafic porphyry that occur in leucomonzogranite dykes tend to be oval in shape with pronounced tapered ends (Fig. 2.4), and the leucomonzogranite shows no chilled or altered margins. These xenoliths show alignment with alkali feldspar megacrysts in the leucomonzogranite dyke (Fig. 2.4 and Fig. 2.5). Feldspar megacrysts within the leucomonzogranite locally penetrate mafic porphyry xenoliths (Fig. 2.5), suggesting that mafic porphyry xenoliths behaved plastically in leucomonzogranite dykes. Figure 2.6 shows a xenolith of mafic porphyry in the leucomonzogranite that displays evidence of chilling and alteration. In this example, the host decreases in grain size, and increases in biotite content towards the xenolith (Fig. 2.6). No inclusions of the leucomonzogranite occur in the mafic porphyry unit, indicating that the leucomonzogranite postdates the mafic porphyry unit.



Samples Collected
Stop 1 - 1, 2, 3, 9, 10, 11, 12, 13, 14, 15
Stop 2 - 4, 5, 6, 7
Stop 3 - 8

Figure 2.3. Detailed map of the study area, showing patchy outcrop of mafic porphyry and locations of various sampling localities.

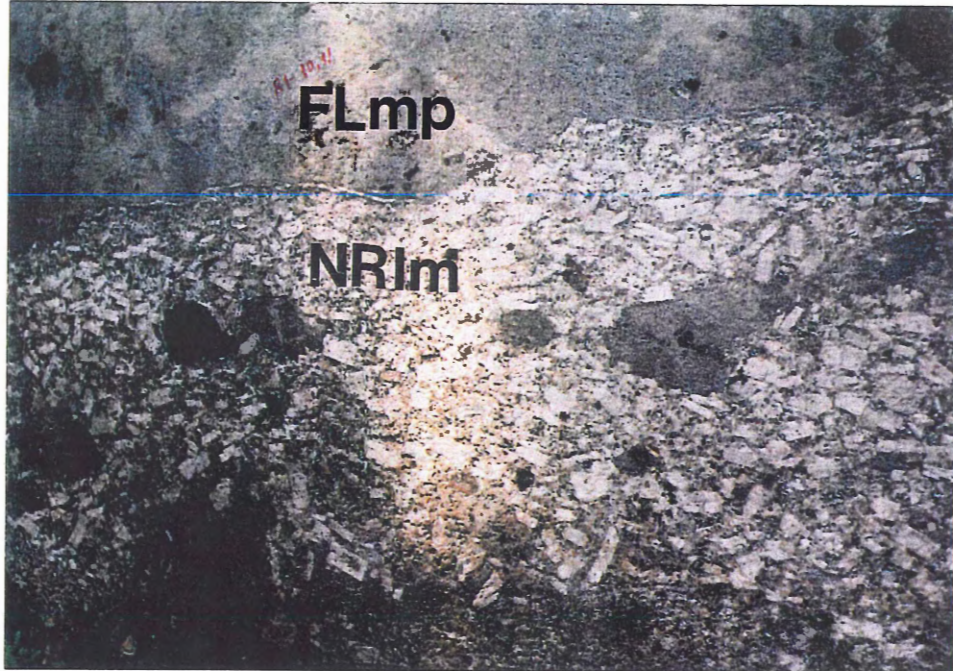


Figure 2.4. Photograph showing mafic porphyry xenoliths present in a leucomonzogranite dyke. Alkali feldspar megacrysts and mafic porphyry xenoliths align parallel to the dyke margins (numbers ~ 2 cm tall) (NRIm=New Ross Leucomonzogranite, FLmp=Falls Lake Mafic Porphyry).

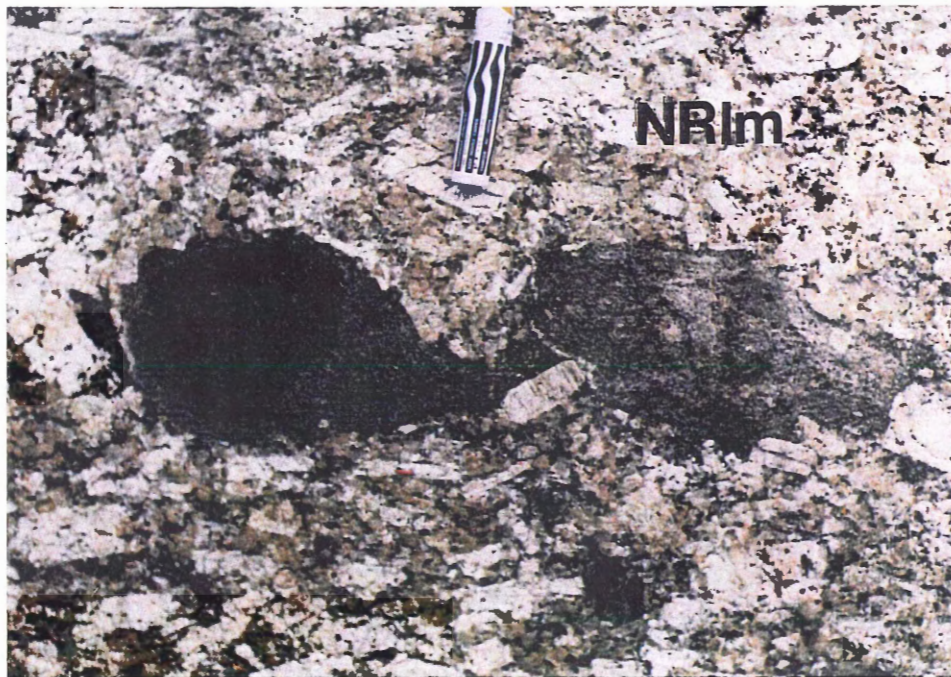


Figure 2.5. Enlarged section of Figure 2.4 showing the elongate, oval shape of mafic porphyry xenoliths. Mafic porphyry xenoliths align with alkali feldspar phenocrysts. Feldspar megacrysts from the leucomonzogranite protrude into the mafic porphyry xenoliths (marker (13cm) for scale).

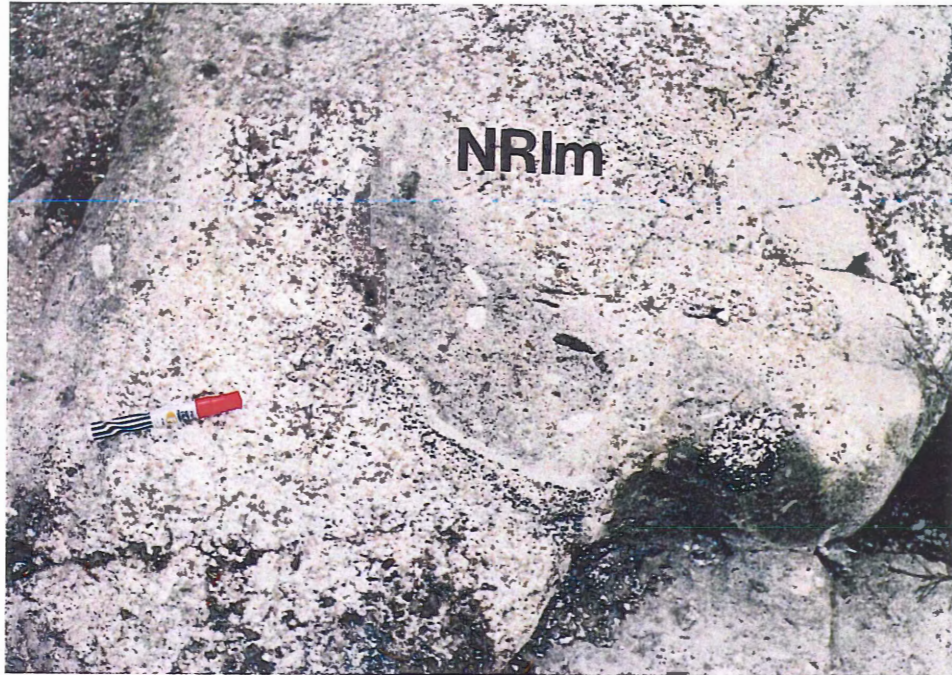


Figure 2.6. Photograph showing a mafic porphyry xenolith with chilled and altered margins. Grain size decreases and in places, biotite content increases in the leucomonzogranite toward the xenolith (marker (13cm) for scale).

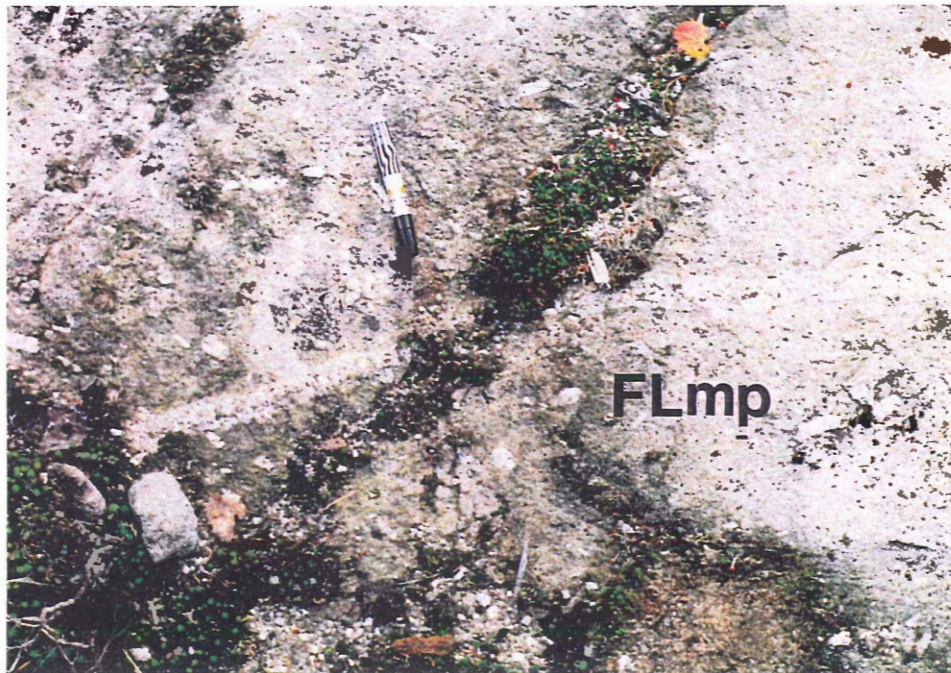


Figure 2.7. Photograph showing the megascopically sharp linear nature of leucomonzogranite contacts which occur where leucomonzogranite intrudes the mafic porphyry (marker (13cm) for scale) (NRIm=New Ross Leucomonzogranite, FLmp=Falls Lake Mafic Porphyry).

2.5.2 Dykes of leucomonzogranite in the mafic porphyry

Dykes of leucomonzogranite cutting the mafic porphyry fall into two groups, those with: a) megascopically sharp and relatively linear contacts, and b) diffuse and irregular contacts. Where dyke contacts are sharp (Figs. 2.7 and 2.8), leucomonzogranite dykes cross-cut the mafic porphyry; however, leucomonzogranite dykes do not truncate crystals in the mafic porphyry, and in some cases dykes are slightly curved (Fig. 2.8). Dykes showing relatively sharp contacts suggest that leucomonzogranite intruded mechanically solid ($C > 0.74$) mafic porphyry.

In other places where the leucomonzogranite intrudes the mafic porphyry, no definitive boundary between the leucomonzogranite and mafic porphyry occurs (Figs. 2.9-2.11). Commonly, leucomonzogranite dykes have irregular contacts. Where leucomonzogranite dyke contacts are irregular, large alkali feldspar megacrysts align with the dyke, and commonly straddle the contact (Fig. 2.10). Some leucomonzogranite dykes occur as concentrations of aligned, large (up to 5 cm) alkali feldspar megacrysts (Fig. 2.11). In Figure 2.11, feldspar megacrysts gradually decrease in concentration away from the centre of the intrusion. Some alkali feldspar megacrysts appear to be xenocrysts in the mafic porphyry (Fig. 2.11), and probably originated from the leucomonzogranite.

2.5.3 Nature of contacts between leucomonzogranite and mafic porphyry

Unusual contact relations also occur at the boundary between larger volumes of leucomonzogranite and mafic porphyry. In some areas contacts are megascopically sharp and linear (Fig. 2.12), and show no evidence of chilling or alteration of either

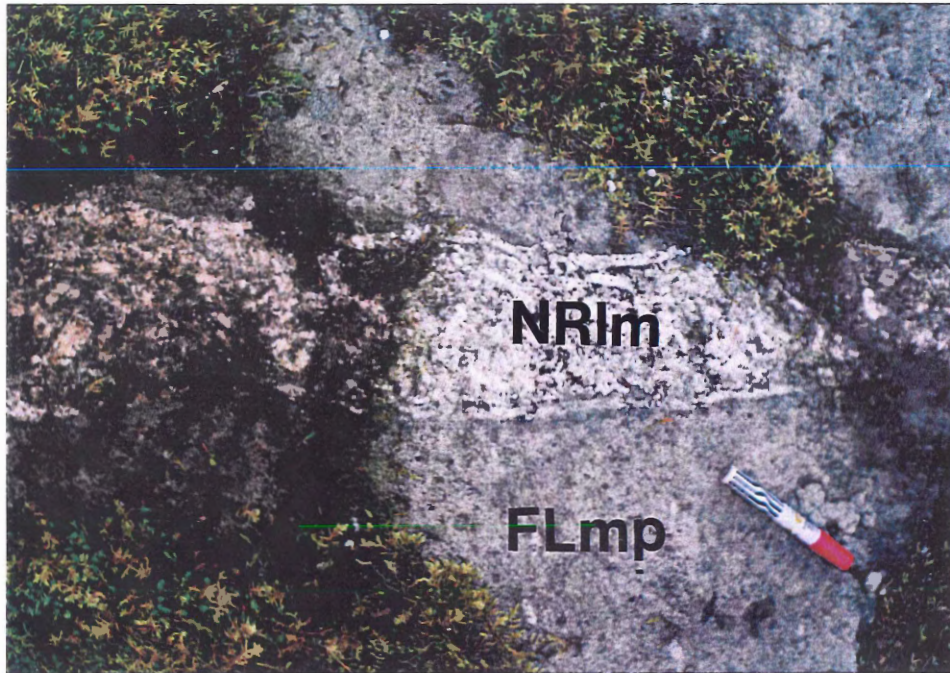


Figure 2.8. Photograph showing the megascopically sharp linear nature of leucomonzogranite dyke contacts, which show curvilinear contacts at smaller scale (marker (13cm) for scale) (NRIm=New Ross Leucomonzogranite, FLmp=Falls Lake Mafic Porphyry).

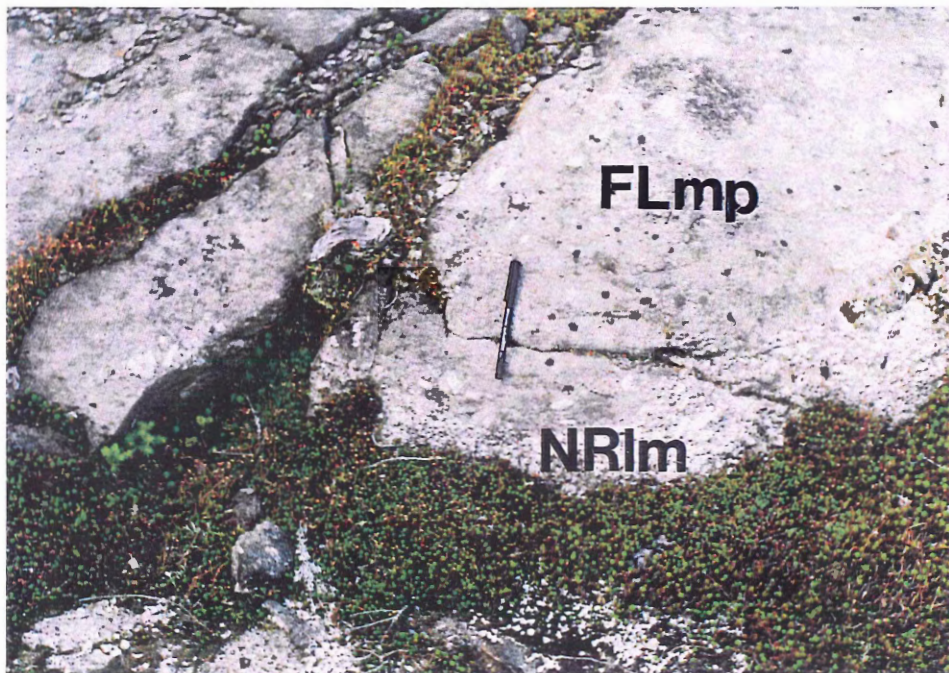


Figure 2.9. Photograph showing the irregular diffuse contact between leucomonzogranite (below) and the mafic porphyry (above). This small intrusion pinches out at the left edge of the photo (pen (15cm) for scale) (NRIm=New Ross Leucomonzogranite, FLmp=Falls Lake Mafic Porphyry).

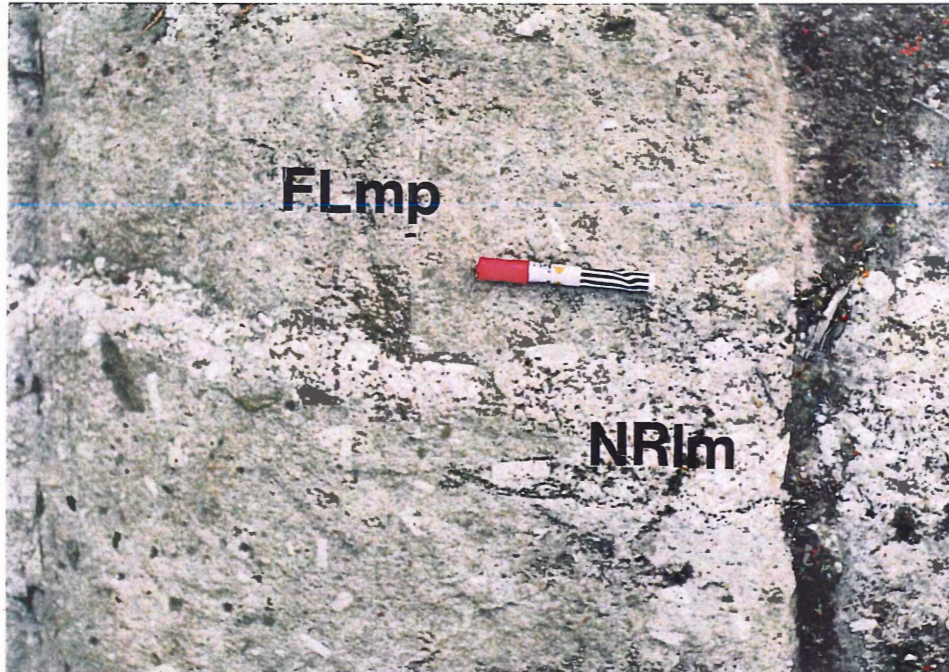


Figure 2.10. Photograph showing alkali feldspar megacrysts which align at the edge of the leucomonzogranite dyke, and cut across the contact (marker (13 cm) for scale) (NRlm=New Ross Leucomonzogranite, FLmp=Falls Lake Mafic Porphyry).

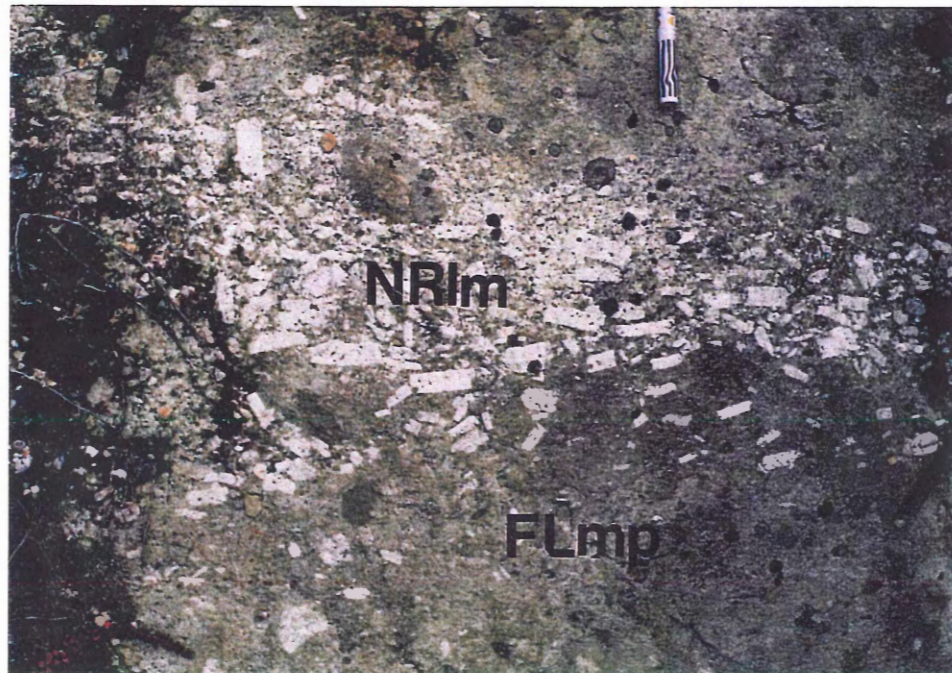


Figure 2.11. Photograph showing dyking of leucomonzogranite, which is marked by fine-grained leucomonzogranite which contains a mafic porphyry xenolith, and a concentration of alkali feldspar megacrysts in mafic porphyry. Away from the dyke, the concentration of feldspar megacrysts gradually decreases (marker (13cm) for scale) (NRlm=New Ross Leucomonzogranite, FLmp=Falls Lake Mafic Porphyry).



Figure 2.12. Photograph showing a megascopically sharp, linear contact between the leucomonzogranite and mafic porphyry units (marker (13cm) for scale) (NRlm=New Ross Leucomonzogranite, FLmp=Falls Lake Mafic Porphyry).

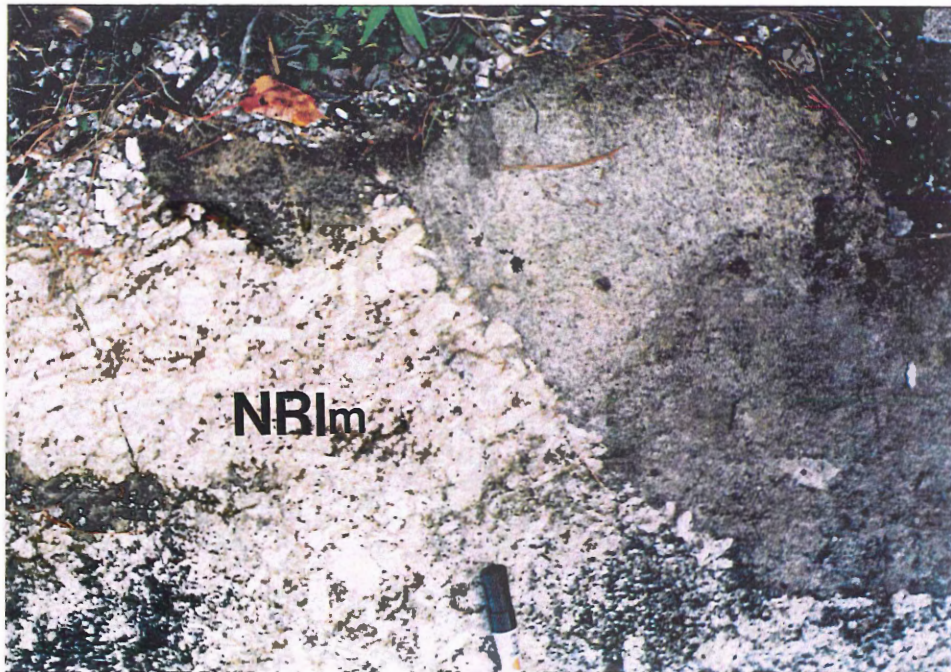


Figure 2.13. Photograph showing an irregular leucomonzogranite/mafic porphyry contact, where alkali feldspar megacrysts cut across the contact and protrude into the mafic porphyry (marker (13cm) for scale) (NRlm=New Ross Leucomonzogranite, FLmp=Falls Lake Mafic Porphyry).

unit. Some megascopically sharp linear contacts are diffuse at smaller scales, and some leucomonzogranite phenocrysts and megacrysts penetrate the mafic porphyry (Fig. 2.13). Some contacts are more diffuse and irregular, and commonly show lobate and cusped contacts (Fig. 2.14). Where contacts are irregular, alkali feldspar megacrysts commonly straddle the contact, and may occur as free-floating crystals in the mafic porphyry (Figs. 2.15 and 2.16).

Where the contact between the leucomonzogranite and mafic porphyry is crenulate and curved, the mafic porphyry usually occurs on the concave side of the contact, and the leucomonzogranite occurs on the convex side (Fig. 2.17). Between concave areas of mafic porphyry, the leucomonzogranite forms wispy, wedge-shaped projections between the two concave contacts (Fig. 2.18). Figure 2.19 (a sketch of Figure 2.18) shows several lobate and cusped contacts between the leucomonzogranite and mafic porphyry. Contacts are crenulate and lobate on several scales, and have a fractal nature (Fig. 2.19).

2.6 Discussion

Field observations (leucomonzogranite dykes, mafic porphyry xenoliths, and leucomonzogranite-mafic porphyry contacts) indicate that the leucomonzogranite postdates the mafic porphyry. Where leucomonzogranite dykes intrude the mafic porphyry, contacts can be sharp or diffuse. Contacts between the leucomonzogranite and mafic porphyry are representative of Type 2 contacts, and have diffuse, irregular and crenulate contacts. Alkali feldspar megacrysts are present in both units, and may have similar origins. To determine precisely the intrusive relationship between the

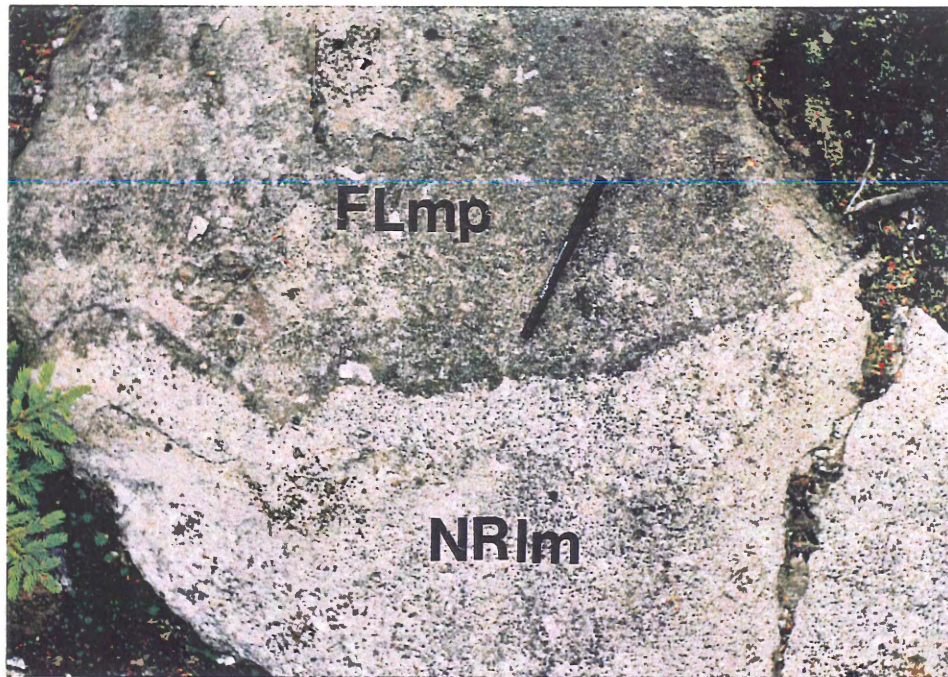


Figure 2.14. Photograph showing an irregular crenulate contact between the leucomonzogranite and mafic porphyry units. These contacts are usually curved, rather than linear (pen for scale) (NRIm=New Ross Leucomonzogranite, FLmp=Falls Lake Mafic Porphyry).

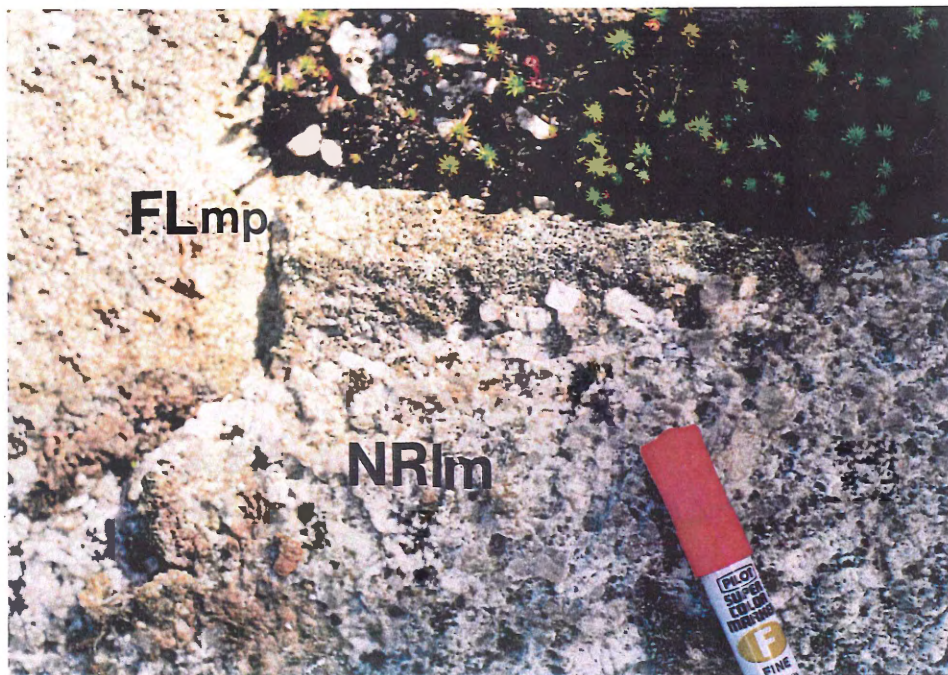


Figure 2.15. Photograph showing phenocrysts of alkali feldspar which cut across the leucomonzogranite/mafic porphyry contact. Some of these phenocrysts appear, at least in two dimensions, to occur free-floating in the mafic porphyry (marker (13cm) for scale) (NRIm=New Ross Leucomonzogranite, FLmp=Falls Lake Mafic Porphyry).

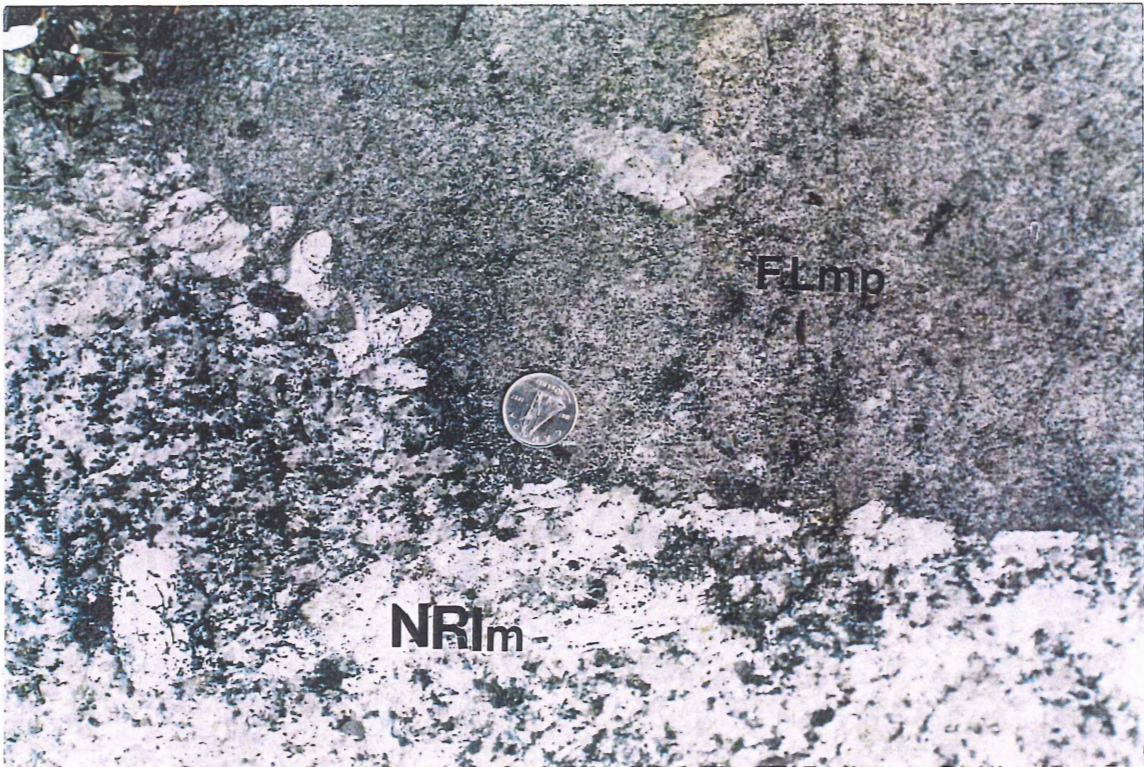


Figure 2.16. Photograph showing irregular contact where feldspar phenocrysts from the leucomonzogranite penetrate the mafic porphyry (dime for scale) (NRIm=New Ross Leucomonzogranite, FLmp=Falls Lake Mafic Porphyry).

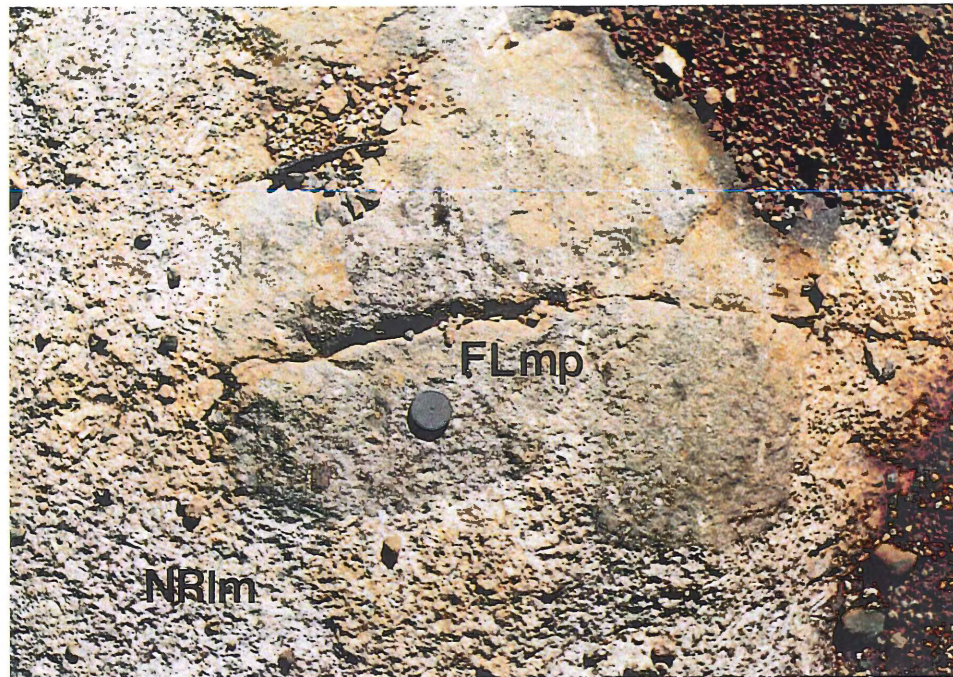


Figure 2.17. Photograph showing the arcuate shape and nature of leucomonzogranite/mafic porphyry contacts. The mafic porphyry occurs on the concave side of the arc, whereas the leucomonzogranite occurs on the convex side. The leucomonzogranite forms a wedge between the two arcuate contacts ("W" shaped) (film canister lid (~3cm) (NRlm=New Ross Leucomonzogranite, FLmp=Falls Lake Mafic Porphyry).

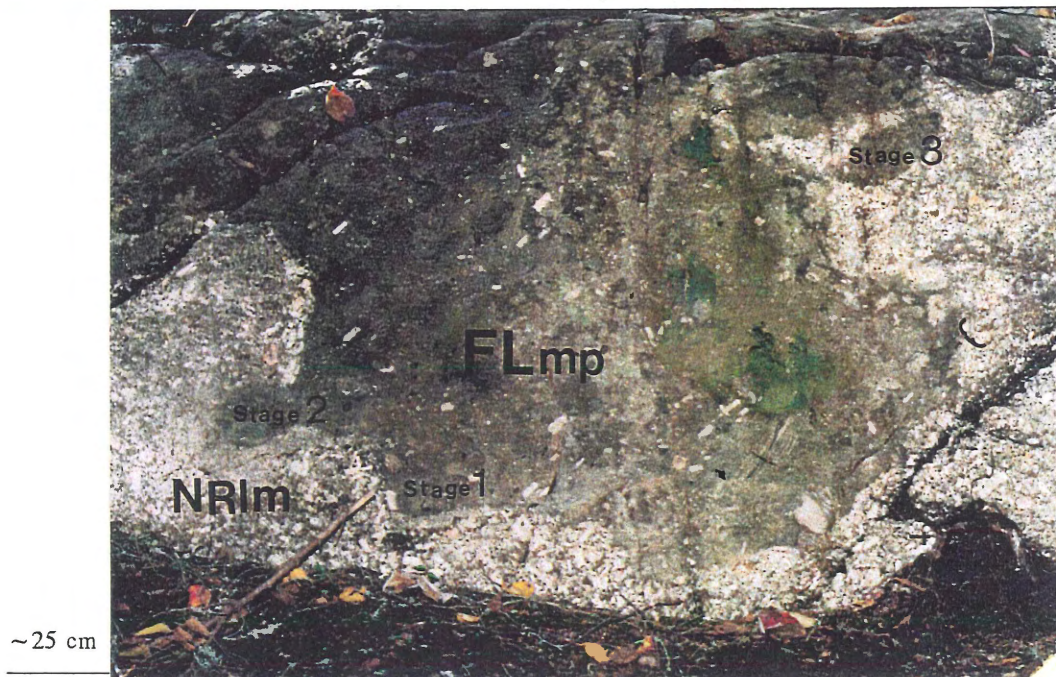


Figure 2.18. Photograph showing crenulate and cusperate contacts between leucomonzogranite and mafic porphyry. Contacts are crenulate at various scales, leading to fractal patterns (NRlm=New Ross Leucomonzogranite, FLmp=Falls Lake Mafic Porphyry). Stages 1, 2, and 3 are for later reference to Figure 5.2.

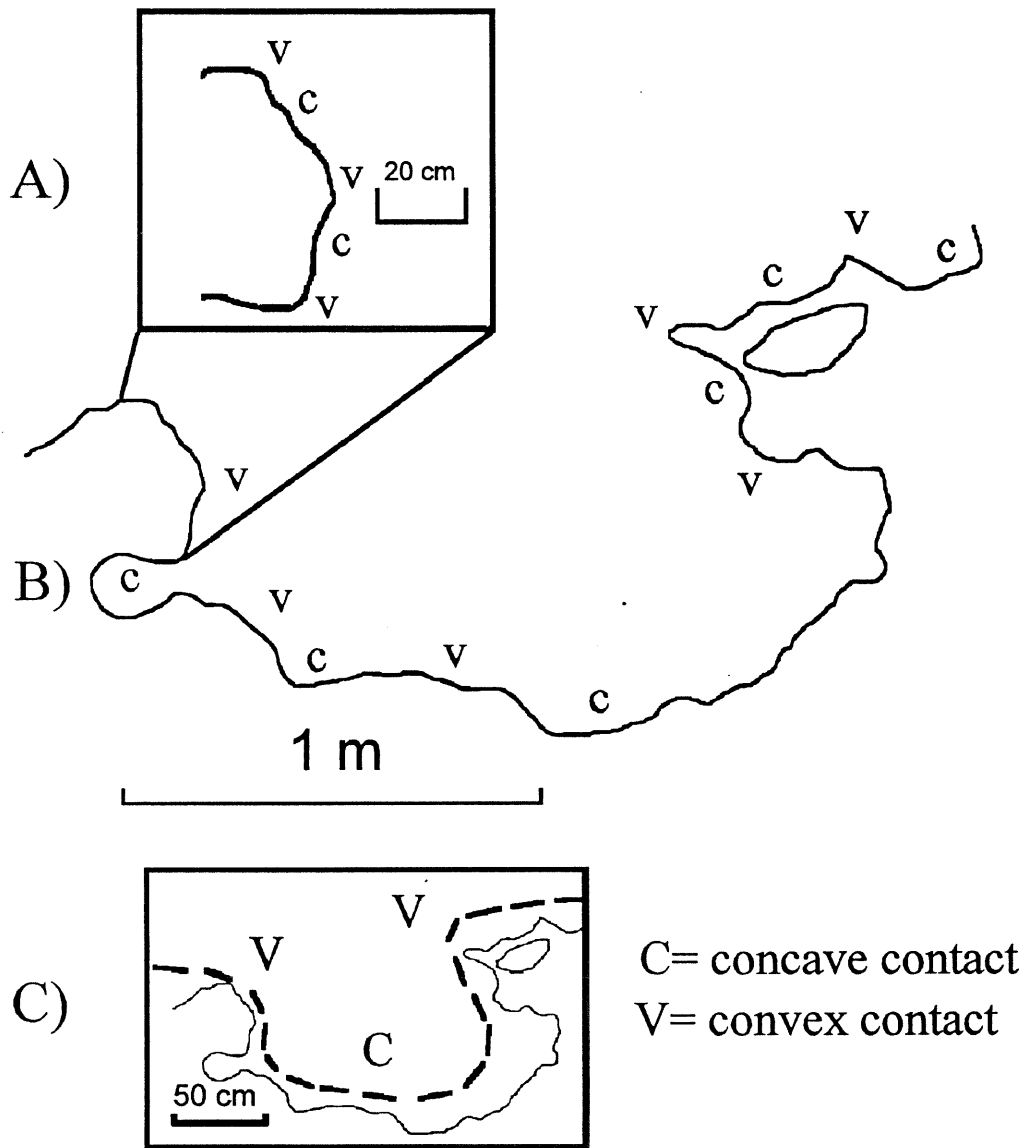


Figure 2.19. Sketch of Figure 2.18 showing contacts between leucomonzogranite and mafic porphyry at various scales. Contacts are crenulate in appearance at several scales, ranging from the centimetre to metre scale (NRlm=New Ross Leucomonzogranite, FLmp=Falls Lake Mafic Porphyry).

leucomonzogranite and mafic porphyry requires an examination of contacts in thin section (Chapter 3), and also requires using mineral chemistry (Chapter 4) to investigate the origins of alkali feldspar megacrysts in the mafic porphyry.

2.7 Conclusions

Cross-cutting dykes of leucomonzogranite, and xenoliths of mafic porphyry in leucomonzogranite suggest that the leucomonzogranite postdates the mafic porphyry. The lack of chilled or altered margins at mafic porphyry-leucomonzogranite contacts suggests no significant temperature difference existed between the leucomonzogranite and mafic porphyry when they came into contact. Magma mingling is suggested by: arcuate and crenulate contacts, feldspar megacrysts which straddle contacts, and phenocrysts from the leucomonzogranite in the mafic porphyry. Field observations suggest that both units were not completely crystallized, however, the precise degree of crystallization of the leucomonzogranite and mafic porphyry at the time of leucomonzogranite intrusion is unclear.

CHAPTER 3: PETROGRAPHY

3.1 Introduction

Characteristics of Type 1 (melt-solid) and Type 2 (melt-melt) contacts at the mesoscopic scale (field relations) are also applicable at the microscopic scale (thin section). Petrographic descriptions in this chapter characterize the leucomonzogranite and mafic porphyry in terms of mineralogy and texture, and clearly distinguish the leucomonzogranite from mafic porphyry. Comparisons of thin sections of contacts between the leucomonzogranite and mafic porphyry with thin sections of both units away from contacts will evaluate whether mingling and mixing of the two units occurs at contacts.

3.2 Petrographic Descriptions

3.2.1 New Ross Leucomonzogranite

The New Ross Leucomonzogranite is a medium- to coarse-grained megacrystic rock and has a hypidiomorphic granular-inequigranular groundmass texture. This unit contains nearly equal amounts of quartz (30%), alkali feldspar (35%), and plagioclase (25%), which together occupy about 90% of the rock volume (Appendix A) (all percentages for leucomonzogranite phases are from visual estimates of thin sections and hand samples).

Biotite commonly ranges between 4-6%, occurring as 2-5mm subhedral plates, and less commonly as small (< 1 mm) inclusions in other grains (Fig. 3.1).

Muscovite ranges between 1-2% and usually occurs as euhedral, 2-5mm plates that

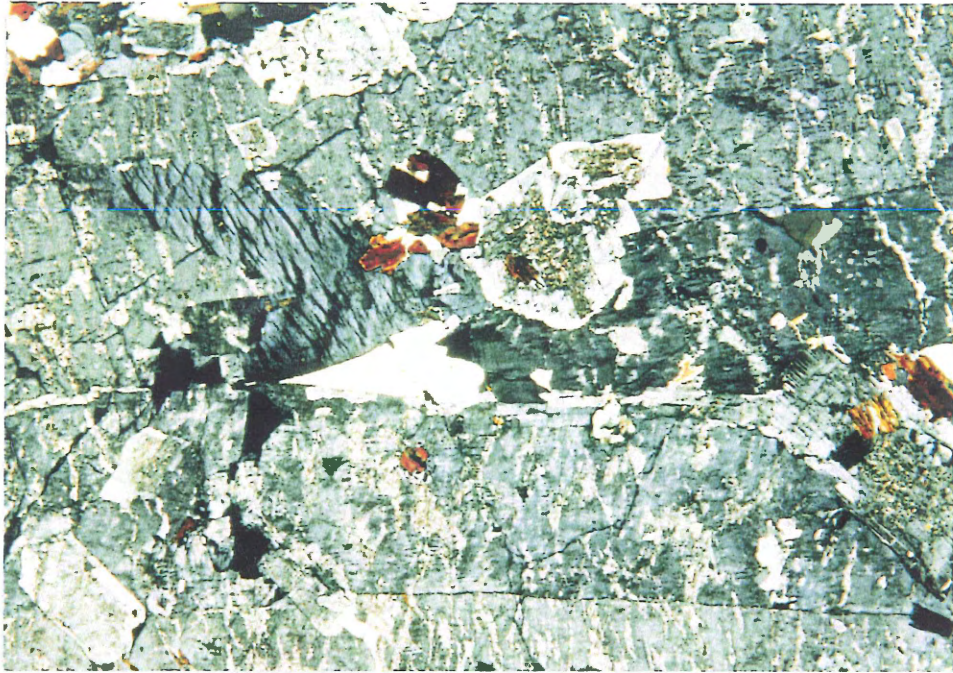


Figure 3.1. Photomicrograph showing small biotite plates occurring as inclusions in alkali feldspar (photo is 20mm x 26mm).

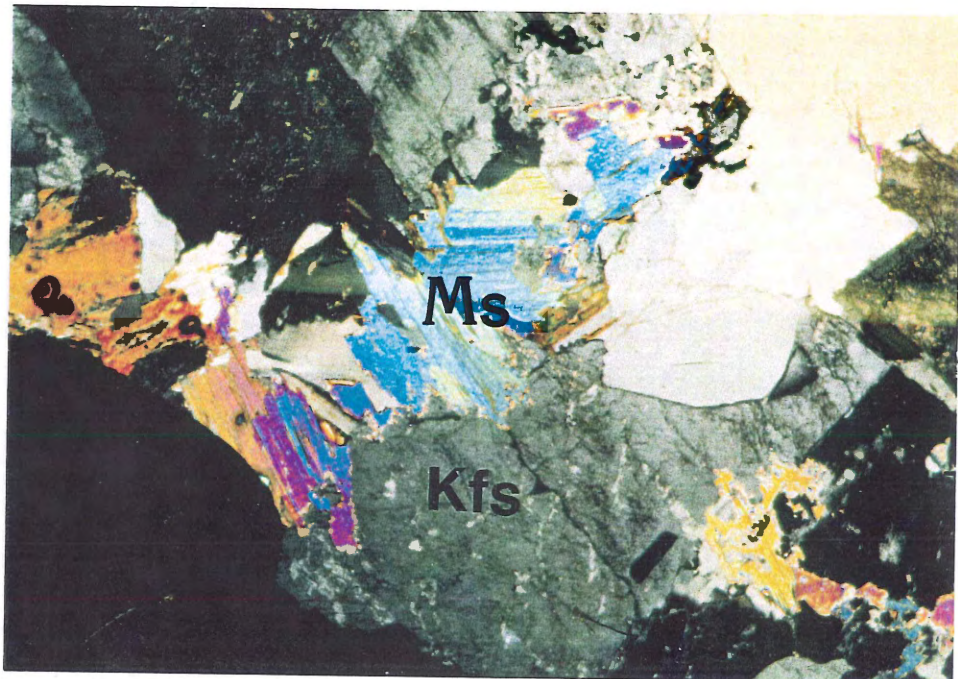


Figure 3.2. Photograph showing muscovite phases in the leucomonzogranite that occur as euhedral plates replacing alkali feldspar (Kfs) (Photo is 4mm x 6mm).

replace alkali feldspar (Fig. 3.2). Muscovite also replaces cordierite, which constitutes ~ 1% of the rock volume. Quartz occurs as inclusion-free, anhedral grains, usually less than 1 cm in length. Plagioclase occurs mainly as unzoned, subhedral-euhedral grains up to 1 cm in length, and commonly shows Carlsbad and albite twinning (Fig. 3.3). Plagioclase grains contain inclusions of biotite, and typically have sausseritized cores (Fig. 3.3). Alkali feldspar megacrysts occur as subhedral, twinned, inclusion-rich, elongate grains, showing perthitic exsolution (Fig. 3.4), reaching lengths of 3-4 cm.

3.2.2 Falls Lake Mafic Porphyry

The Falls Lake Mafic Porphyry groundmass contains quartz, alkali feldspar, plagioclase, biotite, and muscovite. Quartz, alkali feldspar, and plagioclase occur in nearly equal abundances and sizes (up to 3mm), each occupying approximately 25% (visual estimates from thin section) of rock volume (Appendix A). The mafic porphyry groundmass has an inequigranular texture, and in some areas a micrographic texture between alkali feldspar and quartz is common (Fig. 3.5). The mafic porphyry contains larger 5-10 mm phenocrysts of quartz, alkali feldspar, and plagioclase, which constitute ~ 5% of the total rock volume and give the unit its porphyritic texture.

The mafic porphyry groundmass contains between 10-20% biotite and 1-2% muscovite, both phases occurring as individual, small (~ 0.5 mm) plates (Fig. 3.6), and occasionally together in 2-4 mm clusters of small plates (Fig. 3.6). Quartz occurs as inclusion-free, anhedral grains, up to 5 mm in length. Plagioclase occurs

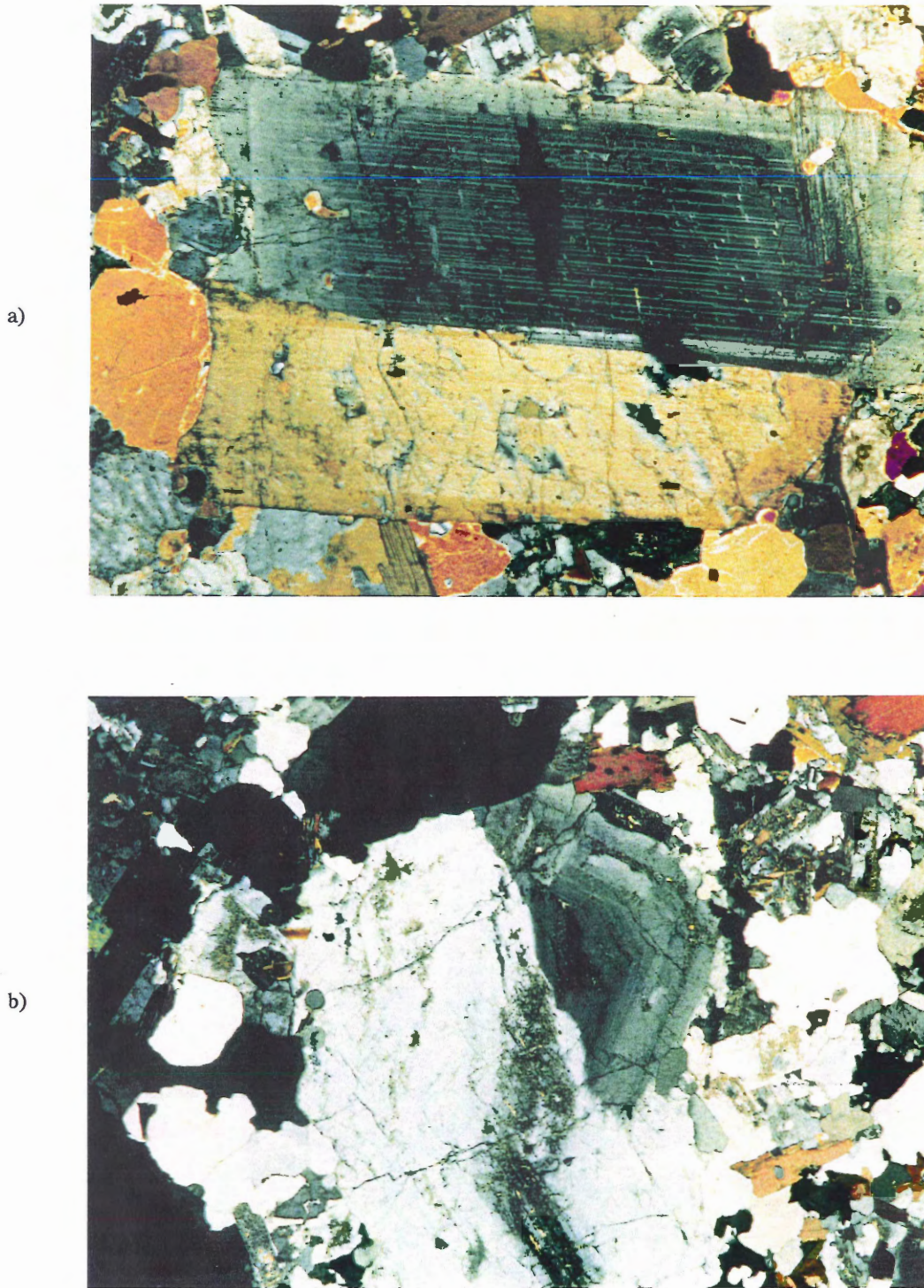


Figure 3.3. a) Photograph of plagioclase in the leucomonzogranite showing Carlsbad twinning and albite twinning (photo is 6mm x 8mm). b) Photograph of plagioclase with a sausseritized core (photo is 4mm x 6mm). Both of these types of twinning are present in plagioclase grains in the leucomonzogranite groundmass, and many of these grains have sausseritized cores.



Figure 3.4. Photograph showing alkali feldspar megacrysts from the leucomonzogranite. Alkali feldspar megacrysts contain inclusions of plagioclase, quartz, and biotite and show rod and film perthitic exsolution (photo is 20mm x 26mm)

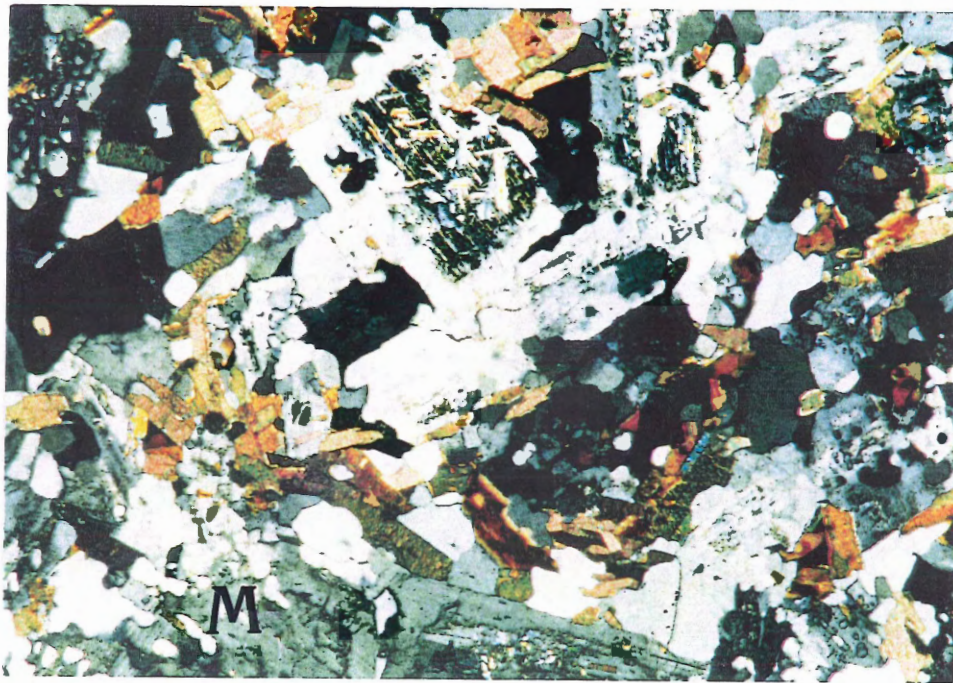


Figure 3.5. Photograph showing an inequigranular texture present in the mafic porphyry groundmass, and also the local occurrence of a micrographic texture (M) between quartz and alkali feldspar (photo is 1mm x 2mm).

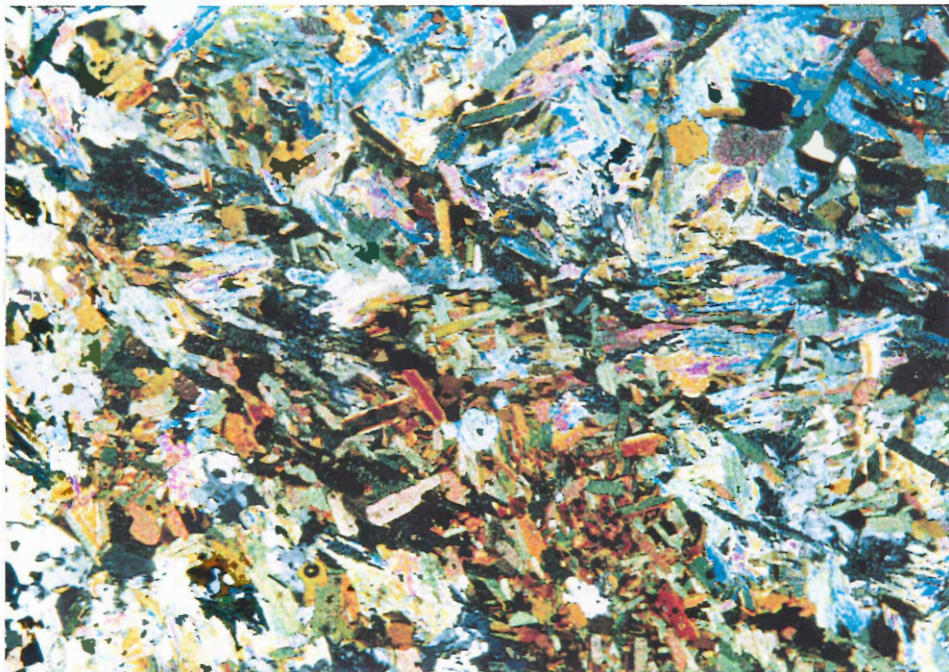


Figure 3.6. Photograph of a cluster of biotite (brown) and muscovite (blue) in the mafic porphyry. These clusters reach lengths up to 8 mm, and may represent the remnants of assimilated country rocks (photo is 4mm x 6mm).

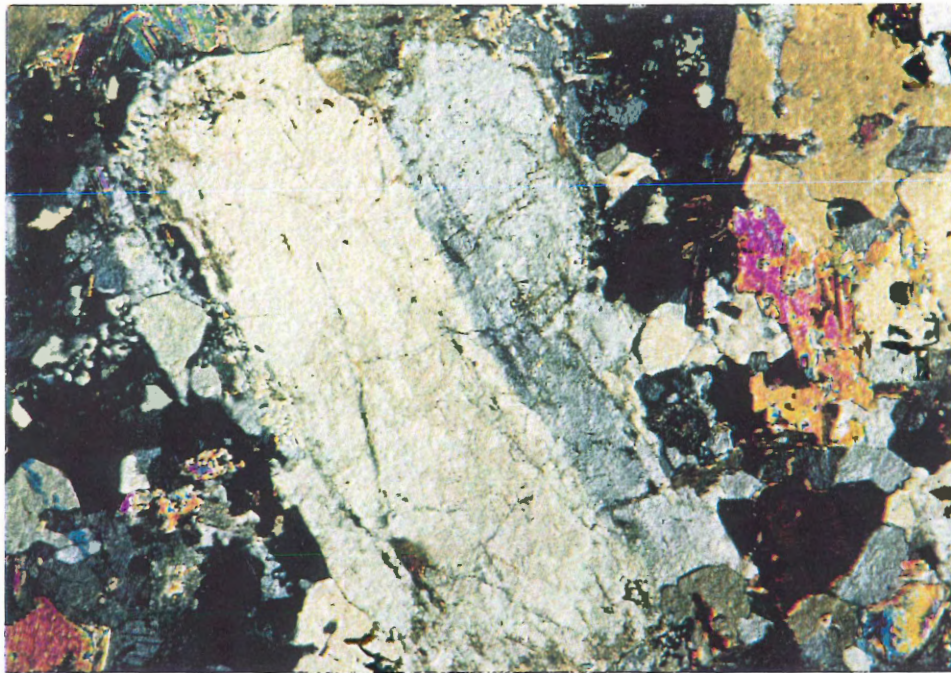
as small, ≤ 5 mm grains with sausseritized cores, and inclusions of small biotite. Plagioclase grains are typically unzoned, and commonly show Carlsbad and albite twinning (Fig. 3.7). Alkali feldspar occurs as untwinned, inclusion-free, sub-rounded grains, usually less than 5 mm in length (Fig. 3.8). Alkali feldspar megacrysts occur locally in the mafic porphyry and are typically larger (4-5 cm) than similar alkali feldspars in the leucomonzogranite (Fig. 3.9).

3.2.3 Contact Descriptions

Contacts between leucomonzogranite and mafic porphyry at thin section scale are diffuse and irregular. Large grains of alkali feldspar, quartz, and plagioclase similar to phases in the leucomonzogranite, and clusters of these grains present in the mafic porphyry near contacts, are anomalous compared to other mafic porphyry phases (Fig 3.10). In thin section, small pockets of mafic porphyry isolated in the leucomonzogranite near contacts and *vice versa*, indicate that mingling between the leucomonzogranite and mafic porphyry occurred near contacts (Figs. 3.10 and 3.11).

Crystals of alkali feldspar, quartz, and plagioclase isolated in the mafic porphyry are commonly sub-rounded, however some are subhedral-euhedral (Fig. 3.10). Some larger grains of alkali feldspar and plagioclase isolated in the mafic porphyry have growths of small quartz grains that outline the large feldspar grains (Figs. 3.9 and 3.12). These small quartz growths appear as concentric rings near the larger feldspar grain margins.

a)



b)



Figure 3.7. Photograph showing plagioclase grains that occur in the mafic porphyry groundmass. Plagioclase grains commonly display a) Carlsbad and b) albite twinning (photos are 4mm x 6mm).

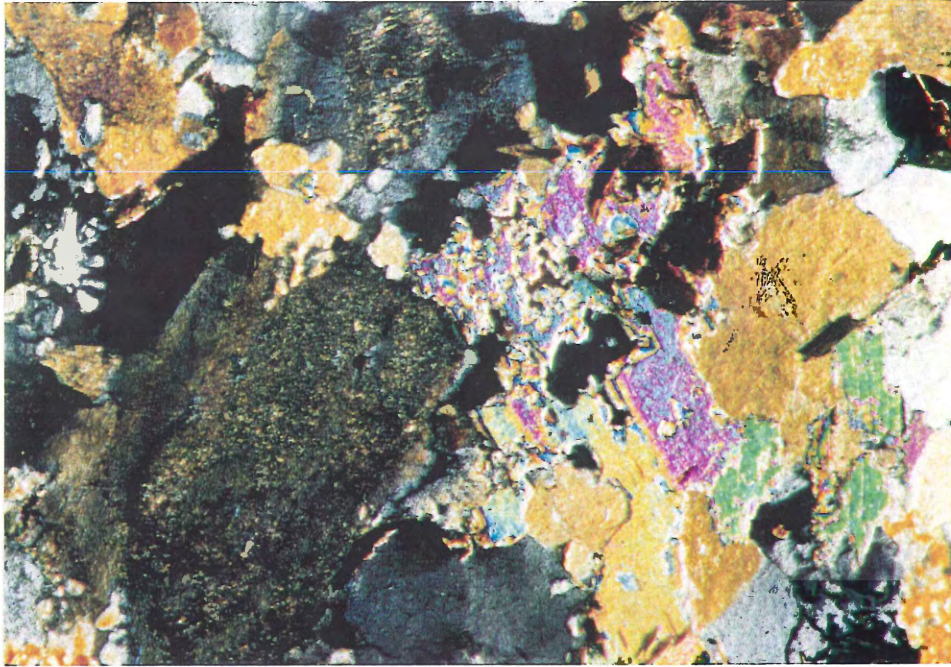


Figure 3.8. Photograph of alkali feldspar phases (Kfs) from the mafic porphyry. Alkali feldspar phases (Kfs) occur as small, rounded, untwinned, inclusion-free phenocrysts (photo is 1mm x 2mm).

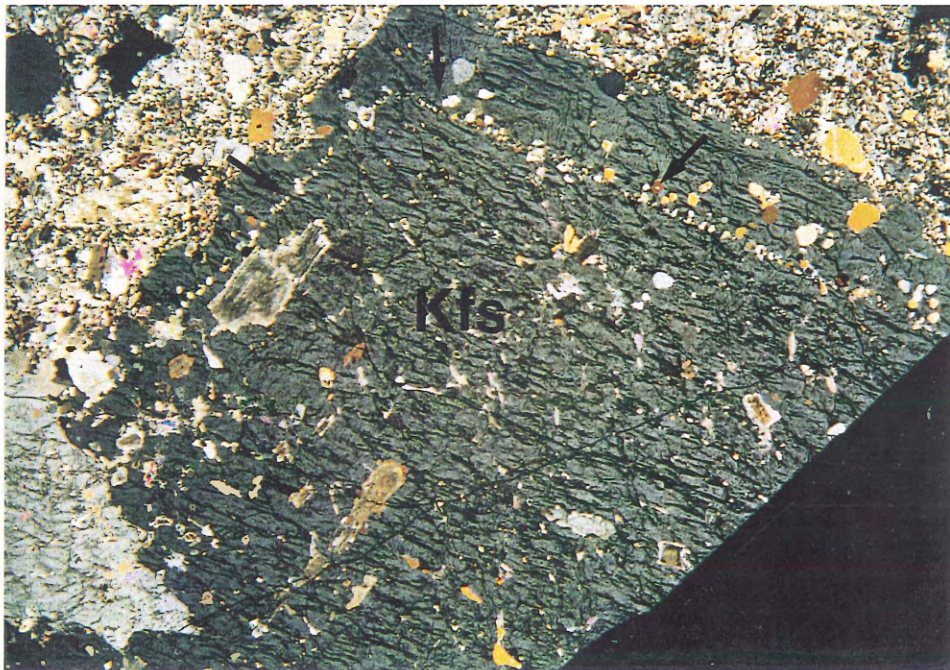


Figure 3.9. Photograph of alkali feldspar megacrysts (Kfs) present in the mafic porphyry. Alkali feldspar megacrysts are similar to alkali feldspar megacrysts present in the leucomonzogranite. Note the concentric ring of small quartz grains near the margin of the alkali feldspar grain (indicated by arrows) (photo is 20mm x 26mm).

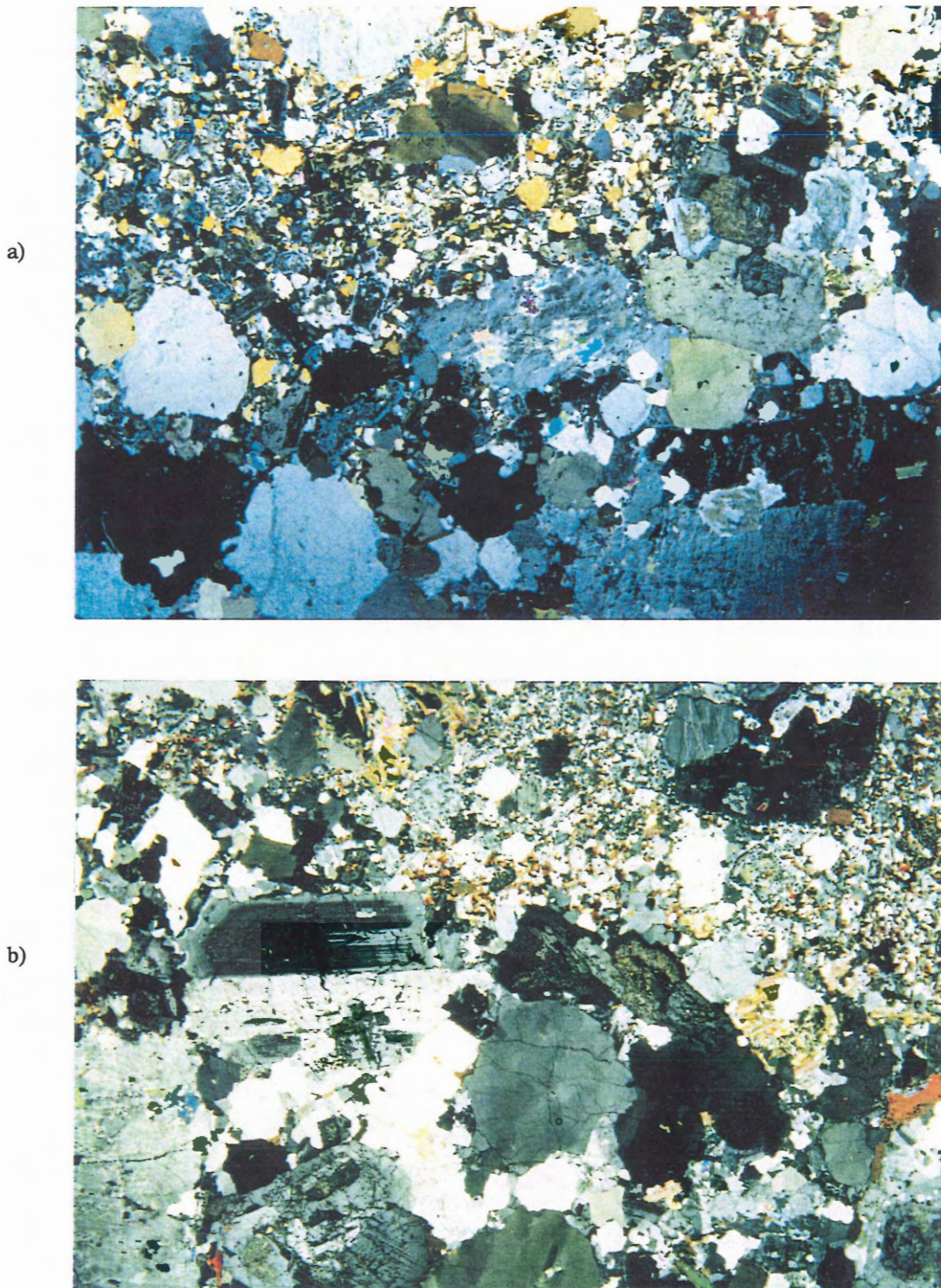


Figure 3.10. a) Photograph showing the irregular nature of leucomonzogranite/mafic porphyry contacts. Large grains isolated in Falls Lake Mafic Porphyry are similar to phases present in the leucomonzogranite (photo is 12mm x 18mm). b) Photograph showing an irregular contact where a cluster of grains from the leucomonzogranite (top right) occurs isolated in the Falls Lake Mafic Porphyry (photo is 20mm x 26mm).

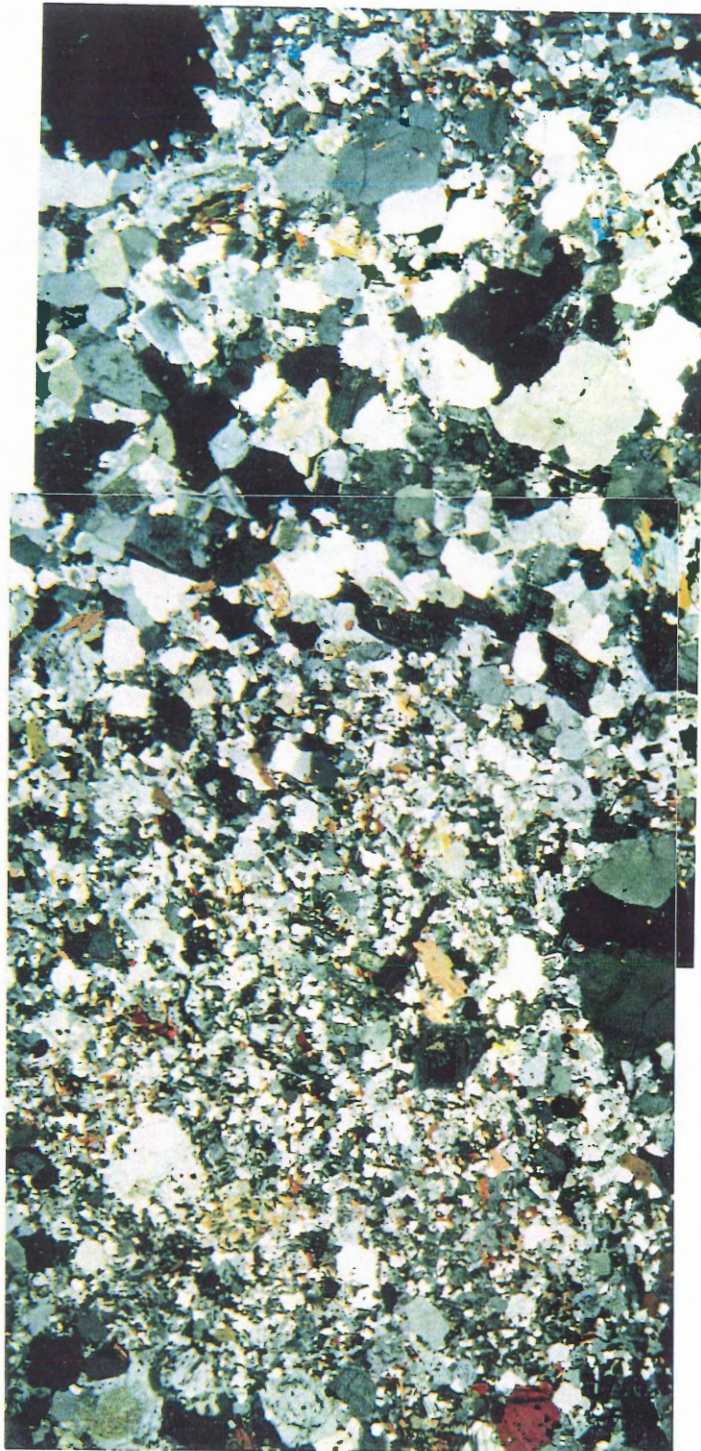


Figure 3.11. Photograph showing mingling between Falls Lake Mafic Porphyry (top and bottom) and New Ross Leucomonzogranite (middle). Mingling causes pockets of one unit to be isolated in the other, giving the units a banded nature at contacts (photo is 20mm x 26mm).

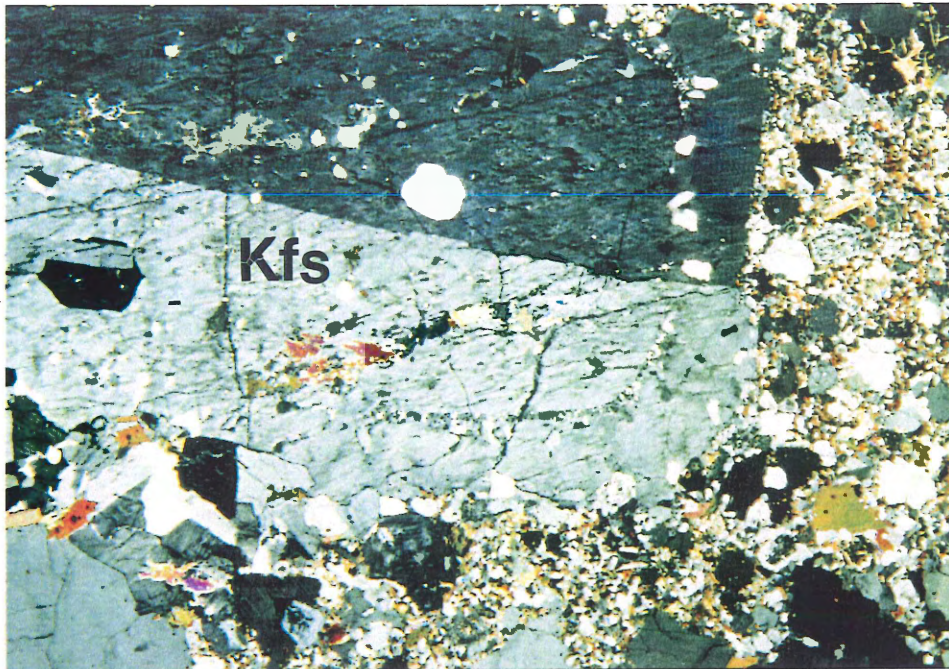


Figure 3.12. Photograph showing concentric zone of quartz grains included in an alkali feldspar xenocryst in the Falls Lake Mafic Porphyry (photo is 12mm x 18mm).

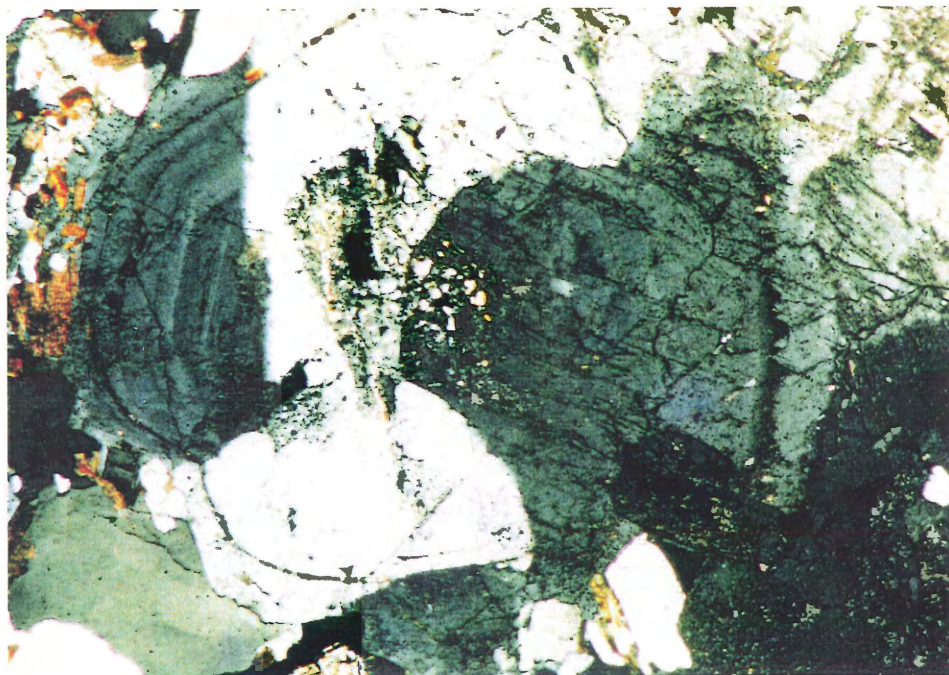


Figure 3.13. Photograph showing zoned plagioclase grains in the Falls Lake Mafic Porphyry near contacts. Zoned plagioclase grains are more common in both units near contacts (photo is 20mm x 26mm)

Some plagioclase grains in the mafic porphyry near contacts show continuous zoning (Fig. 3.13), and some have distinct rims of uniform composition (Fig. 3.14). Plagioclase rims showing different extinction may have different compositions than plagioclase cores, and often contain inclusions of quartz and biotite. In some cases plagioclase grains are mantled by alkali feldspar (anti-rapakivi texture) (Fig. 3.14b). Corroded plagioclase grains are uncommon, but they may occur in the mafic porphyry near contacts (Fig. 3.15). A thin section taken from the dyke-like intrusion (Figure 2.11) shows the alignment of biotite grains with the intrusion contact. Biotite grains near the intrusion contact wrap around larger grains (Fig. 3.16), suggesting that the mafic porphyry was capable of plastic flow when the leucomonzogranite intruded.

3.3 Discussion

Many of the criteria for distinguishing between Type 1 and Type 2 contacts at the field scale are also valid at thin section scale. Type 1 contacts at thin section scale are sharp, and show truncated grains at contacts. Type 2 contacts at thin section scale are irregular, and may show evidence of magma mingling and mixing that are not apparent in the field.

Mingling and mixing of two incompletely crystallized units may result in xenocrysts, which may be present in one or both units; the presence of xenocrysts in either unit suggest that one of these units was partially crystallized, and contained phenocrysts (Barbarin 1988). If two incompletely crystallized magmas mix

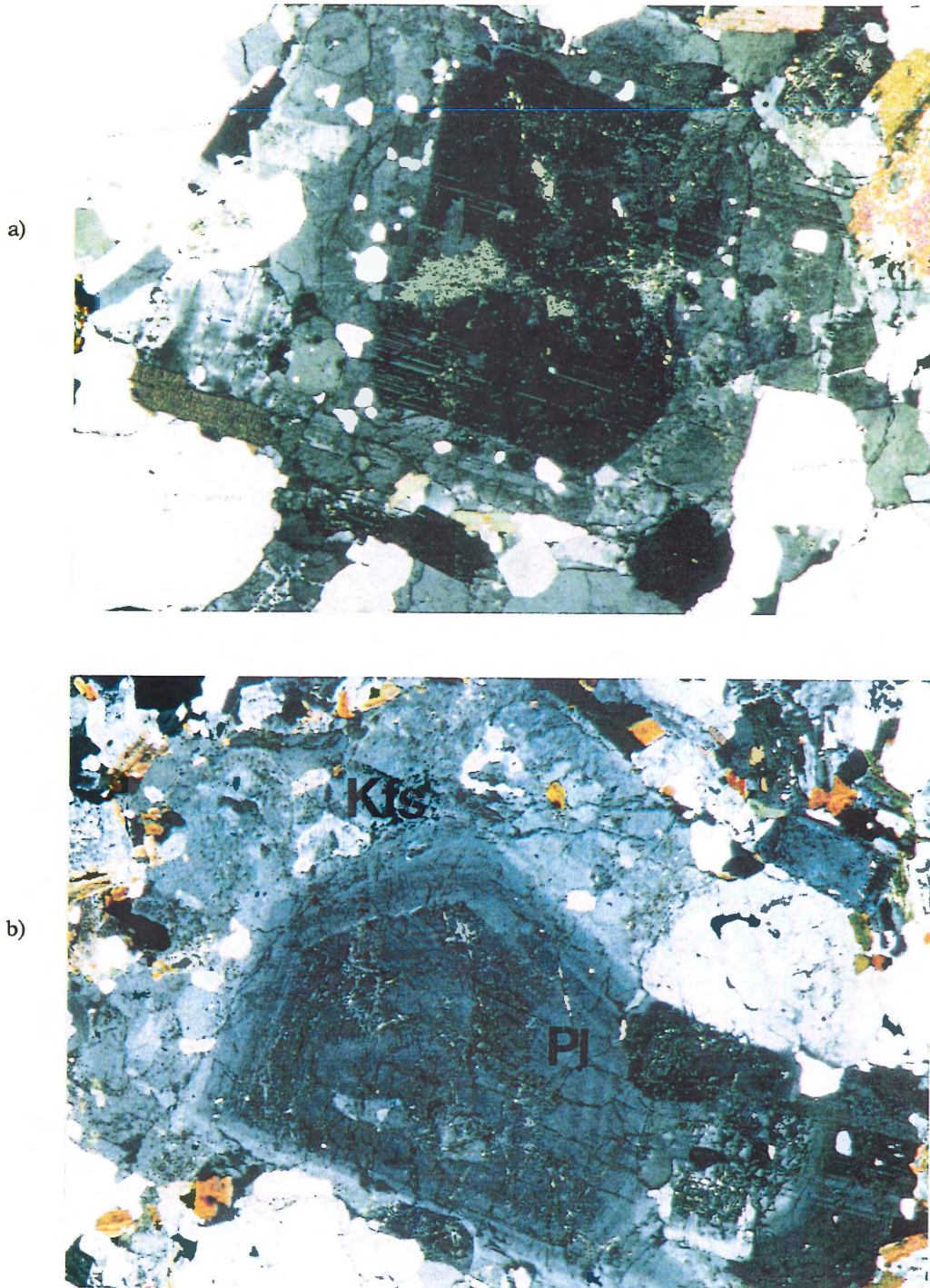


Figure 3.14. a) Plagioclase grain with an unzonated core mantled by an inclusion-rich rim of different composition (photo is 12mm x 18mm). b) Photograph showing plagioclase (Pl) with a rim of alkali feldspar (Kfs) (photo is 12mm x 18mm).

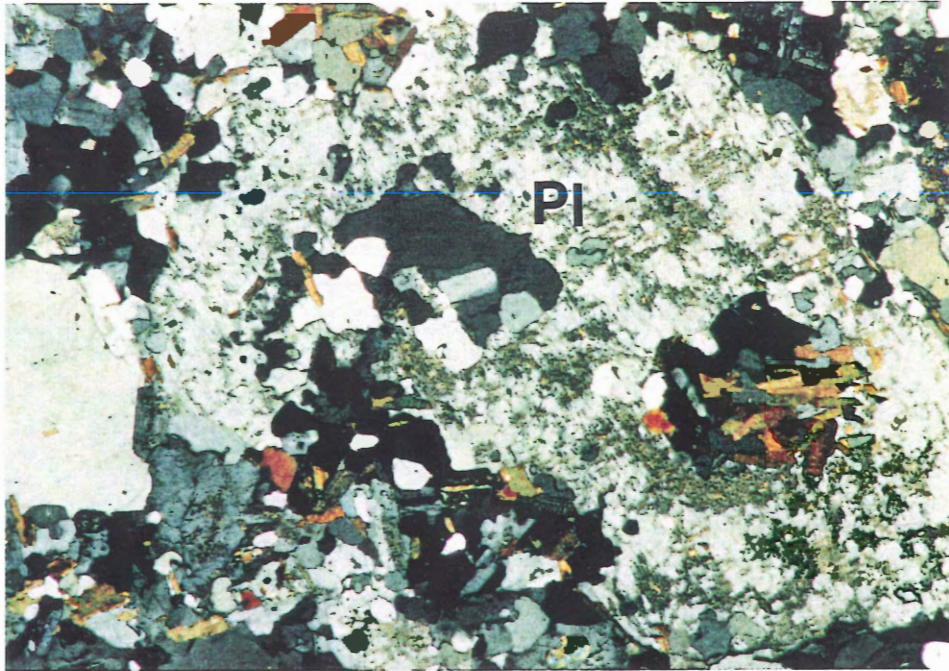


Figure 3.15. Photograph showing corroded plagioclase grain (Pl) in Falls Lake Mafic Porphyry (photo is 20mm x 26mm).

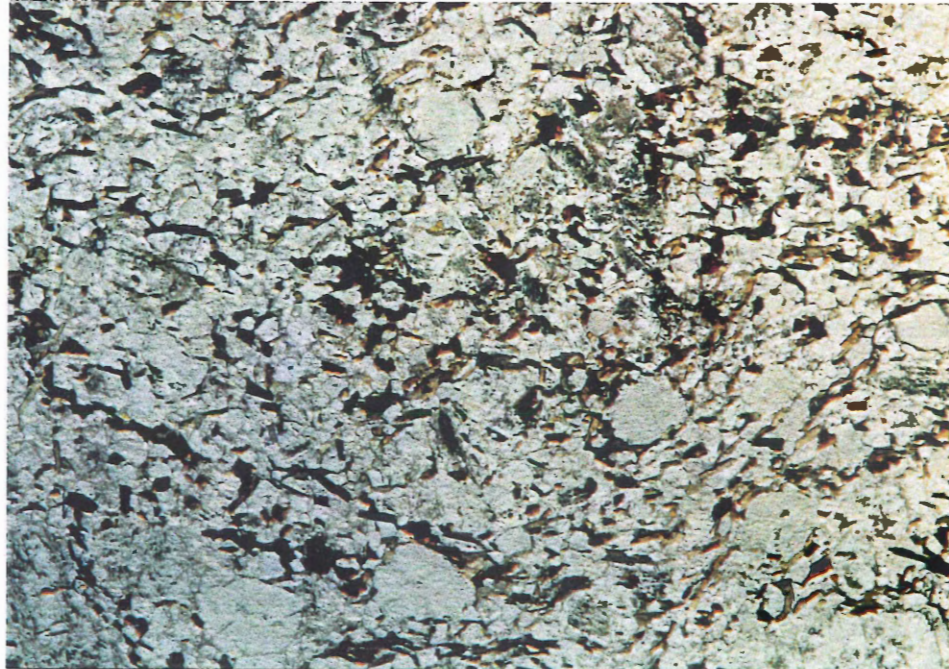


Figure 3.16. Photograph of mafic porphyry near the dike-like contact shown in Figure 2.11. Biotites align parallel to the dike contact (parallel to top of photo), and wrap around larger grains. This suggests that the mafic porphyry behaved plastically when the leucomonzogranite intruded (photo is 20mm x 26mm).

thoroughly, hybrid magmas may result, which contain minerals from both units (Cantagrel et al. 1984; Barbarin 1988).

When a magma incorporates foreign grains, physical and chemical modification of the grains may occur (Hibbard 1981; Hibbard 1991). Grains incorporated from a completely crystallized unit may become fractured and broken, showing evidence of brittle deformation (Type 1). However, transportation of these angular crystals may result in smaller, more rounded crystals. Once present in a foreign magma, these grains may be unstable and react with the magma. Grains reacting with the foreign magma, recrystallize, corrode, or become mantled by a mineral of different composition (Hibbard 1981; Hibbard 1991).

If two mingling magmas have different compositions, chemical transfer occurs between the two magmas until the chemical system reaches equilibrium. Chemical transfer across contacts between two incompletely crystallized magmas may result in zoned plagioclase grains. Hibbard (1981) suggested that zoning and mantling of grains result when magmas of contrasting composition and temperature mix. If the composition of the foreign magma is not significantly different from the original melt, foreign grains may be stable, and may form a seed for further crystallization (Pitcher 1991).

In thin section, contact relations between leucomonzogranite and mafic porphyry are similar to contact relations observed in the field. Significant features include: a) large grains of alkali feldspar, quartz, and plagioclase isolated in the mafic porphyry that are similar to phases present in the leucomonzogranite,

Table 3.1 Comparisons of New Ross Leucomonzogranite and Falls Lake Mafic Porphyry.

Comparisons	New Ross Leucomonzogranite	Contact Zone	Falls Lake Mafic Porphyry
Mineral Assemblage	Kfs, Pl, Qtz, Bt, Ms, Crd	Kfs, Pl, Qtz, Bt, Ms, Crd	Kfs, Pl, Qtz, Bt, Ms, Crd
Crystallization History (from thin section observations)	Bt > Pl > Qtz > Kfs > Crd > Ms	Bt > Pl > Qtz > Kfs > Crd > Ms	Bt > Pl > Qtz > Kfs ≥ Crd > Ms
Grain Size	Coarse-Grained	Variable	Fine-Grained
Texture	Hypidiomorphic granular-inequigranular	Variable	Porphyritic
Alkali Feldspar	-twinned -inclusions of Kfs, Pl, Qtz, Bt, Ms -average 1-3cm grains -subhedral	-twinned -inclusions of Kfs, Pl, Qtz, Bt, Ms -subhedral - subrounded	-clear, subrounded, untwinned grains ≤ 5mm -micrographic growths -subrounded -also occur locally as subhedral alkali feldspar megacrysts -inclusions of Kfs, Pl, Qtz, Bt, Ms
Plagioclase	-no inclusions in rims -inclusions of Bt -sausseritized cores - anhedral - subhedral -grains ≤ 1 cm	-inclusion rich rims -inclusions of Bt, Qtz -sausseritized cores -sometimes zoned -subrounded - subhedral	-no inclusions in rims -inclusions of Bt -sausseritized cores -subhedral -grains ≤ 5mm
Table 3.1 continued			

Table 3.1 continued			
Quartz	-inclusion-free -grains \leq 1cm -anhedral	-inclusions of Bt, Pl	-inclusion-free -anhedral -grains \leq 5mm
Mineral	New Ross Leucomonzogranite	Contact Zone	Falls Lake Mafic Porphyry
Biotite	-large 2-5mm plates	-Predominantly small \leq 5 mm plates	-0.1-0.5mm plates -clumps of smaller grains -larger grains often corroded
Muscovite	-2-5mm plates replacing Kfs	-small \leq 1 mm grains	- ~ 2mm clumps of small 0.5-1 mm plates - ~ 1 mm replacing Kfs

b) alternating bands of leucomonzogranite and mafic porphyry at contacts, and
 c) zoned and mantled plagioclase grains near contacts. These features demonstrate evidence of mingling near contacts, suggesting that both units were incompletely crystallized during intrusion. Contacts between leucomonzogranite and mafic porphyry in thin section support Type 2 contacts.

If large grains of alkali feldspar, quartz, and plagioclase in the mafic porphyry are native to the leucomonzogranite, they are xenocrysts in the mafic porphyry. Xenocrysts can be propelled into and moved through the mafic porphyry by stirring of the two units (Barbarin and Didier 1992). Rounding of the xenocrysts in the mafic

porphyry may occur during the transport of the xenocrysts from the leucomonzogranite to the mafic porphyry. Corroded plagioclase grains in the mafic porphyry may be xenocrysts from the leucomonzogranite that were unstable. However, some xenocrysts of plagioclase in the mafic porphyry were stable and were mantled by plagioclase of different composition. Alkali feldspar megacrysts in the mafic porphyry far from contacts are slightly larger than, but petrographically similar to, alkali feldspar megacrysts from the leucomonzogranite. Intense stirring of the two units is necessary to propel alkali feldspar megacrysts into the mafic porphyry far away from contacts.

The presence of concentric quartz inclusions near the margins of alkali feldspar and plagioclase grains, and zoned and mantled plagioclase grains near contacts, also suggest mixing between leucomonzogranite and mafic porphyry. If large feldspar grains from the leucomonzogranite were introduced into the mafic porphyry during crystallization of the mafic porphyry, crystallizing quartz grains from the mafic porphyry may tend to nucleate on earlier formed grains. By nucleating on the surface of crystallized grains, the small quartz grains require less energy to crystallize. Similar textures described by Hibbard (1991) represent two stages of mixing between coeval magmas. The first stage of mixing results in epitaxial growths on already-formed crystal surfaces. A second stage of mixing then refreshes the hybrid, continuing the crystallization of the initial crystal, locking in the smaller epitaxial grains (Hibbard 1991).

Mingling of two magmas facilitates chemical transfer between the two units by creating larger surface areas where chemical transfer can occur. Zoned feldspar grains may result from chemical transfer of sodium and calcium across contacts between the leucomonzogranite and mafic porphyry in an attempt to reach equilibrium.

3.5 Conclusions

At thin section scale, contact relations agree with field observations. Contacts at thin section scale show no properties of Type 1 contacts, and suggest that the leucomonzogranite and mafic porphyry were incompletely crystallized when they met. Evidence of mingling (diffuse contacts, xenocrysts in mafic porphyry) between the New Ross Leucomonzogranite and Falls Lake Mafic Porphyry occurs near contacts in many thin sections. The degree of mixing and chemical transfer between the two units is unclear, however limited chemical exchange may have occurred across contacts. Large grains of quartz, alkali feldspar, and plagioclase present near contacts in the mafic porphyry are similar to phases present in the leucomonzogranite, and probably originated from the leucomonzogranite. Chapter 4 uses mineral chemistry to examine the origins of larger crystals that occur in the mafic porphyry near contacts, and to determine the degree of chemical transfer between units.

CHAPTER 4: MINERAL CHEMISTRY

4.1 Introduction

Petrographic observations suggest that large alkali feldspar megacrysts, and other large grains in the mafic porphyry near contacts, are xenocrysts from the leucomonzogranite. This chapter uses mineral compositions to distinguish phases in the leucomonzogranite from similar phases in the mafic porphyry. Comparisons of chemical compositions of mineral inclusions in alkali feldspar megacrysts to similar groundmass phases allows assessment of the origin of alkali feldspar megacrysts. Chemical compositions of plagioclase mantles, and zoning trends may reflect mixing and chemical transfer between the leucomonzogranite and mafic porphyry. This chapter presents the mineral chemistry of various phases from the leucomonzogranite and mafic porphyry, and interprets the data in terms of mingling and mixing and chemical transfer.

4.2 Mineral Chemistry

4.2.1 Background

In the New Ross Leucomonzogranite and Falls Lake Mafic Porphyry, plagioclase and alkali feldspar grains commonly contain inclusions of biotite. Biotite inclusions reflect the composition of the melt from which they formed. Compositions of biotite inclusions that occur in alkali feldspar megacrysts may link alkali feldspar megacrysts in the mafic porphyry to the leucomonzogranite.

Zoning occurs in plagioclase grains when the melt from which they crystallize changes composition, temperature, water pressure, or experiences mixing. Melt

composition may change when the melt preferentially crystallizes minerals that deplete the melt in certain elements. Changes in melt composition may also result from diffusion from, or assimilation of another material. Stirring of two incompletely crystallized materials results in various degrees of mingling and mixing of the two units, and enhances chemical reactions between the two units (Barbarin and Didier 1992; Barbarin 1988). Figure 4.1 shows how plagioclase compositions change in a magma in response to temperature changes, water pressure changes, and mixing of two magmas.

Alkali feldspar megacrysts occur: a) widely in the New Ross Leucomonzogranite, b) locally in the Falls Lake Mafic Porphyry, and c) sporadically near and across contacts between these two units. Petrographically, megacrysts from the three occurrences are similar. Alkali feldspar megacrysts commonly contain mineral inclusions of quartz, plagioclase, biotite, and muscovite. The composition of biotite inclusions are representative of the melt in which they formed. Comparing compositions of biotite inclusions in alkali feldspar megacrysts to compositions of biotite phases in the leucomonzogranite and mafic porphyry groundmass helps to constrain the origins of the megacrysts.

4.2.2 Mineral Chemistry

4.2.2.1 Biotite compositions

Groundmass biotites away from contacts in the leucomonzogranite have higher FeO/MgO ratios than groundmass biotites in the mafic porphyry (Table 4.1; Appendix B2). The FeO/MgO ratios for biotites in the leucomonzogranite average

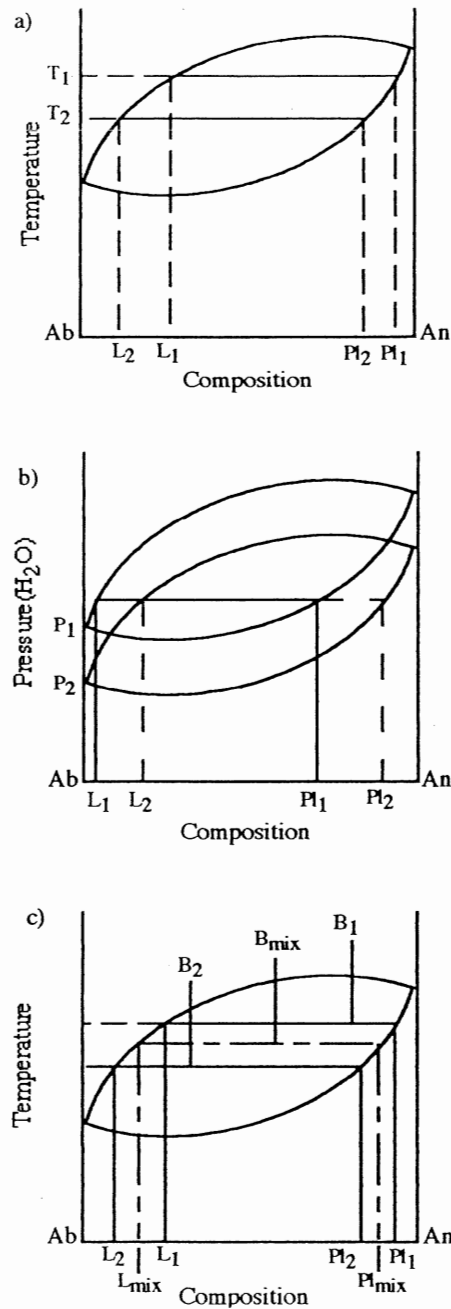


Figure 4.1. Schematic phase diagrams showing how plagioclase compositions (Pl_2) change in response to: a) temperature changes, b) changes in water pressure, and c) magma mixing (B_1 = magma batch 1, B_2 = magma batch 2, and B_{mix} = magma batch after mixing). Magma mixing (c) results in normally zoned plagioclase from B_1 and reversely zoned plagioclase from B_2 . As the temperature changes (a), the composition of the liquid changes, and affects the composition of the crystallizing plagioclase. Water pressure (b) affects the position of the solidus and liquidus curves, which changes the composition of the crystallizing plagioclase. Mixing of two magma batches (c) results in a hybrid magma batch (B_{mix}) which crystallizes plagioclase that has a composition intermediate to the two initial magma batches.

Table 4.1 Comparison of compositions of phases from the New Ross Leucomonzogranite and Falls Lake Mafic Porphyry.

Mineral Composition Comparisons				
Mineral	New Ross Leucomonzogranite	Falls Lake Mafic Porphyry	New Ross Leucomonzogranite near contacts	Falls Lake Mafic porphyry near contacts
Biotite (FeO/MgO) Mean and Std. Dev.	5.12 ± 0.23	3.05 ± 0.12	4.21 ± 0.78	3.50 ± 0.52
Plagioclase $\text{Na}_2\text{O}/(\text{Na}_2\text{O}+\text{CaO})$ Mean and Std. Dev.	-occurs as reversely-zoned grains -albitic compositions 0.78 ± 0.12	-occurs as normally-zoned grains -slightly albitic to intermediate composition 0.65 ± 0.09	-normally- and reversely-zoned grains -non-zoned grains of intermediate composition 0.64 ± 0.21	
Alkali Feldspars	All feldspars are similar in composition in all areas: K rich, small amounts of Na, little or no Ca			
Biotite Inclusions in Alkali Feldspar (FeO/MgO) Mean and Std. Dev.	4.80 ± 0.55	3.85 ± 0.15	3.92 ± 0.77	-wide range of biotite compositions representative of the 4 biotite phases listed above

5.12 ± 0.23 , and are distinct from ratios for biotites in the mafic porphyry, which average 3.05 ± 0.12 (Table 4.1; Appendix B2). Biotites near contacts between the leucomonzogranite and mafic porphyry have compositions intermediate to biotites in both units farther from contacts. Ratios for biotites in the mafic porphyry near contacts (FeO/MgO = 3.5 ± 0.52 ; Appendix B3) are lower than ratios for biotites in the mafic porphyry farther from contacts (Table 4.1). Similarly, biotites in the

leucomonzogranite near contacts ($\text{FeO}/\text{MgO} = 4.21 \pm 0.78$; Appendix B3) have ratios lower than biotite in the leucomonzogranite remote from contacts (Table 4.1).

4.2.2.2 Plagioclase chemistry

Plagioclase phases in the leucomonzogranite away from contacts occur as unzoned grains with average $(\text{Na}_2\text{O})/(\text{Na}_2\text{O}+\text{CaO})$ ratios of 0.78 ± 0.12 , and also occur as reversely-zoned grains (Table 4.1; Appendix B5). Away from contacts in the mafic porphyry, plagioclase phases occur as unzoned grains with average $(\text{Na}_2\text{O})/(\text{Na}_2\text{O}+\text{CaO})$ of 0.65 ± 0.09 , and also occur as normally-zoned grains (Table 4.1; Appendix B6).

Near contacts plagioclase phases occur as unzoned grains with $(\text{Na}_2\text{O})/(\text{Na}_2\text{O}+\text{CaO})$ ratios of 0.64 ± 0.12 , and as both normally- and reversely-zoned grains (Table 4.1; Appendix B7). These three types of plagioclase occur in both of the units near contacts, and are different from plagioclase in both units away from contacts (Fig. 4.2). The zoning of plagioclase grains are a function of how the plagioclase crystal is cut in thin section preparation, and may account for some of the observed unusual zoning trends .

4.2.2.3 Alkali feldspar chemistry

Biotite inclusions in alkali feldspar megacrysts from the leucomonzogranite are different from those in the mafic porphyry (Table 4.2). Iron-Magnesium ratios for biotite inclusions in leucomonzogranite megacrysts average 4.80 ± 0.55 , and are distinct from those in mafic porphyry megacrysts which average 3.85 ± 0.15 (Table 4.7). Biotite inclusions from alkali feldspar megacrysts that occur near contacts have

FeO/MgO ratios similar to biotite in the groundmass near contacts (i.e. intermediate).

Table 4.1 summarizes and compares the mineral chemistry of various phases in the leucomonzogranite and mafic porphyry with similar phases near contacts.

4.3 Discussion

Biotites from the leucomonzogranite have FeO/MgO ratios which are distinctly higher than FeO/MgO ratios for biotites in the mafic porphyry, and biotite phases near contacts have intermediate FeO/MgO ratios. The trend in groundmass biotite compositions (Table 4.1) may represent chemical transfer between the leucomonzogranite and mafic porphyry near contacts, attempting to reach equilibrium (i.e. magma mixing).

Plagioclase near contacts display zoning trends different from similar plagioclase grains away from contacts. If chemical transfer occurred between the mafic porphyry and leucomonzogranite, plagioclase grains in both units near contacts may show irregular zoning trends. Unusual zoning trends in plagioclase grains can also occur if plagioclase grains from one unit occur as xenocrysts in another unit, and become mantled by plagioclase of different composition. The compositions and zoning of plagioclase near and away from contacts suggest that mingling, and possibly mixing occurred between the leucomonzogranite and mafic porphyry (Fig. 4.2).

Biotite inclusions in feldspar megacrysts have various chemical compositions, and distinguish megacrysts in the leucomonzogranite from megacrysts in the mafic porphyry, and suggest that megacrysts formed separately in each unit. The composition of biotites in alkali feldspar megacrysts near contacts suggest that alkali

feldspar megacrysts near contacts formed near contacts after mixing of the leucomonzogranite and mafic porphyry occurred. Some biotite inclusions in megacrysts in the mafic porphyry near contacts have ratios similar to biotite phases that occur in the leucomonzogranite, suggesting that the megacrysts originated in the leucomonzogranite near contacts (i.e. mingling).

4.4 Conclusions

Mineral compositions of biotite inclusions suggest that alkali feldspar megacrysts in the mafic porphyry were not derived from the leucomonzogranite. The mineral chemistry of biotite inclusions from alkali feldspar megacrysts suggest that mixing of the leucomonzogranite and mafic porphyry occurred before alkali feldspar megacrysts formed, and is supported by the crystallization history observed in thin section (Appendix A). Variances in biotite compositions in both units near and far from contacts suggest that chemical transfer occurred between the two units across contacts. Zoning trends in plagioclase grains suggest that chemical exchange occurred across contacts, and that grains from the leucomonzogranite and mafic porphyry occur in each other. Mineral chemistry of phases near contacts suggests that mingling and mixing of the leucomonzogranite and mafic porphyry occurred near contacts, forming hybrid magmas.

CHAPTER 5: DISCUSSION

5.1 Introduction

Field relations, petrographic observations, and mineral compositions suggest that mingling and mixing occurred between the leucomonzogranite and mafic porphyry. This chapter reviews and discusses data gathered from field relations, petrography, and mineral chemistry, and applies these data to Type 1 and Type 2 contacts. Interpretation of the data from earlier chapters determines the behaviour and intrusive history of the leucomonzogranite and mafic porphyry.

5.2 Review of Data

5.2.1 Review

Interpretation of data obtained from field relations, petrography, and mineral chemistry indicate that the leucomonzogranite postdates the mafic porphyry, and that both units were incompletely crystallized when the leucomonzogranite intruded.

5.2.2 Evidence of mingling

Contacts between the leucomonzogranite and mafic porphyry are diffuse and irregular in most areas, and sharp where leucomonzogranite dykes cut the mafic porphyry. Where leucomonzogranite dykes cut the mafic porphyry, contacts are megascopically sharp, however grains do not show truncation (Fig. 1.3b); these contact relations suggest that the mafic porphyry was highly, but not completely crystallized, and may have behaved as a crystal mush ($C \sim 0.74$).

Table 5.1. Evidence of mingling and mixing that occurs in field relations, petrography, mineral composition data.

Criteria	Evidence of Mingling	Evidence of Mixing
Field Relations	-irregular and crenulate contacts (Fig. 2.19) -phenocrysts and megacrysts that bridge contacts (Fig. 2.15 and Fig. 2.16) -xenocrysts from the leucomonzogranite in mafic porphyry near contacts (Fig. 2.14 and Fig 2.16)	-not observable at outcrop scale
Petrography	-diffuse irregular contacts lacking truncated grains (Fig. 3.10) -xenocrysts from the leucomonzogranite in mafic porphyry near contacts (Fig. 3.10)	-mantling and zoning of plagioclase grains (Fig. 3.13 and Fig. 3.14) -epitaxial quartz growths (Fig. 3.12)
Mineral Chemistry	-similarly zoned plagioclase grains present in both units near contacts	-irregular zoning of plagioclase grains at contacts (Table 4.2) -changes in FeO/MgO ratios of biotites near contacts (Table 4.2)

Leucomonzogranite dykes that cut the mafic porphyry contain tapered xenoliths of mafic porphyry showing evidence of plastic deformation. The mafic porphyry xenoliths align with dyke margins, and are penetrated by megacrysts from the leucomonzogranite (Fig. 2.4 and Fig. 2.5). Figure 5.1 shows how leucomonzogranite dykes can incorporate fragments of incompletely crystallized mafic porphyry ($1.0 > C > 0.74$), which behave mechanically as a solid. Leucomonzogranite dykes may heat incorporated mafic porphyry fragments, which behave plastically ($C < 0.74$) (Fig. 5.1, Stage 2). Stresses that occur during leucomonzogranite intrusion can cause

megacrysts from the leucomonzogranite to penetrate mafic porphyry xenoliths, which align with dyke margins and form tapered ends (Fig. 5.1, Stage 3).

Figure 5.2 shows a model formulated from field evidence (Fig. 2.18), suggesting how xenoliths of mafic porphyry form in the leucomonzogranite. If the leucomonzogranite and mafic porphyry were immiscible magmas, stirring may cause viscous fingering (Fig. 5.2, Stages 1 and 2). Viscous fingering occurs when a less viscous magma (mafic porphyry) protrudes into a more viscous magma (leucomonzogranite), and can result in blobs of mafic porphyry isolated in the leucomonzogranite (Fig. 5.3) (Bébién et al. 1987 in Barbarin and Didier 1991).

Some areas where the leucomonzogranite intrudes the mafic porphyry are dyke-like, but have diffuse contacts (Figs. 2.9-2.11). Where leucomonzogranite dyke contacts are diffuse, alkali feldspar megacrysts in the dykes align with each other, and in some cases appear to occur as xenocrysts in the mafic porphyry (Fig. 2.11). The diffuse nature of contacts that occur where the leucomonzogranite intrudes the mafic porphyry, suggest that the mafic porphyry was incompletely crystallized ($C < 0.74$), and behaved plastically when the leucomonzogranite intruded. The differences in the types of contacts (sharp and diffuse) that occur where the leucomonzogranite intrudes the mafic porphyry suggest that the degree of crystallization (C) of the mafic porphyry was higher in some areas than others (Fig. 5.3). Where C was high ($1.0 > C > 0.74$), sharp contacts resulted, and where C was low ($C < 0.74$), diffuse contacts resulted (Fig. 5.3).

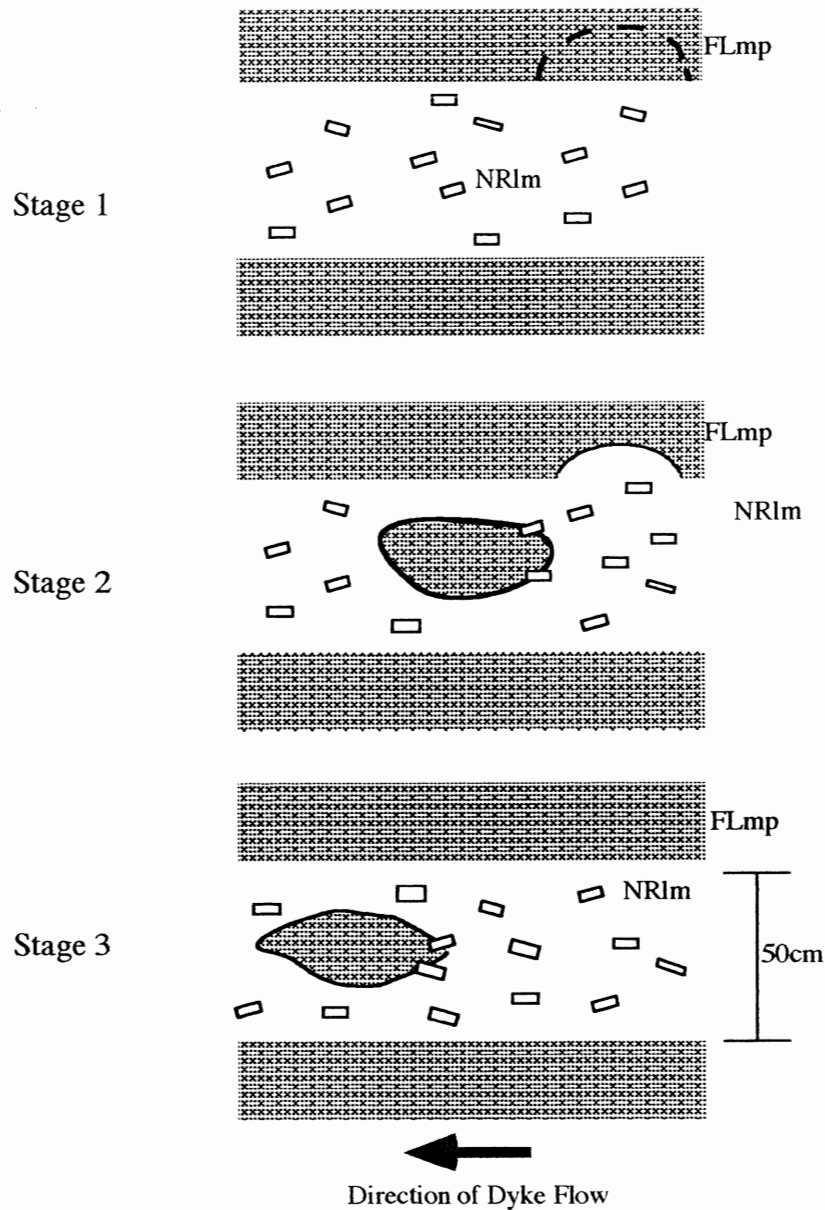


Figure 5.1. Sketch showing the various stages that may occur during the incorporation of mafic porphyry xenoliths by leucomonzogranite dykes (NRIm=New Ross Leucomonzogranite, FLmp=Falls Lake Mafic Porphyry). In Stage 1 the leucomonzogranite plucks a fragment from the wall rocks. The fragment of mafic porphyry behaves plastically during transportation, aligns with dyke margins (Stage 2). The interaction of mafic porphyry xenoliths with the leucomonzogranite dyke during intrusion causes the xenolith to form tapered ends, and in some cases megacrysts from the leucomonzogranite penetrate the xenoliths.

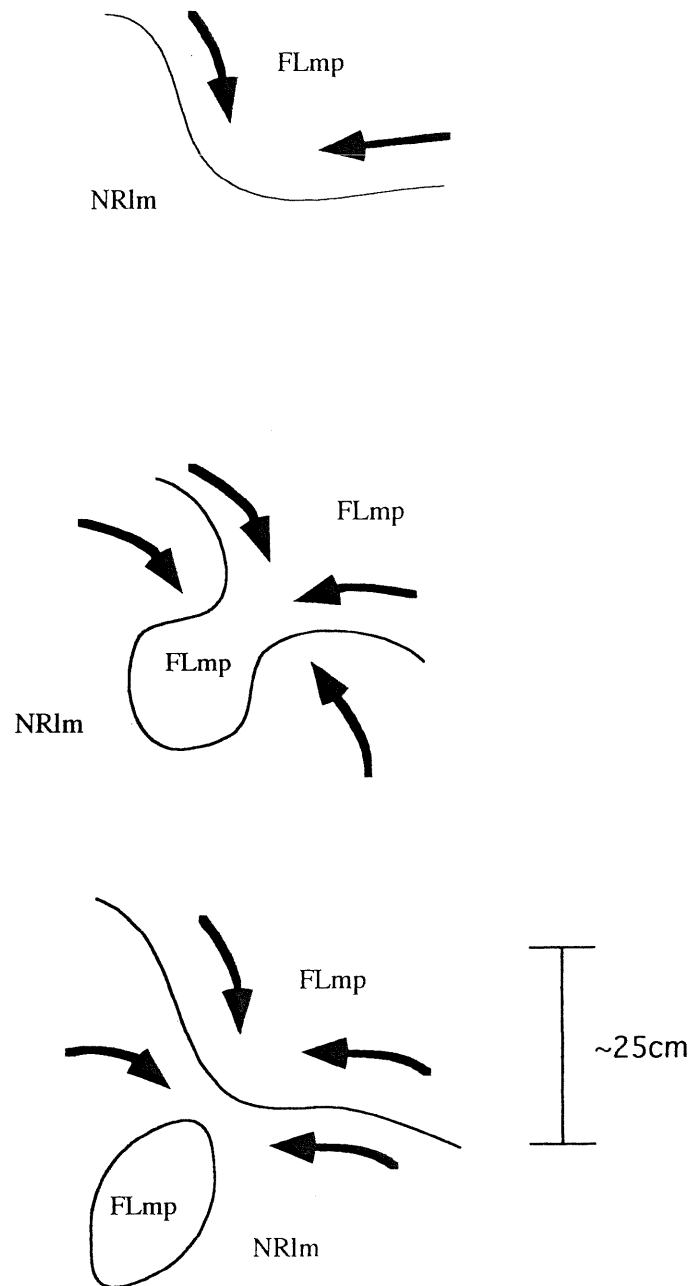


Figure 5.2. Sketch showing how xenoliths of mafic porphyry may be incorporated at contacts between areas of leucomonzogranite and mafic porphyry (NRIm=New Ross Leucomonzogranite, FLmp=Falls Lake Mafic Porphyry). Stirring processes cause the mafic porphyry and leucomonzogranite to behave plastically, and curved contacts form between the two units (Stage 1). Some areas of the mafic porphyry to protrude into the leucomonzogranite (Stage 2), and blobs of mafic porphyry may occur in the leucomonzogranite (Stage 3). This model is formulated on field observations like those shown in Fig. 2.19.

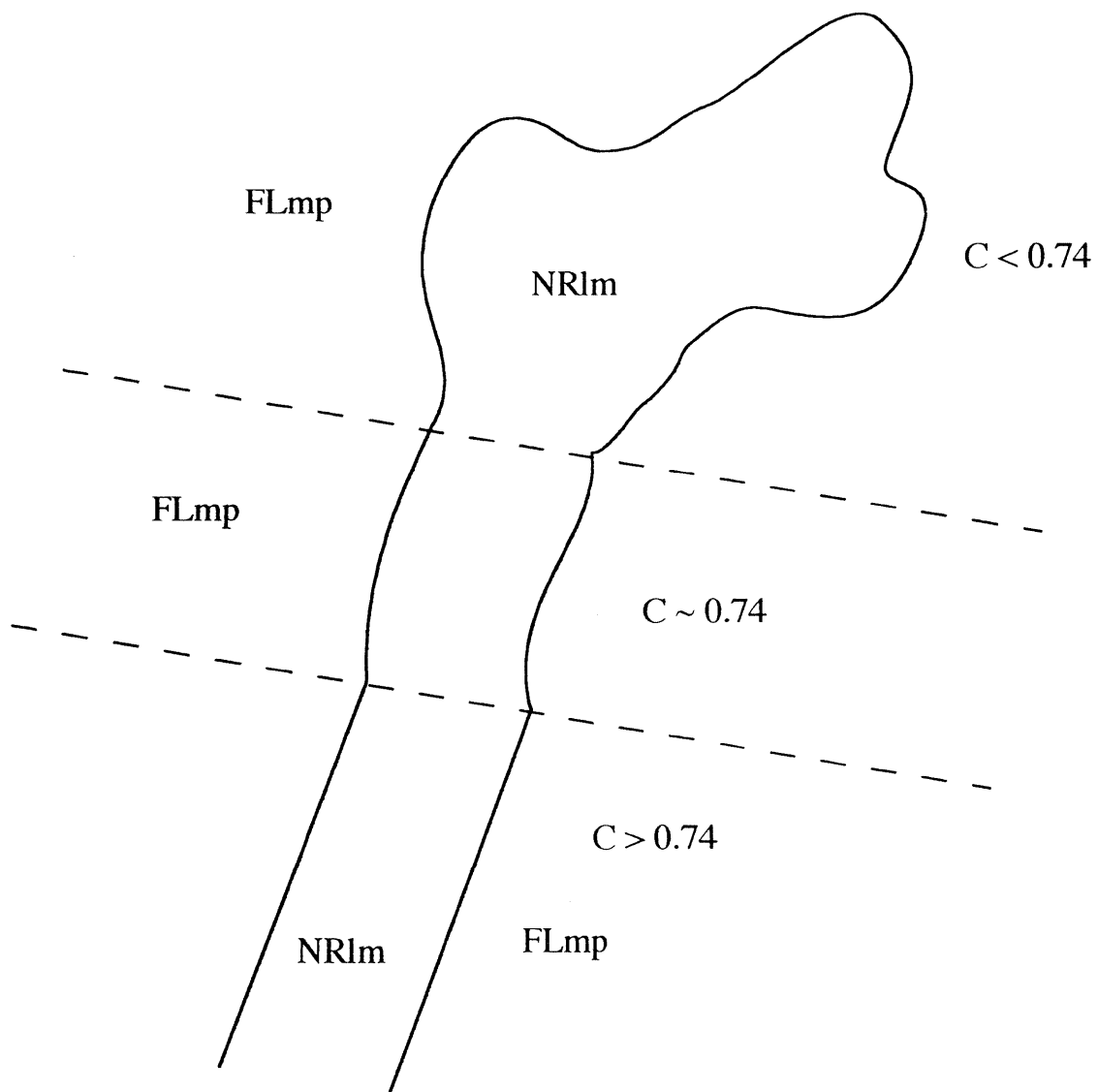


Figure 5.3. Drawing showing how the types of contacts between the leucomonzogranite and mafic porphyry vary according to differences in the degree of crystallization of the mafic porphyry. Where the mafic porphyry is highly crystallized ($C > 0.74$) the mafic porphyry behaves mechanically as a solid (Type 1). Where the mafic porphyry is less crystallized ($C < 0.74$), the mafic porphyry behaves plastically (Type 2). Where the mafic porphyry behaves as a crystal mush ($C \sim 0.74$), Type 1 and Type 2 contacts can result.

The variability of the contact relations may also occur if the mafic porphyry had a uniform crystallization of C near 0.74. In this case, variable degrees of stirring (Table 5.2) can result in the various types of contacts observed. Where significant stirring occur contacts can be lobate and crenulate (like $C > 0.74$; Fig. 5.3), and where stirring is minimal contacts may be linear (like $C < 0.74$; Fig 5.3).

Irregular contacts also occur between large areas of leucomonzogranite and mafic porphyry, and are diffuse, or have lobate and cusped shapes. Diffuse contacts between the leucomonzogranite and mafic porphyry occur at the mesoscopic (field) scale (Fig. 2.15) and at the microscopic (thin section) scale (Fig. 2.10); these contacts contain phenocrysts and megacrysts that straddle contacts, and locally show xenocrysts from the leucomonzogranite isolated in the mafic porphyry near contacts. Because no other large phenocrysts occur in the mafic porphyry near contacts (Fig. 2.15 and Fig. 2.16) large, isolated grains in the mafic porphyry near contacts are not phenocrysts from the mafic porphyry. Xenocrysts from the leucomonzogranite in the mafic porphyry can result when stirring of the two units propels grains from the leucomonzogranite into the mafic porphyry.

Stirring processes can occur during a) magma replenishment, b) ascent processes, and c) convective stirring (Barbarin and Didier 1991; Koyaguchi and Blake 1991) (Table 5.2). Stirring processes cause coeval magmas to interact, and the types of interaction that occur depend on the degree of stirring, and the rheological properties of the two magmas involved. The transport of phases between magmas is

Place of exchanges	Causes	Nature of exchanges	Results
EMPLACEMENT LEVEL (upper crust)	Late injections of mafic magmas	LOCAL MECHANICAL AND CHEMICAL EXCHANGE	Enclaves in monogenic swarms Synplutonic dykes (Net-veined complexes)
	Compositional contrasts between enclaves and host	EXTENSIVE CHEMICAL EXCHANGE	Partial chemical equilibrium and complete isotopic equilibrium between enclaves and host
		LIMITED CHEMICAL EXCHANGE	Fine-grained margins, felsic haloes, and scarce zoned enclaves with discontinuous hybrid zones at enclave-host contacts
MAGMA CONDUITS (dyke swarms)	Relative movement of magmas of contrasted densities	EXTENSIVE MECHANICAL EXCHANGE	Various types of enclave Composite enclaves Xenocrysts
MAGMA CHAMBER (lower crust)	Temperature contrasts	LIMITED CHEMICAL EXCHANGE	Hybrid rocks surrounding enclaves
		THERMAL EXCHANGE	Melting of crustal rocks and production of anatectic melt Chilling of mafic magma (fine grain-size, chilled margins, acicular and hollow crystals)
	Convective stirring Magma fountains	EXTENSIVE MECHANICAL EXCHANGE	(Banded structures) Enclaves Xenocrysts
Compositional contrasts between coeval magmas	EXTENSIVE CHEMICAL EXCHANGE (INTERDIFFUSION)	Hybrid magmas (granites?)	

Table 5.2. Role of the various types of exchange at different structural levels, their causes, and results. Exchanges can occur at the emplacement level, in magma conduits, or in the magma chamber. At the emplacement level, late injections of magma can cause stirring, leading to local mechanical exchanges, and chemical exchanges if there are compositional differences between the two units involved. In magma conduits, extensive mechanical exchange occurs as a result of the relative movement of magmas in the magma conduits. In magma conduits there is limited chemical exchange, and little or no thermal exchanges. Magma chamber interactions can result in thermal and chemical exchange between coeval magmas, and mechanical exchange can occur as a result of convective stirring or stirring caused by magma fountains (after Barbarin and Didier 1992).

controlled by the viscosities, densities, rheologies, and the degree of crystallization of the magmas involved (Barbarin and Didier 1991). If the viscosity and degree of crystallization of the mafic porphyry were low ($C < 0.74$), and the leucomonzogranite was partially crystallized (i.e. contained phenocrysts), stirring may cause the leucomonzogranite to disaggregate near contacts, and might propel phenocrysts from the leucomonzogranite into the mafic porphyry.

Irregular contacts between the leucomonzogranite and mafic porphyry that have lobate and cusped shapes may occur where the rheological properties of the of the leucomonzogranite and mafic porphyry inhibit the transport of phases between the two immiscible magmas. If the leucomonzogranite and mafic porphyry behaved as immiscible magmas, stirring processes might result in lobate and crenulate contacts.

5.2.3. Evidence of mixing

Petrography and mineral compositions provide evidence of local mixing between the leucomonzogranite and mafic porphyry near contacts that is not obvious in the field, suggesting that mixing was restricted to areas near contacts. Mineral compositions of biotite in the leucomonzogranite and mafic porphyry indicate chemical transfer across contacts between the two units. Biotite compositions have intermediate FeO/MgO ratios near contacts, compared to biotite away from contacts in the leucomonzogranite and mafic porphyry (Table 4.1). The intermediate compositions of biotite near contacts indicate that chemical transfer occurred between the leucomonzogranite and mafic porphyry, in response to a chemical disequilibrium between the two units.

The mineral compositions of biotite inclusions in alkali feldspar megacrysts in both units suggests that alkali feldspar megacrysts in both units have different origins. Alkali feldspar megacrysts near contacts formed after chemical exchange occurred across contacts, and included intermediate biotites that formed at contacts. Mineral compositions of zoned and mantled plagioclase in the leucomonzogranite and mafic porphyry away from, and near contacts, indicate that homogenization and hybridization occurred near contacts (Fig. 4.2). Plagioclase compositions in the leucomonzogranite are distinct from plagioclase compositions in the mafic porphyry (Fig. 4.2; Table 4.1); however, plagioclase compositions in the mafic porphyry near contacts are similar to plagioclase compositions in the leucomonzogranite near contacts (Fig. 4.2; Table 4.1). The irregular assemblage of zoned plagioclase near contacts suggest that mingling and mixing occurred between the leucomonzogranite and mafic porphyry.

5.3. Discussion

Evidence provided from field relations, petrography, and mineral compositions suggest that mingling of the leucomonzogranite and mafic porphyry commonly occurred, and that mixing of the two units was restricted to narrow zones near contacts. Barbarin and Didier (1992) stated that two magmas with low viscosities mix more easily than magmas with higher viscosities. The limited degree of mixing, and the occurrence of lobate and cusped contacts between the leucomonzogranite and mafic porphyry suggests that the leucomonzogranite and mafic porphyry had high viscosities when the leucomonzogranite intruded. High viscosities occurred where the

mafic porphyry behaved as a crystal mush ($C \sim 0.74$), during leucomonzogranite intrusion. Barbarin and Didier (1992) stated that thermal transfer occurs several orders of magnitude faster than chemical transfer; The restriction of mixing to contact areas between the leucomonzogranite and mafic porphyry may suggest that both units solidified shortly after meeting, and did not allow for any significant chemical transfer between the two units.

5.4 Possible Models and Explanations

Table 5.3. Criteria present where intrusive-intrusive contacts occur.

CRITERIA	EXPECTED FOR Type 1	EXPECTED FOR Type 2	PRESENT IN THIS STUDY
megascopically sharp cross cutting dykes	yes	possibly	yes
truncated grains	yes	no	no
megascopically sharp linear contacts	yes	possibly	yes
diffuse contacts	not likely	yes	yes
magma mingling near contacts	not likely	yes	yes
magma mixing near contacts	no	not likely	yes
cusped fractal contacts	no	yes	yes
non-chilled, oval xenoliths	no	yes	yes
short interval of SMB intrusion	not likely	yes	yes
non-truncated grains	no	yes	yes
chemical transfer	possibly	yes	yes
hybrid rocks	not likely	yes	yes

The two general models proposed to explain contact relations that occur when one granite intrudes another are Type 1 (magma-solid) and Type 2 (magma-magma) (outlined in Table 1.1). Most of the evidence gathered from Chapters 2, 3, and 4 support Type 2 contacts, and the small amount of evidence supporting Type 1 contacts can also occur in Type 2 situations. Type 1 contacts can occur in Type 2 situations if one of the units behaves locally as a solid ($C \sim 0.74$), however, Type 2 contacts cannot occur in Type 1 situations.

5.5. Conclusions

Interpretations of field relations, petrography, and mineral chemistry suggest that the mafic porphyry was incompletely crystallized when the leucomonzogranite intruded. Xenocrysts present in the mafic porphyry near contacts, and phenocrysts that straddle contacts suggest that the leucomonzogranite was partially crystallized when it intruded. Evidence of magma mingling and magma mixing occurs near contacts where hybrid rocks occur. Magma mingling is common between the leucomonzogranite and mafic porphyry, however, mixing between the leucomonzogranite and mafic porphyry is limited to areas near contacts. The preservation and limited extent of magma mingling and mixing indicates that both units solidified shortly after the leucomonzogranite intruded.

CHAPTER 6: CONCLUSIONS

6.1. Conclusions

The interpretation of field relations, petrographic relations, and the mineral chemistry of phases that occur in the New Ross Leucomonzogranite and Falls Lake Mafic Porphyry indicate that:

- a) the Falls Lake Mafic Porphyry was incompletely crystallized when the New Ross leucomonzogranite intruded, and that the New Ross Leucomonzogranite was partially crystallized at the time of intrusion.
- b) the mafic porphyry had varying degrees of crystallization, behaving mechanically as a solid in some areas, and plastically in others.
- c) magma mingling and magma mixing occurred between the New Ross Leucomonzogranite and the Falls Lake Mafic Porphyry.
- d) where magma mingling occurs between two incompletely crystallized magmas, contacts have a fractal nature, and have crenulate and lobate shapes, and that where magma mingling and mixing occur hybrid rocks may result.

REFERENCES:

- Arzi, A.A., 1978. Critical phenomenon in the rheology of partially melted rocks. *Tectonophysics*, **44**: 173-184
- Abbot, R.N., 1989. Internal structures in part of the South Mountain Batholith, Nova Scotia, Canada. *Geological Society of America Bulletin*, **101**:1493-1506
- Barbarin, B., and Didier, J. 1991. Macroscopic features of mafic microgranular enclaves. *In Developments in Petrology*, **13**, Enclaves and Granite Petrology: 253-262
- Barbarin, B., and Didier, J., 1992. Genesis and evolution of mafic microgranular enclaves through various types of interaction between coexisting felsic and mafic magmas. *Special Paper-Geological Society of America*, **272**:145-153
- Cantagrel, J.-M., Didier, J., and Gourgaud, A. 1984. Magma mixing: origin of intermediate rocks and "enclaves" from volcanism to plutonism. *Physics of the Earth and Planetary Interiors*, **35**: 63-76
- Clarke, D.B., MacDonald, M.A., Reynolds, P.H., and Longstaffe, F.J. 1993. Leucogranites from the eastern part of the South Mountain batholith, Nova Scotia. *Journal of Petrology*, **34**: 653-679
- Didier, J. 1973. Granites and their enclaves: the bearing of enclaves on the origin of granites. *Developments in Petrology*, **3**. 386 pp
- Fernandez, A.N., Barbarin, B. 1991. Relative rheology of coeval mafic and felsic magmas: nature of resulting interaction processes and shape and mineral fabrics of mafic microgranular enclaves. *In Developments in Petrology*, **13**, Enclaves and Granite Petrology: 263-275
- Ham, L.J., and Horne, R.J. 1986. Geology of the South Mountain batholith on the eastern half of NTS sheet 21A/16. Nova Scotia Department of Mines and Energy, Report **86-1**: 149-159
- Ham, L.J. and Horne, R.J. 1987. Geological map of Windsor (N.T.S. sheet 21A\16 east half), Nova Scotia. Nova Scotia Dept. of Mines and Energy. Map 87-7
- Ham, L.J., Marsh, S.W., Corey, M.C., Horne, R.J., and MacDonald, M.A. 1989. Lithochemistry of the Eastern Portion of the South Mountain Batholith, Nova Scotia, N.T.S. map sheets 11D\05, 11D\12, 11D\13, 21A\09, 21A\10, 21A\15, 21A\16, and parts of 21H\01, and 21H\02. Nova Scotia Dept. of Mines and Energy. Open File Report 89-001. 62 pp

- Hibbard, M.J. 1981. The magma mixing origin of mantled feldspars. *Contributions to Mineralogy and Petrology*, **76**: 158-170
- Hibbard, M.J. 1991. Textural anatomy of twelve magma-mixed granitoid systems. *In Developments in Petrology*, **13**, Enclaves and Granite Petrology: 431-444
- Hibbard, M.J., and Watters, R.J. 1985. Fracturing and diking in incompletely crystallized granitic plutons. *Lithos*, **18**: 1-12
- Horne, R.J., MacDonald M.A., Corey, M.C., and Ham, L.J. 1992. Structure and emplacement of the South Mountain Batholith, southwestern Nova Scotia. *Atlantic Geology*, **28**: 29-50
- Koyaguchi, T., and Blake, S. 1991. Origin of mafic enclaves: constraints on the magma mixing model from fluid dynamic experiments. *In Developments in Petrology*, **13**, Enclaves and Granite Petrology: 415-429
- MacDonald, M.A., Horne, R.J., Corey, M.C., and Ham, L.J. 1992. An overview of recent bedrock mapping and follow-up petrological studies of the South Mountain Batholith, southwestern Nova Scotia, Canada. *Atlantic Geology*, **28**: 7-28
- MacDonald, M.A., Corey, M.C., Ham, L.J., and Horne, R.J. 1987. The geology of the South Mountain batholith: NTS map sheets 21A/09, 21A/10, 21A/16 (West). Nova Scotia Department of Mines and Energy, Report **87-1**: 107-121
- Martel, A.T., McGregor, D.C., and Utting, J. 1993. Stratigraphic significance of Upper Devonian and Lower Carboniferous miospores from the type area of the Horton Group, Nova Scotia. *Canadian Journal of Earth Sciences*, **30**: 1091-1098
- Sparkes, R.S.J., and Marshall, L.A. 1986. Thermal and mechanical constraints on mixing between mafic and silicic magmas. *Journal of Volcanology and Geothermal Research*, **29**: 99-124
- van der Molen, I., and Peterson, M.S. 1979. Experimental deformation of partially-melted granite. *Contributions to Mineralogy and Petrology*, **70**: 299-318
- Vernon, R.H. 1991. Interpretation of microstructures of microgranitoid enclaves. *In Developments in Petrology*, **13**, Enclaves and Granite Petrology: 277-291

Appendix A:
Petrographic Descriptions

Appendix A: Petrographic Descriptions

Section #14

From: Sample #14 (leucomonzogranite)

Lithology: Leucomonzogranite

Average Grain Size: ~ 1cm

Texture: hypidiomorphic granular-inequigranular

Crystallization history: Bt > Pl > Qtz > Kfs > Crd > Ms

Mineralogy:

Alkali feldspar- 35%, occurs as large (up to 5cm), Carlsbad twinned, subhedral, grains that often contain inclusions of biotite, quartz, and plagioclase.

Plagioclase-25%, occurs as large, ~ 1cm, subhedral grains that often have sericitized cores. Some grains contain inclusions of biotite. Carlsbad and albite twinning are present in some grains, and zoning is relatively uncommon.

Quartz-30%, occurs as subhedral-anhedral grains up to 1cm in length.

Biotite-4-8%, occurs as large, subhedral-anhedral, 2-5mm plates.

Muscovite-1-3%, occurs as large, subhedral, 2-5mm plates that often replace alkali feldspar.

Appendix A: Petrographic Descriptions

Section #12

From: Sample #12 (mafic porphyry)

Lithology: Mafic Porphyry

Average Grain Size: ~ .5mm

Texture: porphyritic

Crystallization history: Bt > Pl > Qtz > Kfs > Crd > Ms

Mineralogy:

Alkali feldspar-25%, occurs as subrounded, inclusion-free, untwinned grains

Plagioclase-25%, occurs as small, ~ 1mm, grains with sericitized cores. Carlsbad and albite twinned grains present, and zoned grains are relatively uncommon.

Quartz-25%, occurs as inclusion free anhedral grains, < 1mm in length

Biotite-10-20%, variable presence throughout the slide, higher in some areas than others. Occurs as small .5-1mm subhedral plates, and less commonly as larger, 2-4mm clumps of smaller plates of muscovite and biotite.

Muscovite-1-2%, occurs as small .5-1mm plates replacing alkali feldspar, and in 2-4 mm clumps with biotite.

Comments: micrographic texture locally present throughout the mafic porphyry groundmass, and occurs between quartz and alkali feldspar.

-pinitized cordierite occurs in some areas of the mafic porphyry (~ 1%), and is replaced by muscovite.

Appendix A: Petrographic Descriptions

Section #1

From: Sample #1 (across contact)

Lithology:	Leucomonzogranite	Mafic Porphyry
Average Grain Size:	~ 1cm	~ .5mm
Texture:	hypidiomrphic	porphyritic
Crystallization history:	Bt > Pl > Qtz > Kfs > Crd > Ms	Bt > Pl > Qtz > Kfs > Crd > Ms

Mineralogy:

Alkali feldspar	35%	25%
Plagioclase	25%	25%
Quartz	30%	25%
Biotite	4-8%	10-20%
Muscovite	1-3%	1-2%

Comments: minerals from units near contacts are similar in percentage and characteristics to minerals in both units away from contacts.

- micrographic texture common in mafic porphyry
- large biotite and muscovite clumps
- some corroded plagioclase in the mafic porphyry
- evidence of mingling and mixing not prevalent in this section

Appendix A: Petrographic Descriptions

Section #2

From: Sample #2 (across contact)

Lithology:	Leucomonzogranite	Mafic Porphyry
Average Grain Size:	~ 1cm	~ .5mm
Texture:	hypidiomrphic	porphyritic
Crystallization history:	Bt > Pl > Qtz > Kfs > Crd > Ms	Bt > Pl > Qtz > Kfs > Crd > Ms

Mineralogy:

Alkali feldspar	35%	25%
Plagioclase	25%	25%
Quartz	30%	25%
Biotite	4-8%	10-20%
Muscovite	1-3%	1-2%

Comments: minerals from units near contacts are similar in percentage and characteristics to minerals in both units away from contacts.

- layering of leucomonzogranite and mafic porphyry at contacts
- large grains like leucomonzogranite grains in mafic porphyry
- units in layers seem to maintain properties and structure

Appendix A: Petrographic Descriptions

Section #3

From: Sample #3 (across chilled contact)

Lithology:	Leucomonzogranite	Mafic Porphyry
Average Grain Size:	~ 7mm	~ .3mm
Texture:	hypidiomrphic	porphyritic
Crystallization history:	Bt > Pl > Qtz > Kfs > Crd > Ms	Bt > Pl > Qtz > Kfs > Crd > Ms

Mineralogy:

Alkali feldspar	35%	25%
Plagioclase	25%	25%
Quartz	30%	25%
Biotite	4-8%	10-20% (~20% @ contact)
Muscovite	1-3%	1-2%

Comments: minerals from units near contacts are similar in percentage and characteristics to minerals in both units away from contacts.

- biotite increases in size and abundance near contacts
- large biotites near the contact align with the contact
- leucomonzogranite shows a decrease in grain size near contacts

Appendix A: Petrographic Descriptions

Section #4

From: Sample #4 (across contact)

Lithology:	Leucomonzogranite	Mafic Porphyry
Average Grain Size:	~ 5mm	~ .3mm
Texture:	hypidiomorphic	porphyritic
Crystallization history:	Bt > Pl > Qtz > Kfs > Crd > Ms	Bt > Pl > Qtz > Kfs > Crd > Ms

Mineralogy:

Alkali feldspar	35%	25%
Plagioclase	25%	25%
Quartz	30%	25%
Biotite	4-8%	10-20%
Muscovite	1-3%	1-2%

Comments: minerals from units near contacts are similar in percentage and characteristics to minerals in both units away from contacts.

- pockets of mafic porphyry in leucomonzogranite
- leucomonzogranite lacks large alkali feldspars, seems to be finer grained
- diffuse contact, some larger grains isolated in the mafic porphyry
- micrographic texture common in the mafic porphyry

Appendix A: Petrographic Descriptions

Section #5

From: Sample #5 (across contact)

Lithology:	Leucomonzogranite	Mafic Porphyry
Average Grain Size:	~ 5mm	~ .3mm
Texture:	hypidiomrphic	porphyritic
Crystallization history:	Bt > Pl > Qtz > Kfs > Crd > Ms	Bt > Pl > Qtz > Kfs > Crd > Ms

Mineralogy:

Alkali feldspar	35%	25%
Plagioclase	25%	25%
Quartz	30%	25%
Biotite	4-8%	10-20%
Muscovite	1-3%	1-2%

Comments: minerals from units near contacts are similar in percentage and characteristics to minerals in both units away from contacts.

- contact sharp compared to other contacts in study
- micrographic texture common
- plagioclase zoning relatively uncommon

Appendix A: Petrographic Descriptions

Section #6

From: Sample #6 (across contact)

Lithology:	Leucomonzogranite	Mafic Porphyry
Average Grain Size:	~ 5mm	~ .4mm
Texture:	hypidiomrphic	porphyritic
Crystallization history:	Bt > Pl > Qtz > Kfs > Crd > Ms	Bt > Pl > Qtz > Kfs > Crd > Ms

Mineralogy:

Alkali feldspar	35%	25%
Plagioclase	25%	25%
Quartz	30%	25%
Biotite	4-8%	10-20%
Muscovite	1-3%	1-2%

Comments: minerals from units near contacts are similar in percentage and characteristics to minerals in both units away from contacts.

- zoned plagioclase grains more common in both units in this section
- large 3mm corroded plagioclase grain in the mafic porphyry
- large alkali feldspar megacrysts in the leucomonzogranite align with the contact.

Appendix A: Petrographic Descriptions

Section #7

From: Sample #7 (across contact)

Lithology: Leucomonzogranite Mafic Porphyry

Average Grain Size: ~ 4mm ~ .3mm

Texture: hypidiomrphic porphyritic

Crystallization history: Bt > Pl > Qtz > Kfs > Crd > Ms Bt > Pl > Qtz > Kfs > Crd > Ms

Mineralogy:

Alkali feldspar 35% 25%

Plagioclase 25% 25%

Quartz 30% 25%

Biotite 4-8% 10-20%

Muscovite 1-3% 1-2%

Comments: minerals from units near contacts are similar in percentage and characteristics to minerals in both units away from contacts.

- zoned plagioclase grains are more common in this section near contacts
- micrographic texture present in the mafic porphyry, but not common
- 2 large (4-5mm) clumps of biotite and muscovite present in the mafic porphyry

Appendix A: Petrographic Descriptions

Section #10

From: Sample #10 (across contact)

Lithology:	Leucomonzogranite	Mafic Porphyry
Average Grain Size:	~ 4mm	~ .2mm
Texture:	hypidiomrphic	porphyritic
Crystallization history:	Bt > Pl > Qtz > Kfs > Crd > Ms	Bt > Pl > Qtz > Kfs > Crd > Ms

Mineralogy:

Alkali feldspar	35%	25%
Plagioclase	25%	25%
Quartz	30%	25%
Biotite	4-8%	10-20%
Muscovite	1-3%	1-2%

Comments: minerals from units near contacts are similar in percentage and characteristics to minerals in both units away from contacts.

- diffuse contact between the two units, units seem to penetrate each other (i.e. mingle)
- large grains and clumps of large grains from leucomonzogranite present in the mafic porphyry
- zoned plagioclase are more common in both units near contacts
- large 4mm cordierite grain in mafic porphyry, replaced by muscovite
- some of the large grains isolated in the mafic porphyry have quartz concentric quartz growths near the grain margins

Appendix A: Petrographic Descriptions

Section #13A

From: Sample #13 (across contact)

Lithology:	Leucomonzogranite	Mafic Porphyry
Average Grain Size:	~ 5mm	~ .3mm
Texture:	hypidiomorphic	porphyritic
Crystallization history:	Bt > Pl > Qtz > Kfs > Crd > Ms	Bt > Pl > Qtz > Kfs > Crd > Ms

Mineralogy:

Alkali feldspar	35%	25%
Plagioclase	25%	25%
Quartz	30%	25%
Biotite	4-8%	10-20%
Muscovite	1-3%	1-2%

Comments: minerals from units near contacts are similar in percentage and characteristics to minerals in both units away from contacts.

- diffuse contact
- large alkali feldspar grains near contact project into mafic porphyry
- rough alignment of grains with contact
- some large alkali feldspar megacrysts in mafic porphyry have concentric growths near grain margins

Appendix A: Petrographic Descriptions

Section #13B

From: Sample #13 (across contact)

Lithology:	Leucomonzogranite	Mafic Porphyry
Average Grain Size:	~ 5mm	~ .3mm
Texture:	hypidiomrphic	porphyritic
Crystallization history:	Bt > Pl > Qtz > Kfs > Crd > Ms	Bt > Pl > Qtz > Kfs > Crd > Ms

Mineralogy:

Alkali feldspar	35%	25%
Plagioclase	25%	25%
Quartz	30%	25%
Biotite	4-8%	10-20%
Muscovite	1-3%	1-2%

Comments: minerals from units near contacts are similar in percentage and characteristics to minerals in both units away from contacts.

- diffuse contact
- alternating areas of mafic porphyry and leucomonzogranite
- large alkali feldspar grains near contact project into mafic porphyry
- some large alkali feldspar megacrysts in mafic porphyry have concentric growths near grain margins

Appendix A: Petrographic Descriptions

Section #13C

From: Sample #13 (in mafic porphyry near contact)

Lithology: Mafic Porphyry

Average Grain Size: ~ .3mm

Texture: porphyritic

Crystallization history: Bt > Pl > Qtz > Kfs > Crd > Ms

Mineralogy:

Alkali feldspar 25%

Plagioclase 25%

Quartz 25%

Biotite 10-20%

Muscovite 1-2%

Comments: minerals from units near contacts are similar in percentage and characteristics to minerals in both units away from contacts.

- alignment of biotites with direction of contact, biotites wrap around larger grains
- a few large grains present in the mafic porphyry groundmass
- large grains have concentric quartz growths near grain margins

Appendix B: Mineral Chemistry

Analytical Methods

Mineral compositions used in this thesis were obtained at Dalhousie University, using a JEOL 733 Electron Microprobe with four wavelength dispersive spectrometers, and an Oxford Link eXL energy dispersive system. The energy dispersive system was used for all elements, and has a resolution of 137 eV at 5.9 KeV. The slides, and the areas of the slides to be probed, were selected and done by the author. Biotite and plagioclase phases from the leucomonzogranite, mafic porphyry, and areas near the contacts between these two units were probed, and the mineral compositions of these phases were used to determine the effects of magma mingling and magma mixing. Each spectrum was acquired for 40 seconds with an accelerating voltage of 15 Kv and a beam current of 15 nA. The probe spot size is approximately 1 micron, and the data was corrected using Link's ZAF matrix correction program. The accuracy for major elements was $\pm 1.5-2.0$ % relative. The geological standards used in the analysis for this thesis are:

Si, Al, K -	Sanidine
Na -	Jadite
Mg, Ti, Ca -	K-Kaersutite
Fe -	12422 Garnet
Mn -	Manganese Oxide (MnO ₂)

The data listed in this appendix are selected analyses, and do not include mineral compositions of probed phases that were incorrect, or poorly chosen.

Point	SiO ₂	TiO ₂	FeO	MgO	Total	FeO/MgO	Unit
135	34.46	3.33	21.23	6.95	95.01	3.06	FLmp
114	35.11	3.73	20.66	6.50	95.50	3.18	FLmp
115	34.90	3.78	22.06	6.83	96.22	3.23	FLmp
134	34.54	3.79	20.97	6.86	95.93	3.06	FLmp
131	34.76	2.96	21.56	7.24	96.16	2.98	FLmp
132	35.18	3.41	20.84	7.34	95.54	2.84	FLmp
130	34.71	3.30	21.89	7.21	96.38	3.04	FLmp
133	34.51	2.98	21.54	7.13	96.13	3.02	FLmp
					Average=	3.05	
					Std. Dev. =	0.12	
77	34.89	3.45	23.36	5.04	96.76	4.64	NRIm
216	34.22	3.25	24.12	4.67	95.75	5.17	NRIm
206	34.48	3.75	23.71	4.60	96.71	5.16	NRIm
69	34.28	3.85	23.81	4.39	96.27	5.43	NRIm
205	34.13	3.20	24.36	4.62	95.51	5.27	NRIm
222	34.50	3.30	23.83	4.76	95.74	5.00	NRIm
217	34.38	2.76	24.58	5.00	96.61	4.92	NRIm
223	34.69	3.35	23.27	4.66	95.01	5.00	NRIm
199	34.03	3.44	24.20	4.53	95.49	5.35	NRIm
218	34.57	3.55	24.08	4.53	95.71	5.31	NRIm
73	34.78	3.66	23.17	4.60	96.33	5.03	NRIm
					Average=	5.12	
					Std. Dev. =	0.23	

Table B1. Microprobe data obtained from groundmass biotites in the leucomonzogranite (NRIm) and mafic prophyry (FLmp).

Point	SiO ₂	FeO	MgO	Total	FeO/MgO	Location	Type
4	34.35	21.77	6.33	94.73	3.44	Contact	b (mp)
108	34.62	21.60	6.57	96.05	3.29	Contact	b (mp)
88	35.08	21.47	6.60	96.57	3.25	Contact	b (mp)
9	36.10	21.75	6.36	96.99	3.42	Contact	b (mp)
52	34.28	21.28	6.76	94.47	3.15	Contact	b (mp)
111	34.81	21.40	7.04	96.21	3.04	Contact	b (mp)
26	34.08	24.43	4.85	95.43	5.03	Contact	b (mp)
60	34.83	23.52	5.79	96.36	4.07	Contact	b (mp)
31	34.54	22.73	5.92	95.62	3.84	Contact	b (mp)
101	34.77	22.14	6.38	96.43	3.47	Contact	b (mp)
7	34.40	21.41	6.31	94.19	3.39	Contact	b (mp)
106	34.70	21.19	7.02	95.85	3.02	Contact	b (mp)
5	35.57	19.99	5.91	93.32	3.38	Contact	b (mp)
17	34.89	23.43	5.94	96.93	3.95	Contact	b (mp)
57	34.42	21.44	6.73	95.32	3.19	Contact	b (mp)
				Average=	3.53		
				Std. Dev. =	0.52		
58	34.97	23.03	5.16	95.82	4.47	Contact	b (lm)
11	35.12	22.44	5.82	96.34	3.86	Contact	b (lm)
104	35.39	21.47	6.41	95.87	3.35	Contact	b (lm)
18	34.83	23.09	5.05	95.54	4.57	Contact	b (lm)
30	34.23	24.78	4.53	96.42	5.47	Contact	b (lm)
55	34.99	21.42	6.04	95.35	3.55	Contact	b (lm)
29	33.89	23.42	4.43	94.25	5.29	Contact	b (lm)
91	33.71	22.64	6.10	94.93	3.71	Contact	b (lm)
90	34.89	22.05	6.08	96.57	3.62	Contact	b (lm)
				Average=	4.21		
				Std. Dev. =	0.78		

Table B2. Microprobe data obtained from biotites near contacts in the leucomonzogranite (b(lm)) and mafic porphyry (b(mp)).

Point	SiO ₂	FeO	MgO	Total	FeO/MgO	Location	Type
84	34.86	21.78	6.18	96.22	3.52	Contact	bik
95	34.91	21.54	6.19	95.96	3.48	Contact	bik
86	34.73	21.51	6.62	96.42	3.25	Contact	bik
98	34.71	22.37	5.98	96.26	3.74	Contact	bik
41	33.89	22.92	5.36	94.84	4.28	Contact	bik
10	34.85	21.89	6.16	95.54	3.56	Contact	bik
85	34.66	21.50	5.90	95.24	3.64	Contact	bik
264	34.36	22.7	6.18	95.94	3.67	Contact	bik
265	35.04	22.59	6.33	96.59	3.57	Contact	bik
266	34.25	20.76	5.86	93.03	3.54	Contact	bik
250	34.17	23.19	4.75	95.14	4.88	Contact	bik
251	34.05	21.82	5.9	93.79	3.70	Contact	bik
280	33.90	25.03	4.11	96.27	6.09	Contact	bik
				Average=	3.92		
				Std. Dev. =	0.77		
196	34.77	23.44	4.69	95.27	4.99	NRIm	bik
190	34.52	21.34	6.52	94.03	3.27	NRIm	bik
75	35.04	23.61	4.69	96.92	5.04	NRIm	bik
224	35.25	23.80	5.03	96.96	4.73	NRIm	bik
74	35.28	23.57	4.89	96.93	4.82	NRIm	bik
197	34.35	24.40	4.98	96.09	4.90	NRIm	bik
184	34.99	23.31	4.79	94.98	4.87	NRIm	bik
193	34.60	23.97	4.68	96.18	5.12	NRIm	bik
76	35.26	22.50	5.05	96.36	4.46	NRIm	bik
198	34.58	24.34	4.57	96.38	5.32	NRIm	bik
188	34.50	23.75	5.05	96.02	4.71	NRIm	bik
183	33.38	24.26	4.50	94.14	5.40	NRIm	bik
				Average=	4.80		
				Std. Dev. =	0.55		
179	34.35	22.04	6.04	95.27	3.65	FLmp	bik
181	34.25	22.19	5.79	94.82	3.83	FLmp	bik
180	34.33	22.83	5.77	95.79	3.96	FLmp	bik
182	34.60	22.94	5.78	95.91	3.97	FLmp	bik
				Average=	3.85		
				Std. Dev. =	0.15		

Table B3. Microprobe data obtained from inclusions in alkali feldspar megacrysts in the leucomonzogranite, mafic porphyry, and near contacts (bik = biotite in alkali feldspar, NRIm = leucomonzogranite, FLmp = mafic porphyry).

Point	SiO2	CaO	Na2O	K2O	Total	Loaction	Na2O/(Na2O+CaO)	Type	Grain #
203	68.99	0.03	9.99	0.09	99.09	NRIm	1.00	pc1	1
204	68.39	0.25	9.86	0.01	98.40	NRIm	0.98	pc2	1
201	63.67	3.79	8.33	0.26	99.37	NRIm	0.69	pi1	1
202	60.79	6.00	7.62	0.29	99.23	NRIm	0.56	pi2	1
200	63.42	4.09	8.18	0.31	99.85	NRIm	0.67	pr	1
221	63.77	3.52	9.11	0.17	99.29	NRIm	0.72	pc	2
220	65.12	2.75	8.96	0.26	99.55	NRIm	0.76	pi	2
210	64.42	2.77	9.34	0.26	99.27	NRIm	0.77	pr	2
215	65.60	1.98	9.51	0.31	99.40	NRIm	0.83	pc	3
214	64.87	1.76	7.48	2.86	99.63	NRIm	0.81	pi1	3
213	63.46	3.71	8.66	0.30	99.36	NRIm	0.70	pi2	3
212	65.22	2.16	9.59	0.29	99.54	NRIm	0.82	pr	3
211	61.25	5.29	8.10	0.13	99.27	NRIm	0.60	pc	4
210	64.67	2.76	8.61	0.40	98.44	NRIm	0.76	pi1	4
209	70.22	0.11	8.57	-0.04	99.01	NRIm	0.99	pi2	4
208	65.39	2.34	8.63	0.52	99.11	NRIm	0.79	pi3	4
207	66.60	1.73	9.08	0.17	99.75	NRIm	0.84	pr	4
208	62.89	4.76	8.82	0.26	100.45	NRIm	0.65	pr	5
209	65.75	1.52	10.08	0.22	99.65	NRIm	0.87	pi	5
210	64.7	3.03	9.8	0.3	100.55	NRIm	0.76	pc	5
211	65.77	1.57	8.95	0.59	99.48	NRIm	0.85	pr	6
212	69.1	0.77	8.22	0.20	99.08	NRIm	0.91	pi	6
213	68.49	0.59	10.00	0.04	99.72	NRIm	0.94	pc	6
214	65.07	2.00	8.97	0.49	98.49	NRIm	0.82	pr	7
215	64.34	3.12	9.1	0.22	100.00	NRIm	0.74	pi	7
216	64.49	0.55	6.37	2.98	97.68	NRIm	0.92	pc	7
217	65.68	1.96	9.54	0.32	99.96	NRIm	0.83	pr	8
218	62.18	5.12	7.97	0.34	100.20	NRIm	0.61	pi	8
219	62.17	4.81	8.18	0.11	99.28	NRIm	0.63	pc	8
						Average	0.78		
						Std. Dev.	0.12		

Table B4. Microprobe data obtained from plagioclase grains in the leucomonzogranite (pc = plagioclase core, pi = plagioclase intermediate, pr = plagioclase rim, NRIm = leucomonzogranite)

Point	SiO ₂	CaO	Na ₂ O	K ₂ O	Total	Location	Na ₂ O/(Na ₂ O+CaO)	Type	Grain #
121	62.72	4.80	8.70	0.58	101.22	FLmp	0.64	pc	1
120	61.87	5.26	8.52	0.65	100.92	FLmp	0.62	pr	1
122	61.29	5.54	8.23	0.36	100.85	FLmp	0.60	pc	2
123	65.01	-0.03	1.26	14.95	100.51	FLmp	1.03	pr	2
178	61.79	5.12	8.39	0.32	99.73	FLmp	0.62	pc	3
177	61.97	5.16	8.24	0.35	100.19	FLmp	0.61	pi	3
176	62.10	4.96	8.23	0.36	100.41	FLmp	0.62	pr	3
128	62.65	4.55	8.71	0.49	100.84	FLmp	0.66	pc	4
171	63.82	3.81	8.35	0.22	99.51	FLmp	0.69	pi1	4
170	64.06	3.93	7.39	0.36	99.19	FLmp	0.65	pi2	4
175	63.55	3.88	8.39	0.24	99.12	FLmp	0.68	pi3	4
129	62.21	4.95	8.63	0.40	101.44	FLmp	0.64	pr	4
168	61.85	5.57	7.89	0.43	100.32	FLmp	0.59	pc	5
174	61.73	5.38	7.62	0.49	99.23	FLmp	0.59	pi1	5
167	62.30	5.24	6.93	0.39	99.41	FLmp	0.57	pi2	5
173	61.89	5.13	7.87	0.40	99.75	FLmp	0.61	pi3	5
166	63.94	3.56	8.43	0.29	99.36	FLmp	0.70	pr	5
165	62.14	5.37	7.84	0.41	100.28	FLmp	0.59	pc	6
164	61.77	5.30	8.01	0.56	99.75	FLmp	0.60	pi1	6
163	61.26	5.62	7.53	0.35	99.89	FLmp	0.57	pi2	6
162	63.41	3.97	8.95	0.19	99.84	FLmp	0.69	pr	6
172	63.07	4.01	8.05	0.10	98.18	FLmp	0.67	pc	7
169	64.86	2.78	8.35	0.46	98.70	FLmp	0.75	pr	7
261	64.68	4.12	8.42	0.24	101.32	FLmp	0.67	pr	8
262	62.67	5.43	8.31	0.16	100.98	FLmp	0.60	pc	8
263	65.03	3.13	8.68	0.25	100.11	FLmp	0.73	pr	9
264	61.64	5.73	7.66	0.27	100.42	FLmp	0.57	pc	9
265	61.02	6.11	7.62	0.28	100.65	FLmp	0.55	pi	9
						Average	0.65		
						Std. Dev.	0.09		

Table B5. Microprobe data obtained from plagioclase grains in the mafic porphyry (pc = plagioclase core, pi = plagioclase intermediate, pr = plagioclase rim, FLmp = mafic porphyry).

Point	SiO ₂	CaO	Na ₂ O	K ₂ O	Total	Location	Side	Type	Grain #	Na ₂ O/(Na ₂ O/CaO)
156	61.33	5.45	7.67	0.16	99.44	Contact		pc	1	0.58
155	61.57	5.45	7.85	0.20	99.51	Contact		pi	1	0.59
154	61.38	5.29	8.34	0.30	99.82	Contact		pr	1	0.61
151	58.78	7.36	6.97	0.32	99.41	Contact		pc	2	0.49
149	60.70	6.37	7.64	0.45	100.21	Contact		pi1	2	0.55
148	63.91	4.00	8.11	0.38	99.78	Contact		pi2	2	0.67
147	59.40	7.07	7.10	0.28	99.46	Contact		pc	3	0.50
146	59.36	6.69	7.50	0.24	99.36	Contact		pi1	3	0.53
145	62.15	4.57	8.71	0.46	99.63	Contact		pi2	3	0.66
144	64.42	3.34	9.04	0.40	100.16	Contact		pr	3	0.73
223	68.48	0.05	11.29	0.02	99.73	Contact	lm	pr	4	1.00
224	65.59	1.82	10.04	0.32	100.46	Contact	lm	pi	4	0.85
225	62.71	4.32	8.57	0.47	100.26	Contact	lm	pc	4	0.66
226	63.78	3.79	9.06	0.24	100.38	Contact	mp	pr	5	0.71
227	63.09	4.27	8.80	0.17	99.78	Contact	mp	pi	5	0.67
228	63.33	4.45	8.80	0.32	100.87	Contact	mp	pc	5	0.66
229	60.90	6.38	7.51	0.24	100.72	Contact	lm	pr	6	0.54
230	67.85	0.49	8.89	0.41	98.12	Contact	lm	pc	6	0.95
231	61.82	5.47	8.12	0.24	100.80	Contact	lm	pr	7	0.60
232	61.56	5.49	8.36	0.24	100.71	Contact	lm	pc	7	0.60
233	62.93	4.81	8.66	0.19	100.80	Contact	lm	pr	8	0.64
234	62.56	5.11	7.92	0.27	100.42	Contact	lm	pc	8	0.61
235	63.62	4.04	8.72	0.21	100.06	Contact	lm	pr	9	0.68
236	60.00	7.25	7.40	0.11	100.87	Contact	lm	pi	9	0.51
237	59.10	7.31	7.37	0.26	100.15	Contact	lm	pc	9	0.50
238	65.12	2.98	9.26	0.32	100.51	Contact	lm	pr	10	0.76
239	63.23	4.79	8.72	0.40	101.22	Contact	lm	pi	10	0.65
240	62.11	4.95	8.29	0.24	99.63	Contact	lm	pc	10	0.63
241	62.84	4.11	8.23	0.24	98.83	Contact		cp	11	0.67
242	63.55	4.14	9.13	0.10	100.53	Contact		cp	11	0.69
243	64.60	3.55	9.21	0.40	101.30	Contact	lm	pr	12	0.72
244	59.63	7.61	7.12	0.26	101.15	Contact	lm	pi	12	0.48
245	59.39	7.57	7.31	0.20	100.77	Contact	lm	pc	12	0.49
246	59.80	6.91	7.79	0.07	100.49	Contact	mp	pr	13	0.53
247	61.45	5.62	7.56	0.16	99.08	Contact	mp	pc	13	0.57
248	63.18	4.52	9.39	0.06	101.21	Contact	mp	pr	14	0.68
249	58.03	8.53	6.68	0.13	100.73	Contact	mp	pc	14	0.44
250	63.85	4.17	8.67	0.28	100.71	Contact	lm	pr	15	0.68
251	66.66	0.90	8.32	0.62	98.03	Contact	lm	pi	15	0.90
								Average		0.64
								Std. Dev.		0.12

Table B6. Microprobe data obtained from plagioclase grains at and near contacts (pc = plagioclase core, pi = plagioclase intermediate, pr = plagioclase rim, lm = leucomonzogranite, mp = mafic porphyry).